THESIS

’t Hooft anomaly, Lieb-Schultz-Mattis theorem, and boundary of topological phases

Ryohei Kobayashi
Department of Physics, Graduate School of Science, The University of Tokyo

January, 2019

Abstract

We review recent developments of symmetry protected topological phases and Lieb-Schultz-Mattis mechanism, associated with original results by the author related to the topic. The original result consists of two parts.

First, we examine (3+1)d topological ordered phases with C_k rotation symmetry. We show that some rotation symmetric (3+1)d topological orders are anomalous, in the sense that they cannot exist in standalone (3+1)d systems, but only exist on the surface of (4+1)d SPT phases. For (3+1)d discrete gauge theories, we propose anomaly indicator that can diagnose the $\mathbb{Z}_k$ valued rotation anomaly. Since (3+1)d topological phases support both point-like and loop-like excitations, the indicator is expressed in terms of the symmetry properties of point and loop-like excitations, and topological data of (3+1)d discrete gauge theories (Sec.3.2).

Second, we examine the Lieb-Schultz-Mattis theorem in lattice systems, which dictates that a trivial symmetric insulator is prohibited if lattice translation symmetry and $U(1)$ charge conservation are both preserved. We generalize the Lieb-Schultz-Mattis theorem to systems with higher-form symmetries, which act on extended objects of dimension $n > 0$. The prototypical lattice system with higher-form symmetry is the pure abelian lattice gauge theory whose action consists only of the field strength. We first construct the higher-form generalization of the Lieb-Schultz-Mattis theorem with a proof. We then apply it to the $U(1)$ lattice gauge theory description of the quantum dimer model on bipartite lattices. Finally, using the continuum field theory description in the vicinity of the Rokhsar-Kivelson point of the quantum dimer model, we diagnose and compute the mixed 't Hooft anomaly corresponding to the higher-form Lieb-Schultz-Mattis theorem (Sec.5.3).

Publication List

This thesis is mainly based on the following two papers that I was involved in.

1. The description in Chapter 3 is presented in an unpublished paper [1]:
   R. Kobayashi and K. Shiozaki, "Anomaly indicator of rotation symmetry in (3+1)D topological order", arXiv: 1901.06195.

2. The results shown in Chapter 5 is mostly following [2]:
   R. Kobayashi, K. Shiozaki, Y. Kikuchi and S. Ryu, "Lieb-Schultz-Mattis type theorem with higher-form symmetry and the quantum dimer models", Phys. Rev. B **99**, 014402 (2019), selected as *Editors' suggestion*.

Acknowledgements

First and foremost, it is a pleasure to express my sincere gratitude to my advisor Masaki Oshikawa for his guidance and advice. I would also like to thank Yuji Tachikawa and Chang-Tse Hsieh for intensive discussions on anomalies in discrete gauge theories, which are of great help in clarifying many points in my project.

Due to my long-term stay at the university of Chicago, I deeply thank to Shinsei Ryu for kindly having accepted my visit and supervised me during my stay in Chicago. His profound physical insight always amazed me and helped me to accomplish our project about the Lieb-Schultz-Mattis mechanism. It was certainly fortunate to work with Yuta Kikuchi in Chicago, who patiently helped me to understand anomalies involving higher-form symmetries.

During my Master program there has been several collaborations that I was involved in, and I feel deep appreciations for having such brilliant collaborators: Kohei Kawabata, Ning Wu, Hosho Katsura, Yuya Nakagawa, Yoshiki Fukusumi, Masaki Oshikawa, Yuta Kikuchi, Shinsei Ryu and Ken Shiozaki. I am especially grateful to Ken Shiozaki for helping me to understand from basics to advanced topic of SPT phases, accepting my visit to Yukawa institute of theoretical physics in Kyoto university, and encouraging me to work on gapped boundaries of topological phases, which turns into one of the main subjects in my thesis.

I acknowledge financial support that I had received from Institute for Solid State Physics (ISSP), without which my stay in Chicago would have been impossible. I should acknowledge Advanced Leading Graduate Course Photon Science (ALPS) of Japan Society for the Promotion of Science (JSPS) as well.

At last but not least, I would like to thank my parents, Hideki Kobayashi and Keiko Kobayashi, for their tremendous support.

Contents

Chapter 1

Introduction

Recent years have witnessed tremendous progress in understanding of topological phases of matter. Especially, condensed matter theorists have discovered symmetry protect topological (SPT) phases, which are certain gapped phases of condensed matter systems at zero temperature. Theoretical and experimental study on SPT phases have elucidated the mechanism for emergence of distinct quantum phases in the presence of the global symmetry. Roughly speaking, distinct phases can appear in a phase diagram, since global symmetry in general constrains the possible path in the phase diagram which can bring the initial ground state living on a certain point in the phase diagram, to the final state on the other point; such continuous deformation of parameters in the phase diagram is allowed only when the process respects the symmetry. As a result, the phase diagram can be divided into distinct phases, where a single phase is defined as an equivalence class of ground states, whose equivalence relation is defined by continuous deformation of parameters respecting the symmetry.

The classification of SPT phases is an important problem in condensed matter physics. A great leap towards the complete classification of SPT phases has been made by recognizing that the $(d+1)$ dimensional SPT phases are equivalent to the 't Hooft anomaly on the d dimensional boundary of the SPT phase, which is represented as "anomaly inflow" assumption. Such field theoretical perspective of SPT phases brought significant attention of high energy theorists, which has paved the way to discovering new class of 't Hooft anomalies in quantum field theory (QFT). For example, people realized that the anomalies are present in bosonic systems with help of the discovery of bosonic SPT phases, while the anomalies had been thought to be present only in fermionic systems.

While the 't Hooft anomalies are applied to classify SPT phases, they are also exploited to constrain vacuum structure of the low energy (IR) theory. For instance, it was recently discovered that the $SU(N)$ pure Yang-Mills theory at $\theta = \pi$ suffers from 't Hooft anomaly involving the center symmetry and CP symmetry, which dictates the breaking of CP symmetry with at least two-fold ground state degeneracy. Such spectral constraint thanks to 't Hooft anomalies is known as Lieb-Schultz-Mattis (LSM) mechanism in condensed matter literature. LSM mechanism is applied for quantum many-body system defined on a lattice, possessing both internal and lattice symmetries. Roughly speaking, LSM theorem prohibits a symmetric gapped phases without ground state degeneracy (i.e., trivial symmetric insulator) with input of combination of internal and lattice symmetries. Such theorem of LSM-type is empirically known to manifest itself as a consequence of 't Hooft anomaly in the continuum infrared limit. More concretely, in the IR theory where lattice symmetry such as translational symmetry can be treated as internal symmetry, LSM-type constraint is understood as a mixed 't Hooft anomaly involving internal and lattice symmetries.

The thesis is largely devoted to the review of recent development in SPT phases and LSM mechanism, and their intimate relation to 't Hooft anomalies. Associated with the review, we illustrate the original results by the author in Section 3.2, 5.3.

The thesis is organized as follows. In Chapter 2, we begin with reviewing the anomaly inflow observed in the Haldane chain, which realizes a bosonic SPT phase protected by $\mathbb{Z}_2 \times \mathbb{Z}_2$ symmetry. We will see that the boundary of the Haldane chain transforms as a nontrivial projective representation under $\mathbb{Z}_2 \times \mathbb{Z}_2$ symmetry, which is shown to offer the simplest example of 't Hooft anomaly in (0+1)d system. The anomaly (i.e., phase ambiguity of partition function under gauge transformation) on the boundary is cancelled by the SPT phase in the bulk. Next, we review the classification of bosonic SPT phases protected by onsite symmetries based on group cohomology in arbitrary dimensions. We analyze the boundary properties of these SPT phases characterized by the element of group cohomology $\mathcal{H}^{d+1}(G, U(1))$, and observe that the symmetry acts on boundaries in non-onsite fashion, which prevents us from gauging the symmetry on the boundary.

In Chapter 3, we examine boundary states of SPT phases protected by (non-onsite) spacetime symmetries. Interestingly, the boundaries of SPT phases can sometimes host gapped phases, where ground states have nontrivial degeneracy to account for anomalies. Specifically, we are interested in topological ordered phases without symmetry breaking, realized on the boundaries of SPT phases. We first review the study of (2+1)d gapped boundaries realized on the surface of (3+1)d bosonic SPT phases protected by reflection symmetry in Ref. [3]. We will see that path integral on the SPT phase in the bulk is expressed by the data of topological order on the boundary, which enables us to evaluate anomalies by the TQFT data on surface and is called "anomaly indicator formula" .

Next, we generalize the anomaly indicator formula to (3+1)d topological ordered phases regarded as boundaries of (4+1)d SPT phases (see Sec.3.2). For (3+1)d discrete gauge theories with C_k rotation symmetry around an axis, we obtain the indicator formula which makes possible to compute anomalies from the data of (3+1)d topological order and symmetry properties of quasiparticles in discrete gauge theories.

In Chapter 4, we examine topological phases and anomalies based on "higher-form symmetries", which is generalized concept of ordinary global symmetries proposed in Ref. [4]. Higher-form symmetries (p-form symmetries) are global symmetries whose charged objects are of dimension p, e.g., lines for $p = 1$, membranes for $p = 2$, and so on. Especially, by enumerating several known concrete examples, we will see that 1-form symmetries are ubiquitous in pure gauge theories, where gauge invariant line operators become charged objects. We will see that higher-form symmetries can also be gauged, which enables us to discuss anomalies based on p-form symmetries. As an application, we review the mixed 't Hooft anomaly between CP and $\mathbb{Z}_N$ 1-form symmetry (center symmetry) in (3+1)d $SU(N)$ pure Yang-Mills theory at $\theta = \pi$, recently discussed in Ref. [5]. As a result of the anomaly, one can dictate that the CP symmetry must be broken at $\theta = \pi$ at zero temperature.

In Chapter 5, we discuss the constraint on low-energy spectral properties of many-body systems deduced from 't Hooft anomaly, which is akin to CP breaking in $SU(N)$ pure Yang-Mills theory enforced by the mixed anomaly. Such spectral constraint thanks to 't Hooft anomalies is known as Lieb-Schultz-Mattis (LSM) mechanism in condensed matter literature. After reviewing intimate relation of the LSM theorem defined on lattice systems and 't Hooft anomalies in continuum theory, we construct the generalized LSM theorem based on higher-form symmetry and lattice translational symmetry, which corresponds to anomaly constraint based on the mixed 't Hooft anomaly involving these two symmetries in continuum IR limit. The generalized theorem is applied to pure gauge theories constructed on lattice (see Sec.5.3). As a demonstration, we apply the generalized LSM theorem to the quantum dimer model on a bipartite lattice, which is known to be equivalent to the pure $U(1)$ lattice gauge theory, where both $U(1)$ 1-form symmetry and lattice symmetry are present. We diagnose a corresponding mixed 't Hooft anomaly involving these two symmetries at the continuum field theory that describes the vicinity of the quantum critical (Rokhsar-Kivelson) point.

Chapter 2

Classification of SPT phases

2.1 bosonic SPT in (1+1)d

Symmetry protected topological (SPT) phase [6] is a certain equivalence class of ground states of quantum many-body systems at zero temperature. Here, we consider systems with the following properties;

- gapped,
- without ground state degeneracy on arbitrary closed spatial manifolds,
- G-symmetric, without spontaneous symmetry breaking. G can be internal as well as spacetime symmetries.

Namely, we deal with unique ground state of a many-body system respecting G-symmetry. We define an equivalence relation for ground states $|\psi\rangle, |\psi'\rangle$ of different systems, if there exists G-symmetric continuous deformation of the system without closing gap, which interpolates $|\psi\rangle$ and $|\psi'\rangle$.

In QFT language, our situation corresponds to assuming that the theory has a mass gap, and the Hilbert space in the long distance limit is one-dimensional on any closed spatial manifold. Such class of QFT is known as invertible topological field theory.

An important problem in condensed matter theory is the general classification of SPT phases, which is completely resolved in the case of free fermion systems via K-theory. For interacting systems, condensed matter theorists have approached to the problem by constructing explicit lattice Hamiltonian and then finding observables which can probe distinct phases from each other.

One way to identify observables which differentiate distinct phases is putting a system on a space with boundary. For example, let us consider the nontrivial SPT phase (known as the Haldane phase in the literature) in 1+1 dimension protected by $\mathbb{Z}_2 \times \mathbb{Z}_2$ symmetry. The Haldane phase is realized by the following Hamiltonian of one dimensional chain of qubits

$$H_{\mathrm{Haldane}} = -\sum_{j=1}^{N-1} Z_j X_{j+\frac{1}{2}} Z_{j+1} - \sum_{j=1}^{N} Z_{j-\frac{1}{2}} X_j Z_{j+\frac{1}{2}}, \tag{2.1}$$

where X, Y, Z are Pauli operators acting on qubits. $\mathbb{Z}_2 \times \mathbb{Z}_2$ symmetries are generated by

$$U^{(a)} = \prod_{j=1}^{N} X_j, \qquad U^{(b)} = \prod_{j=1}^{N+1} X_{j-\frac{1}{2}}, \tag{2.2}$$

where a, b denotes two generators of $\mathbb{Z}_2 \times \mathbb{Z}_2$. Since the Hamiltonian is the sum of commuting projectors, the ground state $|\psi\rangle$ is characterized by the following conditions

$$Z_j X_{j+\frac{1}{2}} Z_{j+1} |\psi\rangle = |\psi\rangle , \qquad Z_{j-\frac{1}{2}} X_j Z_{j+\frac{1}{2}} |\psi\rangle = |\psi\rangle , \tag{2.3}$$

for all j. In the presence of boundaries, it turns out that the symmetry acts only on boundary degrees of freedom. To see this, we express the action of symmetry transformations restricted on ground state manifolds

$$U^{(a)} = \prod_{j=1}^{N} X_j = Z_{\frac{1}{2}} \otimes Z_{N+\frac{1}{2}}, \qquad U^{(b)} = \prod_{j=1}^{N+1} X_{j-\frac{1}{2}} = X_{\frac{1}{2}} Z_1 \otimes Z_N X_{N+\frac{1}{2}}, \tag{2.4}$$

where we used the conditions (2.3) which is satisfied for ground states. Symmetry transformation clearly decomposes into local actions on boundary degrees of freedom, which are the form of $U^{(g)} = U_L^{(g)} \otimes U_R^{(g)}$ for $g \in \mathbb{Z}_2 \times \mathbb{Z}_2$. The key observation is that the $\mathbb{Z}_2 \times \mathbb{Z}_2$ symmetry acts on each boundary L, R as the nontrivial projective representation characterized by $\omega \in \mathcal{Z}^2(\mathbb{Z}_2 \times \mathbb{Z}_2, U(1))$, which is robust against any redefinition of symmetry actions via local unitary transformations, and hence discriminates the system from the trivial product state of qubits as SPT phases.

We note that the projective action on boundary of Haldane phase provides us the simplest example of 't Hooft anomaly in 0+1 dimensional quantum theory. An 't Hooft anomaly is defined as an obstruction to promoting the global symmetry to local gauge symmetry. Concretely, we say that symmetry G of a theory has an 't Hooft anomaly if the partition function $Z[A]$ with the background G-gauge field is transformed as

$$Z[A + \mathrm{d}\alpha] = Z[A] \exp(\mathrm{i}\mathcal{A}[\alpha, A]) \tag{2.5}$$

under G-gauge transformation $A \to A + \mathrm{d}\alpha$, and $\mathcal{A}[\alpha, A]$ cannot be canceled by introducing local counterterms.

In our case, 't Hooft anomaly manifests itself as phase ambiguity of partition function of the theory coupled to background gauge field, as shown in Fig.2.1. Namely, the partition function of a boundary of a half infinite chain coupled with background gauge field is $\mathrm{tr}_{\mathcal{H}}[U^{(g)} e^{-\beta H}]$, where $g \in \mathbb{Z}_2 \times \mathbb{Z}_2$ is the holonomy of background $\mathbb{Z}_2 \times \mathbb{Z}_2$ gauge field, and $\mathcal{H}$ is the Hilbert space of ground states. Then, 't Hooft anomaly is expressed as phase ambiguity of partition function under gauge transformation

$$\mathrm{tr}_{\mathcal{H}}[U^{(g)} U^{(h)} e^{-\beta H}] = \omega(g, h)^{-1} \cdot \mathrm{tr}_{\mathcal{H}}[U^{(gh)} e^{-\beta H}], \tag{2.6}$$

caused by projective action of global symmetry on the Hilbert space. Such phase ambiguity of (0+1)-dimensional action is not cancellable by introducing local counterterm at the boundary (which amounts at most to changing the phase ω by coboundary). However, this phase ambiguity depends only on background $\mathbb{Z}_2 \times \mathbb{Z}_2$ gauge field, and can be cancelled by boundary variation of topological action of background gauge field living in (1+1)-dimensional bulk. Here we recall briefly how such (1+1)-dimensional topological action cancels the phase ambiguity on the boundary.

The bulk partition function $Z[M, A]$ in terms of $G = \mathbb{Z}_2 \times \mathbb{Z}_2$ background gauge field A is defined on an oriented closed 2d surface M. To construct topological action, we first triangulate M as a simplical complex, and assign a local ordering[1] on 1-simplices. Group elements of G are living on 1-simplices, and the configuration of group elements satisfies a “fusion rule” $g_{(01)} g_{(12)} = g_{(02)}$ on each

[1] a local ordering is an assignment of orientation on each 1-simplex, where the orientation of 1-simplices rounding a 2-simplex never becomes cyclic.

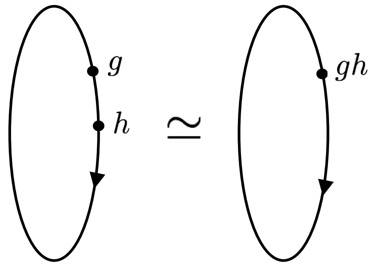

Figure 2.1: The above two configurations of background gauge field in (0+1)-dimensional boundary are gauge equivalent, characterized by holonomy gh (black dots denote symmetry defects). However, gauge invariance of partition function is violated due to 't Hooft anomaly (2.6).

2-simplex $\sigma = (012)$, which stands for flatness of G-field. Then, we can represent the flat background gauge field for G by a network of symmetry defects on M, which is specified by a configuration of group elements on 1-simplices. We assign a Boltzmann weight $\omega(g, h)$ on each 2-simplex, which is regarded as a junction of two symmetry defects. The partition function is obtained by the product of Boltzmann weight for all 2-simplices,

$$Z^{\mathrm{DW}}_{(1+1)\mathrm{d}}[M, A] = \prod_{\sigma} \omega(g, h)^{\epsilon(\sigma)}, \tag{2.7}$$

where the product runs over all 2-simplices in M, and ϵ is an orientation of a 2-simplex (see Fig.2.2).

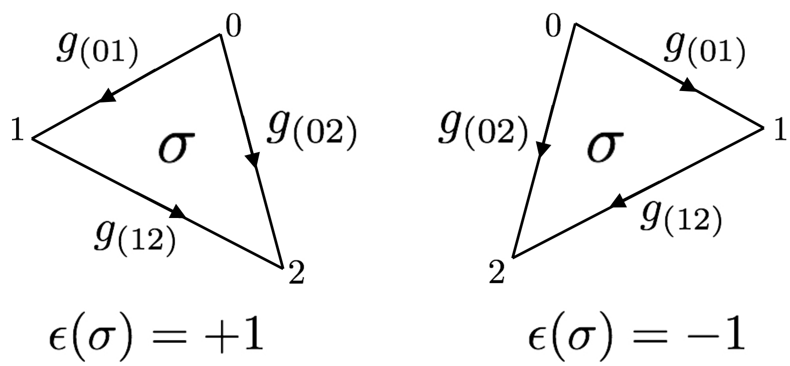

Figure 2.2: orientation of 2-simplices.

We require that the theory only depends on topology of M and hence independent of how we triangulate the manifold. This requirement boils down to cocycle condition for ω (see Appendix A),

$$\omega(g, h)\omega(gh, k) = \omega(g, hk)\omega(h, k), \tag{2.8}$$

as illustrated in Fig.2.3.

For closed M, we can also check that the partition function is invariant under the shift of ω by a coboundary, which corresponds to adding local counterterm to each 1-simplex

$$\omega \mapsto \omega + \mathrm{d}\alpha, \tag{2.9}$$

where $\alpha \in \mathcal{C}^1(G, U(1))$ and $\mathrm{d}\alpha(g, h) := \alpha(g)\alpha(gh)^{-1}\alpha(h)$. This means that only $[\omega] \in \mathcal{H}^2(G, U(1))$ matters for specifying a theory up to addition of local counterterm, reflecting $\mathcal{H}^2(G, U(1))$ classification of (1+1)-dimensional SPT phase. The bulk theory turns out to be essentially Dijkgraaf-Witten

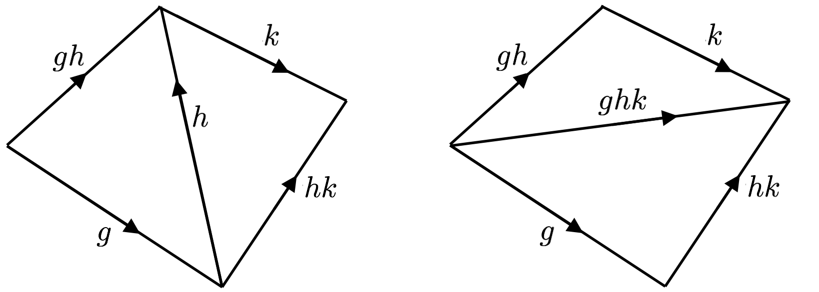

$$\omega(g,h)\omega(h,k)^{-1} = \omega(g,hk)\omega(gh,k)^{-1}$$

Figure 2.3: Invariance of Boltzmann weight under the change of triangulation leads to cocycle condition of ω.

gauge theory [7, 8], although the gauge field is treated as background gauge field, instead of dynamical field to be summed over in path integral.

In the presence of a boundary, gauge transformation between two gauge equivalent configuration shown in Fig.2.1 is realized on the boundary of M by adding a 2-simplex with a Boltzmann weight $\omega(g,h)$ on a tip of the bulk (see Fig.2.4). This manifestly cancels anomalous phase ambiguity of a boundary. Concretely,

$$Z_{(0+1)\mathrm{d}}[\partial M, A] Z^{\mathrm{DW}}_{(1+1)\mathrm{d}}[M, A] \tag{2.10}$$

is gauge invariant. Such mechanism for canceling 't Hooft anomalies by bulk theory is called anomaly inflow. Various examples of SPT phase in higher dimension also suggests the ubiquity of anomaly inflow in SPT phases. Specifically, bosonic SPT phase protected by any onsite symmetry G in any $d+1$ dimension is classified by elements of group cohomology $\omega \in \mathcal{H}^{d+1}(G, U(1))$, and 't Hooft anomaly on its boundary is canceled by variation of Dijkgraaf-Witten topological action specified by ω in the bulk.

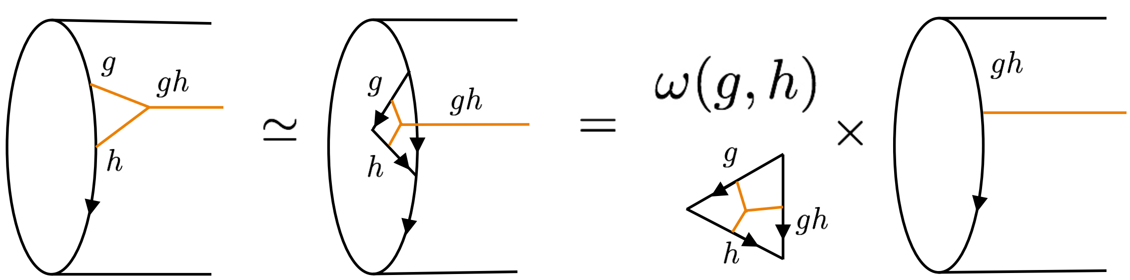

Figure 2.4: The symmetry defect on a boundary is split by attaching a 2-simplex on a tip of the cigar. The Boltzmann weight of an attached 2-simplex is $\omega(g,h)$, which cancels the phase ambiguity on the boundary.

2.2 bosonic SPT in $(d+1)$d

Similarly, the Dijkgraaf-Witten type topological action in $(d+1)$-dimension is constructed on a triangulation of $(d+1)$d spacetime manifold M with local ordering on its 1-simplices. We can locally define a numbering of $(d+2)$ vertices as $v_0, v_1, \ldots, v_{d+1}$ of a $(d+1)$ simplex $(v_0 v_1 \ldots v_{d+1})$

induced by local ordering, where a 1-simplex $(v_j v_{j+1})$ is oriented from v_j to v_{j+1} for all j. Flat G-gauge field configuration is expressed as assignment of a group element $g_{(ij)}$ on each 1-simplex (ij) for $i<j$, satisfying the fusion rule $g_{(01)}g_{(12)}=g_{(02)}$ for all 2-simplex (012). We assign a Boltzmann weight $\omega(g_{(01)},g_{(12)},\dots g_{(d,d+1)})\in\mathcal{Z}^{d+1}(G,U(1))$ on each $(d+1)$-simplex $(012\dots d+1)$, then the topological action is just given by product of Boltzmann weight for the whole spacetime,

$$Z^{\mathrm{DW}}_{(d+1)\mathrm{d}}[M,A]=\prod_{\sigma}\omega(g_{(01)},g_{(12)},\dots g_{(d,d+1)})^{\epsilon(\sigma)},\tag{2.11}$$

where the product runs over $(d+1)$-simplices in M, and $\epsilon(\sigma)$ is an orientation of σ.

One can also formulate such bosonic SPT phases of Dijkgraaf-Witten type in Hamiltonian formalism. To do this, we first introduce dynamical degree of freedom $g_i\in G$ on each 0-simplex i, which is regarded as a matter field coupled with background G-gauge field $g_{(ij)}$. G-gauge transformation is defined as

$$\begin{cases} g_i & \mapsto \alpha_i g_i, \\ g_{(ij)} & \mapsto \alpha_i g_{(ij)}\alpha_j^{-1} \quad \text{for } i<j, \end{cases}\tag{2.12}$$

where $\alpha_i\in G$. Gauge invariant topological action of matter fields $\{g_i\}$ is given by

$$Z^{\mathrm{DW}}_{(d+1)\mathrm{d}}[M,A]=\frac{1}{|G|^{N_0}}\sum_{\{g_i\}}\prod_{\sigma}\omega(g_0^{-1}g_{(01)}g_1,g_1^{-1}g_{(12)}g_2,\dots g_d^{-1}g_{(d,d+1)}g_{d+1})^{\epsilon(\sigma)},\tag{2.13}$$

where N_0 is the number of 0-simplices. We obtain the effective action of background gauge field in the form of (2.11) by integrating out the matter field. In the absence of background gauge field, the topological action becomes

$$Z^{\mathrm{matter}}_{(d+1)\mathrm{d}}[M]:=Z^{\mathrm{DW}}_{(d+1)\mathrm{d}}[M,A=0]=\frac{1}{|G|^{N_0}}\sum_{\{g_i\}}\prod_{\sigma}\omega(g_0^{-1}g_1,g_1^{-1}g_2,\dots g_d^{-1}g_{d+1})^{\epsilon(\sigma)}.\tag{2.14}$$

We remark that $Z^{\mathrm{matter}}_{(d+1)\mathrm{d}}[M]=1$ for closed M. For convenience, we define

$$\nu(g_0,g_1,\dots,g_{d+1}):=\omega(g_0^{-1}g_1,g_1^{-1}g_2,\dots g_d^{-1}g_{d+1}),\tag{2.15}$$

which satisfies $\nu(g_0,g_1,\dots,g_{d+1})=\nu(gg_0,gg_1,\dots,gg_{d+1})$ for $g\in G$ by definition.

Now we provide the lattice Hamiltonian of matter fields for the Hilbert space constructed on a boundary $\Sigma=\partial M$ of spacetime manifold M. Namely, when the $(d+1)$d manifold M has a boundary Σ, we define a quantum state $|\Psi_M\rangle$ on d-dimensional manifold Σ is constructed via path integral of the topological action on M

$$\Psi_M(\{g_i\}_{i\in\Sigma})=\frac{1}{|G|^{N_0^{\mathrm{int}}}}\sum_{g_i\in\text{internal of }M}\prod_{\sigma}\nu(g_0,g_1,\dots,g_{d+1})^{\epsilon(\sigma)},\tag{2.16}$$

where N_0^{int} is the number of 0-simplices in the internal of M. The wave function $\Psi_M(\{g_i\}_{i\in\Sigma})$ on Σ is given by path integral of topological action under the boundary condition $\{g_i\}$ on Σ. Since $Z^{\mathrm{matter}}_{(d+1)\mathrm{d}}[\Sigma\times S^1]=1$, the Hilbert space has one dimension for all closed oriented Σ. For simplicity, let us work on the Hilbert space on $\Sigma=S^d$, whose ground state wave function is given by path integral (2.16) on $M=D^{d+1}$. We choose the triangulation of D^{d+1} such that there is only one 0-simplex v_* in the internal of D^{d+1}; $N_0^{\mathrm{int}}=1$. Then, the ground state wave function becomes

$$\Psi(\{g_i\}_{i\in S^d})=\frac{1}{|G|}\sum_{g_*}\prod_{\sigma}\nu(g_*,g_1,\dots,g_{d+1})^{\epsilon(\sigma)}.\tag{2.17}$$

Actually, each summand in (2.17) $\prod_\sigma \nu(g_*, g_1, \ldots, g_{d+1})^{\epsilon(\sigma)}$ is independent of the choice of g_*, since

$$\left(\prod_\sigma \nu(g_*, g_1, \ldots, g_{d+1})^{\epsilon(\sigma)}\right) \cdot \left(\prod_\sigma \nu(g'_*, g_1, \ldots, g_{d+1})^{\epsilon(\sigma)}\right)^{-1} = Z^{\text{matter}}_{(d+1)\text{d}}[S^{d+1}] = 1, \tag{2.18}$$

where S^{d+1} is given by attaching two D^{d+1}s along $S^d = \partial D^{d+1}$, and the partition function on S^{d+1} is evaluated as the product of Boltzmann weight in each D^{d+1}. Thus, (2.17) becomes

$$\Psi(\{g_i\}_{i\in S^d}) = \prod_\sigma \nu(1, g_1, \ldots, g_{d+1})^{\epsilon(\sigma)}, \tag{2.19}$$

or equivalently,

$$|\Psi\rangle = \sum_{\{g_i\}, i\in S^d} \prod_\sigma \nu(1, g_1, \ldots, g_{d+1})^{\epsilon(\sigma)} |\{g_i\}\rangle . \tag{2.20}$$

up to normalization factor. We can explicitly construct the commuting projector Hamiltonian whose ground state is given by (2.20). To do this, we note that $|\Psi\rangle$ is transformed by a unitary operator $U(\nu)$ from a product state

$$|\Psi\rangle = U(\nu) \sum_{\{g_i\}, i\in S^d} |\{g_i\}\rangle = U(\nu) \cdot \left(\bigotimes_{i\in S^d} \sum_{g_i \in G} |g_i\rangle \right), \tag{2.21}$$

where

$$U(\nu) = \sum_{\{g_i\}, i\in S^d} \prod_\sigma \nu(1, g_1, \ldots, g_{d+1})^{\epsilon(\sigma)} |\{g_i\}\rangle \langle\{g_i\}| . \tag{2.22}$$

Then, the Hamiltonian is given by

$$H(\nu) = U(\nu) H_0 U(\nu)^{-1}, \tag{2.23}$$

where H_0 is a Hamiltonian whose ground state is written as $\bigotimes_{i\in S^d} \sum_{g_i\in G} |g_i\rangle$,

$$H_0 = -\sum_{i\in S^d} P_i, \quad P = \frac{1}{|G|} \sum_{g,h\in G} |g\rangle \langle h| . \tag{2.24}$$

At hindsight, the Haldane chain we have introduced in (2.1) is the nontrivial SPT Hamiltonian written in the form of (2.23) $H_{\text{Haldane}} = U(\nu) H_0 U(\nu)^{-1}$, where

$$H_0 = \sum_i X_i + X_{i+1/2} \tag{2.25}$$

is a projector onto a trivial product state $\bigotimes (|0\rangle + |1\rangle)$, and

$$U(\nu) = \prod_i CZ_{i,i+1/2} CZ_{i+1/2,i+1}, \tag{2.26}$$

where $CZ_{i,j} := \mathrm{i}^{(1-Z_i)(1-Z_j)/2}$. The phase shift of CZ_{ij} on a state $|g_i, g_j\rangle$ corresponds to a 2-cocycle $\nu(0, g_i, g_j)$ in $\mathcal{Z}^2(\mathbb{Z}_2^a \times \mathbb{Z}_2^b, U(1))$ represented by

$$\nu(0,0,0) = \nu(0,0,1) = \nu(0,1,0) = 1, \quad \nu(0,1,1) = -1, \tag{2.27}$$

or equivalently $\omega = \exp(\mathrm{i}\pi \cdot a \cup b)$, where a (resp. b) is background $\mathbb{Z}_2^a$ (resp. $\mathbb{Z}_2^b$) gauge field.

2.2.1 boundary of $(d+1)$d SPT phases

For later convenience, let us refer to how global symmetry acts on boundaries of $(d+1)$d SPT phases labeled by elements of $\mathcal{H}^{d+1}(G, U(1))$. To do this, we simply locate the SPT ground state (2.20) on a space M^d with boundaries,

$$|\Psi\rangle = \sum_{\{g_i\}, i \in M^d} \prod_{\sigma} \nu(1, g_1, \ldots, g_{d+1})^{\epsilon(\sigma)} |\{g_i\}\rangle \,. \tag{2.28}$$

In the presence of boundaries, the wave function on the bulk is generally no longer invariant under global symmetry $U_0(g) : \{g_i\} \mapsto \{gg_i\}$, reflecting the anomalous nature of boundaries. The symmetry action on $|\Psi\rangle$ becomes

$$\begin{aligned} U_0(g) |\Psi\rangle &= \sum_{\{g_i\}, i \in M^d} \prod_{\sigma} \nu(1, gg_1, \ldots, gg_{d+1})^{\epsilon(\sigma)} |\{gg_i\}\rangle \\ &= \sum_{\{g_i\}, i \in M^d} \prod_{\sigma} \nu(g^{-1}, g_1, \ldots, g_{d+1})^{\epsilon(\sigma)} |\{g_i\}\rangle \end{aligned} \tag{2.29}$$

Thus, the variation of wave function under symmetry action is evaluated as

$$\begin{aligned} \frac{[U_0(g)\Psi](g_1, \ldots, g_{d+1})}{\Psi(g_1, \ldots, g_{d+1})} &= \prod_{\sigma} \frac{\nu(g^{-1}, g_1, \ldots, g_{d+1})^{\epsilon(\sigma)}}{\nu(1, g_1, \ldots, g_{d+1})^{\epsilon(\sigma)}} \\ &=: \prod_{\sigma} f_d(g_1, \ldots, g_{d+1})^{\epsilon(\sigma)}, \end{aligned} \tag{2.30}$$

where we defined a d-cochain f_d defined on M^d as

$$f_d(g_1, \ldots, g_{d+1}) := \frac{\nu(g^{-1}, g_1, \ldots, g_{d+1})}{\nu(1, g_1, \ldots, g_{d+1})}. \tag{2.31}$$

In the expression of (2.30), $(d+1)$-simplex σ is taken as $(*, 1, \ldots, d)$, where $1, \ldots, d$ are 0-simplices contained in M^d. If we assign ordering on 0-simplices such that $*$ is labeled by the smallest number, the orientation $\epsilon(\sigma)$ of σ coincides with that of d-simplices $(1, \ldots, d)$ on M^d. Therefore,

$$\frac{[U_0(g)\Psi](g_1, \ldots, g_{d+1})}{\Psi(g_1, \ldots, g_{d+1})} = \prod_{\sigma \in M^d} f_d(g_1, \ldots, g_{d+1})^{\epsilon(\sigma)}, \tag{2.32}$$

where the product runs over d-simplices of M^d. Actually, f_d is a d-coboundary; $f_d = \mathrm{d}f_{d-1}$, since

$$\begin{aligned} f_d(g_1, \ldots, g_{d+1}) &= \frac{\nu(g^{-1}, g_1, \ldots, g_{d+1})}{\nu(1, g_1, \ldots, g_{d+1})} \\ &= \nu(g^{-1}, 1, g_2, \ldots g_{d+1}) \nu(g^{-1}, 1, g_1, g_3, \ldots g_{d+1})^{-1} \ldots \nu(g^{-1}, 1, g_1, \ldots g_d)^{(-1)^d} \\ &=: \mathrm{d}f_{d-1}(g_1, \ldots g_{d+1}), \end{aligned} \tag{2.33}$$

where we used cocycle condition of ν in the second line, and defined $(d-1)$-cochain f_{d-1} as

$$f_{d-1}(g_1, \ldots, g_d) = \nu(g^{-1}, 1, g_1, \ldots, g_d). \tag{2.34}$$

Thus, the shift of wave function (2.32) under symmetry action reduces to boundary variation supported on ∂M^d,

$$\frac{[U_0(g)\Psi](g_1,\ldots,g_{d+1})}{\Psi(g_1,\ldots,g_{d+1})} = \prod_{\sigma\in\partial M^d} f_{d-1}(g_1,\ldots,g_d)^{\epsilon(\sigma)}. \tag{2.35}$$

Thus, the system with the boundary is invariant under the modified symmetry transformation

$$U(g) := U_0(g)\cdot V^{-1}_{\{g_i\}}, \tag{2.36}$$

where $V_{\{g_i\}}$ represents boundary variation,

$$V_{\{g_i\}} = \prod_{\sigma\in\partial M^d} \nu(g^{-1},1,g_1,\ldots,g_d)^{\epsilon(\sigma)}. \tag{2.37}$$

Importantly, in (2.37) the symmetry action is realized in non-onsite fashion on boundaries, as the factor $\nu(g^{-1},1,g_1,\ldots,g_d)$ covers d sites.

2.3 CZX model: $\mathbb{Z}_2$ SPT in (2+1)d

Here we provide an example of sophisticated lattice model realizing nontrivial bosonic $\mathbb{Z}_2$ SPT phase in (2+1) dimension, which is extensively referred in later discussions [9]. This model corresponds to the generator of $\mathcal{H}^3(\mathbb{Z}_2,U(1))\cong\mathbb{Z}_2$. We demonstrate anomalous symmetry action (2.37) in the model. The CZX model is a (2+1) dimensional system of qubits on a square lattice, where each site contains four qubits, as shown in Fig.2.5.

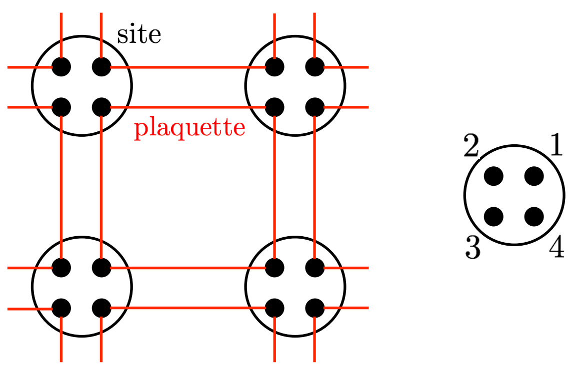

Figure 2.5: CZX model on a square lattice. The site of square lattice is represented as a big circle. Each site contains four qubits (black dots). We assign a counterclockwise numbering on four qubits contained in a single site. Plaquettes are represented as red squares.

The generator of onsite $\mathbb{Z}_2$ symmetry U_{CZX} is given by the product of onsite operators $X_s(CZ)_s$ for all sites,

$$U_{CZX} = \prod_{s\in\text{site}} X_s(CZ)_s, \tag{2.38}$$

where $X_s = X_1X_2X_3X_4$, $(CZ)_s = CZ_{12}CZ_{23}CZ_{34}CZ_{41}$. The numbering of four qubits in a single site is illustrated in Fig.2.5. Since X_s and $(CZ)_s$ commute with each other and square to 1, it follows that U_{CZX} is indeed a generator of onsite $\mathbb{Z}_2$ symmetry; $(X_s(CZ)_s)^2 = 1$. The ground state $|\Psi\rangle$ is given by tensor product of entangled states on plaquettes,

$$|\Psi\rangle = \bigotimes_{p\in\text{plaquette}} |\Psi_p\rangle = \bigotimes_{p\in\text{plaquette}} \frac{1}{\sqrt{2}}(|0000\rangle + |1111\rangle), \tag{2.39}$$

where the entangled state $(|0000\rangle+|1111\rangle)/\sqrt{2}$ on each plaquette is defined for four qubits on vertices of a plaquette, which is illustrated in Fig.2.5. The ground state $|\Psi\rangle$ respects the $\mathbb{Z}_2$ symmetry (2.38). [2] The ground state is expressed in the form of product of locally entangled states, but the state turns out to reside in nontrivial SPT phase, thanks to the mismatch between entanglement structure and lattice structure.

Next, let us write down the Hamiltonian which respects the symmetry (2.38), with its ground state $|\Psi\rangle$. Naively we expect that the sum of projectors onto $(|0000\rangle + |1111\rangle)$ for each plaquette works as Hamiltonian,

$$H = -\sum_{p\in\text{plaquette}} (|1111\rangle\langle 0000| + |0000\rangle\langle 1111|), \tag{2.40}$$

since its ground state becomes $|\Psi\rangle$. However, this Hamiltonian does not respect the symmetry (2.38) due to noncommutativity between $\prod_s CZ_s$. To make it commute with $\mathbb{Z}_2$ generator, we define the Hamiltonian as

$$H_{CZX} = -\sum_{p\in\text{plaquette}} (|1111\rangle\langle 0000| + |0000\rangle\langle 1111|) \otimes_\alpha P_p^\alpha, \tag{2.41}$$

where P_p^α $(\alpha = u, d, l, r)$ acts on the two spins in the up, down, left, right neighboring half-plaquette respectively (see Fig.2.6), as a projector onto states in which two spins of a half-plaquette are equal; $P_p^\alpha = |00\rangle\langle 00| + |11\rangle\langle 11|$. Then, the Hamiltonian is commutative with $\mathbb{Z}_2$ generator; $[H_{CZX}, U_{CZX}] = 0$.

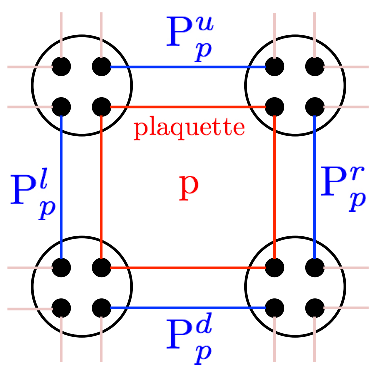

Figure 2.6: Projectors P_p^α $(\alpha = u, d, l, r)$ are defined for two spins in the half-plaquettes (blue lines) neighboring the plaquette p.

Now we examine the boundary of the CZX model. We do this by simply cutting the lattice to make a boundary. Plaquettes on the cut is devided into two half-plaquettes, while the site is not

[2]Since $|\Psi\rangle$ is manifestly left invariant under $\prod_s X_s$, the nontrivial part of seeing this is invariance of $|\Psi\rangle$ under $\prod_s CZ_s$ operator. For each adjacent pair of two plaquettes, we see that $\prod_s CZ_s$ contains two CZ operators connecting the pair of plaquettes. These two CZ operators always pick up identical phase shift ± 1 when operated on each summand of $|\Psi\rangle$, hence the product of these two CZ operators are 1. Since $\prod_s CZ_s$ is written as the product of such pair of CZ operators connecting adjacent two plaquettes, we see that $\prod_s CZ_s |\Psi\rangle = |\Psi\rangle$.

devided by the cut, respecting the lattice structure (see Fig. 2.7). Let us see how the symmetry acts on the boundary. Since the neighboring qubits in a single half-plaquette are fully entangled due to the projector $\{P_p^\alpha\}$, two qubits sharing a half-plaquette effectively behave as a single qubit. Then, the $(CZ)_s$ operator on a site acts as a CZ operator covering two effective spins. Hence, the symmetry generator U_{CZX} operates on the boundary degree of freedom in non-onsite fashion as we indicated in (2.36),

$$U_{\mathbb{Z}_2} = \prod_j X_j CZ_{j,j+1}, \tag{2.42}$$

where j labels the position of qubits on a boundary.

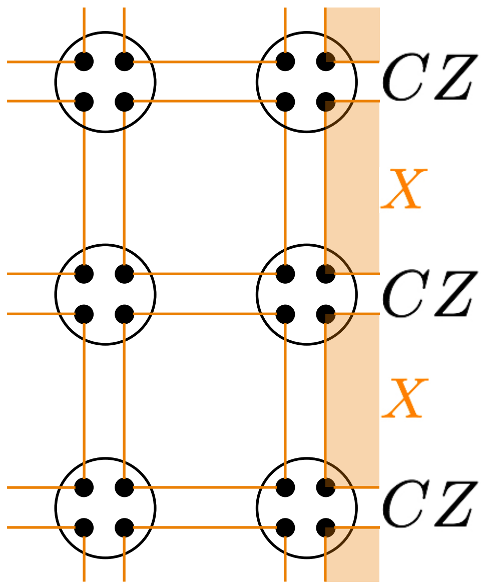

Figure 2.7: Boundary on the CZX model. Projectors P_p^α on boundary dangles each pair of spins sharing a half-plaquette, effectively making the pair a single qubit.

In our Hamiltonian, we remark that all configuration of composite qubits on the boundary are degenerate (i.e., the effective Hamiltonian on the boundary is zero). In Ref. [10], it is proven that the boundary is gapless even after adding perturbations on the boundary, if $\mathbb{Z}_2$ symmetry is not broken on the boundary.

Finally, let us briefly mention recent development about the boundary of CZX model. In Ref. [10], it was revealed that the CZX model can have a *gapped boundary* without nontrivial degeneracy at the ground state, if we choose the boundary of the CZX model such that the boundary cuts a site into two half-circles, instead of cutting plaquettes. Namely, the spectral properties of the boundary generally depend on how we realize boundaries on the model. [3]

[3] Generally, gapped boundary for G-SPT phases are realized by "symmetry extension" mechanism. Roughly speaking, symmetry extension is a procedure of lifting (pulling back) the SPT phase characterized by $[\omega] \in \mathcal{H}^n(G, U(1))$ to a cocycle of larger group $G \subset H$, $[\omega] \in \mathcal{H}^n(H, U(1))$, via the exact sequence $1 \to K \to H \to G \to 1$. Here, if $[\omega]$ becomes a *trivial* cocycle in $\mathcal{H}^n(H, U(1))$ (it is possible even if $[\omega]$ is nontrivial in $\mathcal{H}^n(G, U(1))$), we have a trivial H-SPT phase after symmetry extension. Thus, we can have a H-symmetric gapped domain wall which connects between a G-SPT phase characterized by $[\omega]$ and a trivial product state. For example, gapped boundary of CZX model is constructed via symmetry extension $1 \to \mathbb{Z}_2 \to \mathbb{Z}_4 \to \mathbb{Z}_2 \to 1$. Accordingly, the gapped boundary effectively possess $H = \mathbb{Z}_4$ symmetry, where $K = \mathbb{Z}_2 \subset H$ acts nontrivially only on boundaries. See Ref. [10] for detail.

2.4 Cobordism and generator manifolds

In this section, we briefly review the relationship between cobordism theory and SPT phases. As we introduced in Section 2.1, SPT phases are described by unitary invertible topological field theories, in the low energy (long distance) limit. Invertible topological field theories are a class of topological QFT with one dimensional Hilbert space on any closed spatial manifolds. The classification of SPT phase is determined by the equivalence class of theories under deformation of continuous parameters, which is equivalent to the isomorphism class of invertible topological phases up to the equivalence relation under continuous deformation.

As an input of the theory, let (M, η, A) be a triple of a closed $(d+1)$d manifold M, a structure η (e.g., Spin, $\mathrm{Pin}_{\pm}, \dots$) on M, and background G-gauge field A. Here, we recall that the G-gauge field can be regarded as a map $A : M \mapsto BG$, where BG is a classifying space of G. When the theory has no symmetry $G = \mathrm{id}$, we simply put a single point as a classifying space, $BG = pt$. In general, for a topological space X, a degree-d η-bordism (M, η, f) to X is defined as a closed d-manifold M with structure η, together with a continuous map $f : M \mapsto X$. Hence, we can see that the G-gauge field $A : M \mapsto BG$ provides a degree-d η-bordism to BG.

Then, partition function $\mathcal{Z}$ of an invertible topological phase defines a map from a degree-d η-bordism specified by (M, η, A), to $U(1)$ (see Corollary 3.5. of Ref. [11]). Actually, it is known [11, 12] that the partition function $\mathcal{Z}$ becomes a function of a certain equivalence class of bordisms called the η bordism group; two η-bordisms on X are equivalent $(M_1, \eta_1, f_1) \sim (M_2, \eta_2, f_2)$ if there exists a $(d+1)$-dimensional η-manifold with boundary $\partial N = M_1 \sqcup \overline{M}_2$ and a map $g : N \mapsto X$ that reduces to $(M_1, \eta_1), (M_2, \eta_2)$ on the two components of ∂N. We can define an Abelian group structure on the equivalence class of bordisms defined above, which we call the η bordism group denoted as $\Omega^{\eta}_{d+1}(X)$. Here, the group multiplication is defined via disjoint union of d-manifolds (M_1, η_1) and (M_2, η_2), and the inverse element of (M, η, f) is defined via orientation reversing of M.

The partition function of invertible topological phase gives a map from η-bordism group $\Omega^{\eta}_{d+1}(BG)$ to $U(1)$; $\mathcal{Z} \in \mathrm{Hom}(\Omega^{\eta}_{d+1}(BG), U(1))$. Further, it is known that the value of the partition function determines the isomorphism class of invertible topological field theories in the following sense;

there is a 1-1 correspondence between the following sets,

- *the set of isomorphism classes of $d+1$-dimensional unitary invertible topological field theories with structure η, and*
- *the cobordism group* $\mathrm{Hom}(\Omega^{\eta}_{d+1}(BG), U(1))$,

where two sets are related by giving partition function of the theory $\mathcal{Z} \in \mathrm{Hom}(\Omega^{\eta}_{d+1}(BG), U(1))$.

Now let us turn to the classification of SPT phases, which is captured by isomorphism class of invertible topological phases, up to the equivalence relation under continuous deformation.

When the bordism group $\Omega^{\eta}_{d+1}(BG)$ contains a free part, then the corresponding cobordism group $\mathrm{Hom}(\Omega^{\eta}_{d+1}(BG), U(1))$ has continuous a $U(1)$ part. Physically, this means that we have a continuous parameter in the SPT phase which can be varied continuously without closing gap. For example, let us consider a (3+1)d oriented bordism group equipped with $U(1)$ background gauge field $\Omega^{SO}_4(BU(1)) = \mathbb{Z}^2$. In this case, one of the free parts corresponds to the theta term labeled by $\theta \in \mathbb{R}/2\pi\mathbb{Z}$,

$$\mathcal{Z}[A] = \exp\left[\mathrm{i}\theta \int_M \frac{F}{2\pi} \wedge \frac{F}{2\pi}\right]. \tag{2.43}$$

Therefore, we should regard two theories which differs by the theta term as an identical SPT phase. Thus, the classification of SPT phase is given by the torsion part of the η bordism group $\mathrm{Tor}\Omega^{\eta}_{d+1}(X)$.

Chapter 3

Gapped boundary of SPT phase protected by spacetime symmetry

In this section, we discuss boundary states of SPT phases protected by spacetime symmetry; e.g. reflection, time reversal and point-group symmetry. Such SPT phases can also host gapped boundaries.

3.1 R anomaly in (2+1)d topological order

To see this, let us begin with the case of (3+1)d bosonic SPT phase protected by reflection symmetry R ($\mathsf{R}^2 = 1$) solely, which sends spatial coordinate $(x, y, z) \mapsto (-x, y, z)$ in 3d Euclidian space. One illustrative way to consider the reflection SPT is the "dimension reduction" approach [13–15] developed in Ref. [13], which argues that the (3+1)d reflection SPT phase is adiabatically connected to the trivial product state *except for the reflection plane* $x = 0$, by a sequence of symmetry respecting local unitary transformations. Following Ref. [13], let us consider a small region V in the 3d bulk away from reflection plane. Due to short-range entangled nature of SPT phase, [1] one can think of a local unitary transformation U_V supported on V, which brings the state of the Hilbert space $\mathcal{H}_V$ into a trivial product state. Acting $U_V U_{\mathsf{R}(V)}$ makes the state of $\mathcal{H}_V$ and $\mathcal{H}_{\mathsf{R}(V)}$ product states in symmetry respecting fashion, where $U_{\mathsf{R}(V)}$ is a reflection partner of U_V supported on $\mathsf{R}(V)$. Then, by operating a sequence of local unitaries in the form of $U_V U_{\mathsf{R}(V)}$, we can connect the SPT phase into a product state by reflection symmetric unitary circuits, except for the vicinity of the reflection plane. Therefore, we expect that anomalous nature of the boundary state of reflection SPT phase is totally encoded in what happens in the reflection plane. The vicinity of the reflection plane is effectively a (1+1)d system, where reflection symmetry R acts as *onsite* symmetry.

Thus, by the dimension reduction procedure the anomaly of (2+1)d boundary of reflection SPT comes down to the (1+1)d boundary of (2+1)d SPT protected by onsite $\mathbb{Z}_2$ symmetry. We can think of the situation after the dimension reduction procedure as a "T-junction", which is described in Fig.3.1.

Now we are ready to construct a possible gapped boundary of (3+1)d reflection SPT phase [16–18]. We demonstrate that the surface state can be gapped with $\mathbb{Z}_2$ topological order ($\mathbb{Z}_2$ gauge theory, or toric code). Let us consider a (2+1)d system of qubits on a square lattice, where each edge contains one qubit. Following the dimension reduction approach, the anomalous surface state is

[1] It is believed that the ground state of SPT phase can be smoothly deformed into a trivial product state of local degrees of freedom, by a sequence of local unitary operators. Gapped states with such property are called short-range entangled states.

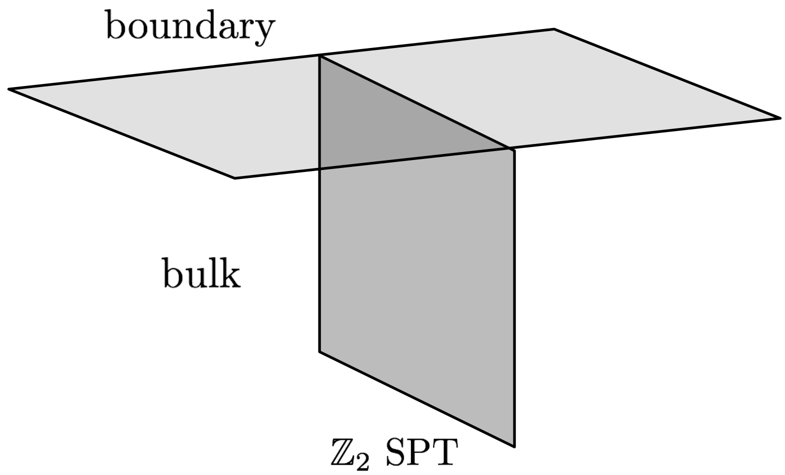

Figure 3.1: After dimension reduction, the geometry looks like a T-junction, where a surface theory is connected to a $\mathbb{Z}_2$ SPT phase by a junction at the reflection line.

realized by simply locating a boundary of (2+1)d CZX model (see Sec.2.3) with onsite $\mathbb{Z}_2$ symmetry on a reflection line $x = 0$. We consider reflection symmetry on a square lattice such that the reflection line intersects with edges, see Fig. We recall that $\mathbb{Z}_2$ symmetry is encoded in anomalous way at the (1+1)d boundary of the CZX model (2.42); $U_{\mathbb{Z}_2} = \prod_i X_i CZ_{i,i+1}$. Thus, the action of reflection symmetry on qubits on the surface is realized as

$$\mathsf{R} : X_j \mapsto Z_{j-1} X_j Z_{j+1}, \quad Y_j \mapsto -Z_{j-1} Y_j Z_{j+1}, \quad Z_j \mapsto -Z_j \qquad \text{at } x = 0, \tag{3.1}$$

and $X_{x,y} \mapsto X_{x,-y}$ (resp. Y, Z) otherwise. Next, we move to construct the Hamiltonian. The conventional lattice Hamiltonian for toric code on a square lattice is defined as

$$H = -\sum_s A_s - \sum_p B_p, \tag{3.2}$$

where $A_s := \prod_{s\in\partial i} X_i$ is the product of four X operators at edges touching a vertex s, and $B_p := \prod_{i\in\partial p} Z_i$ is the product of four Z operators at edges rounding a plaquette p. If we identify X as electric field and Z as gauge field which defines parallel transport, enforcing $A_s = 1$ is regarded as Gauss law constraint, allowing us to identify the system as $\mathbb{Z}_2$ gauge theory. Although the model (3.2) manifestly does not respect the reflection symmetry (3.1), one can construct the symmetric commuting projector model, just by slightly deforming local Hamiltonians touching the reflection line. Let us modify the local Hamiltonian A_s adjacent to the reflection line as

$$\begin{cases} A_s = \left[\prod'_{s\in\partial i} X_i\right] Y_{s-\vec{y}/2} Z_{s+\vec{x}/2-\vec{y}}, & s_x = -1/2 \\ A_s = -\left[\prod'_{s\in\partial i} X_i\right] Y_{s-\vec{y}/2} Z_{s-\vec{x}/2+\vec{y}}, & s_x = 1/2 \end{cases} \tag{3.3}$$

where $\left[\prod'_{s\in\partial i} X_i\right]$ stands for product of X at edges touching a vertex s, except for the edge below s. We illustrate the redefined operators in Fig.3.2 (a). We can immediately see that the above modification provides a commuting projector model which respects the reflection symmetry (3.1). The ground state satisfies $A_s = B_p = 1$ everywhere.

With or without modifications, the Hamiltonian (3.2) hosts quasiparticle excitations with anyonic statistics labeled as $1, e, m, \psi$ respectively. 1 stands for a trivial excitation (i.e., nothing). e is an electric particle which violates the Gauss law constraint; we say that e is at a vertex s if $A_s = -1$.

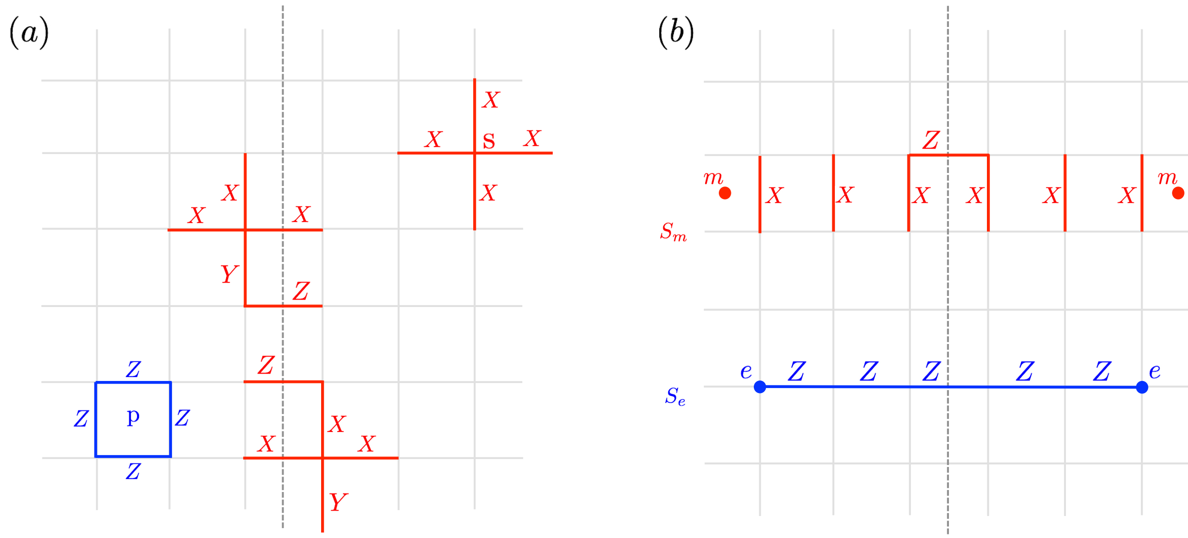

Figure 3.2: (a) Toric code on a square lattice. Qubits on the reflection line (gray dotted line) transforms in anomalous way (3.1) under reflection symmetry. To respect symmetry, A_s operators (red operators) touching the reflection line are modified. B_s operators (blue operators) need not be modified. (b) Open string operators S_m, S_e which create quasiparticles at two ends of strings. When a string operator intersects the reflection line, there exists a Z operator at the intersection which is mapped $Z \mapsto -Z$ by reflection. Hence, we have $\mathsf{R} : S_e \mapsto -S_e, S_m \mapsto -S_m$.

Respectively, m is a magnetic vortex characterized as $B_p = -1$; if e goes around a vortex m, the wave function picks up Aharonov-Bohm phase (holonomy) -1. Finally, ψ is given by fusing e and m together; ψ becomes a fermion due to nontrivial mutual statistics between e and m, though both e and m are bosons. Since the effective theory on the surface is specified by giving the data of quasiparticles on the surface controlled by unitary braided fusion category (UBFC), we expect that anomalous nature can be expressed as the data of UBFC.

Thus, let us take a look at how the reflection symmetry acts on quasiparticle excitations. Quasiparticles e (resp. m) are created by acting an open string operator S_e (resp. S_m) on the ground state (see Fig.3.2 (b)).

By locating quasiparticle excitations in reflection symmetric fashion, we can discuss the eigenvalue of reflection symmetry for the excited states. We denote η_p as the eigenvalue of R on the state $|p, \mathsf{R}(p)\rangle$ where an anyon p and its reflection partner $\mathsf{R}(p)$ are located in reflection symmetric way, $\mathsf{R}\,|p, \mathsf{R}(p)\rangle = \eta_p\,|p, \mathsf{R}(p)\rangle$. (In our case reflection symmetry does not change the label of anyons, $\mathsf{R}(e) = e$ and $\mathsf{R}(m) = m$, but labels could be permuted in general.) When we have non-anomalous reflection symmetry we manifestly have $\eta_e = \eta_m = 1$. However, in the case of anomalous symmetry realization (3.1), we have $\eta_e = \eta_m = -1$, since string operators act nontrivially under reflection symmetry for the modified Hamiltonian

$$\mathsf{R} : \qquad S_e \mapsto U_{\mathbb{Z}_2} S_e U_{\mathbb{Z}_2} = -S_e, \qquad S_m \mapsto U_{\mathbb{Z}_2} S_m U_{\mathbb{Z}_2} = -S_m, \tag{3.4}$$

when the configuration of string operators are taken reflection symmetric (see Fig.3.2 (b)). According to fusion rule $\psi = e \times m$, η_ψ is automatically determined to be 1 by $\eta_\psi = \eta_e \eta_m$.

We have observed that the symmetry property of anyons $\eta_e = -1, \eta_m = -1$ occurs at the boundary of (3+1)d SPT phase protected by reflection symmetry. There are four choices of symmetry properties η when R does not permute anyons since we have $\eta_p^2 = 1$ due to $\mathsf{R}^2 = 1$, which is summarized in Table 3.1. Among them, we expect that the $eMmM$ fractionalization pattern $\eta_e =$

SET	η_e	η_m	η_ψ
$e1m1$	1	1	1
$e1mM$	1	-1	-1
$eMm1$	-1	1	-1
$eMmM$	-1	-1	1

Table 3.1: Pattern of the action of reflection symmetry on anyons. The case of $\eta_e = \eta_m = -1$ ($eMmM$) becomes anomalous, which is realized on the surface of (3+1)d SPT.

$\eta_m = -1$ becomes anomalous, which cannot be realized by a standalone (2+1)d system. Actually, it is known that the R anomaly in (2+1)d bosonic gapped boundary is detected by the $\mathbb{Z}_2$-valued quantity called "anomaly indicator" [16],

$$\exp\left(\frac{2\pi \mathrm{i}\nu}{2}\right) = \frac{1}{\mathcal{D}} \sum_{\bar{p}=\mathsf{R}(p)} d_p \eta_p e^{i\theta_p}, \tag{3.5}$$

where d_p is quantum dimension of p, $\mathcal{D}$ is total dimension characterized by $\mathcal{D}^2 := \sum_p d_p^2$, and θ_p is $\mathbb{R}/2\pi\mathbb{Z}$-valued topological spin of p. Summation runs over particles such that $\bar{p} = \mathsf{R}(p)$, since a reflection symmetric state $|p, \mathsf{R}(p)\rangle$ exists only when p and $\mathsf{R}(p)$ can fuse into vacuum. Anomaly indicator is calculated by input of topological data and symmetry action on quasiparticles of surface theory, and we have $\nu = 1 \bmod 2$ in $eMmM$ fractionalization pattern implying R anomaly, while $\nu = 0$ otherwise. Let us derive the expression of anomaly indicator (3.5), following Ref. [3].

(3+1)d SPT phase protected by reflection symmetry is argued to have $\mathbb{Z}_2 \times \mathbb{Z}_2$ classification corresponding to unoriented bordism in (3+1)d, $\Omega_4^O(pt) = \mathbb{Z}_2 \times \mathbb{Z}_2$. [2] This bordism group is generated by two manifolds, $\mathbb{RP}^4$ and $\mathbb{CP}^2$. Thus, anomaly on (2+1)d is detected by partition function of bulk SPT on generator manifolds; $\mathcal{Z}(\mathbb{RP}^4) = \pm 1$, $\mathcal{Z}(\mathbb{CP}^2) = \pm 1$. Given input data of surface theory, these partition functions are calculated as

$$\mathcal{Z}(\mathbb{RP}^4) = \frac{1}{\mathcal{D}} \sum_{\bar{p}=\mathsf{R}(p)} d_p \eta_p e^{i\theta_p}, \tag{3.6}$$

$$\mathcal{Z}(\mathbb{CP}^2) = \frac{1}{\mathcal{D}} \sum_{p} d_p^2 e^{i\theta_p} = e^{\frac{2\pi \mathrm{i}}{8} c_-}, \tag{3.7}$$

where c_- is chiral central charge of the surface theory. In this thesis, we will be focusing on the case of $\mathbb{RP}^4$, which corresponds to anomaly indicator (3.5) introduced in the previous section. The calculation of $\mathcal{Z}(\mathbb{CP}^2)$ is performed by basically the same method, see Ref. [3] for detail.

3.1.1 Evaluation of bulk partition function

We compute the partition function on a 4d or 5d manifold of rather complicated shape (such as $\mathbb{RP}^4$ or the lens space), by decomposing the manifold into simpler manifolds which are easier to evaluate, and computing the partition function part by part. This procedure is performed via applying the gluing relation for the path integral. Here, let us review some axiomatic properties of path integral for topological field theories, which is required for explicit computations, following Ref. [3, 19].

To consider the path integral on $(D+1)$d manifold M^{D+1}, we first specify the configuration of fields on boundary $c \in \mathcal{C}(\partial M^{D+1})$, where $\mathcal{C}(\partial M^{D+1})$ denotes a set of boundary conditions. For

[2] To be precise, the classification of $(d+1)$d SPT is given by Anderson dual of unoriented bordism $(D\Omega_O)^{d+1} := \mathrm{Tor}\Omega_{d+1,O} + \mathrm{Free}\Omega_{d+2,O}$. In our case, we have trivial free part since $\Omega_{5,O}(pt) = \mathbb{Z}_2$.

example, in the case of $D = 3$ Turaev-Viro topological field theories which encodes UBFC data of 3d topological phases, $\mathcal{C}(M^D)$ stands for the set of all configurations of anyon diagrams on M^D. If M^D has boundary, we denote $\mathcal{C}(M^D; c)$ as the configuration space of anyon diagrams on M^D, under the boundary condition c on ∂M^D.

Then, we define the Hilbert space $\mathcal{V}(M^D; c)$ as the configuration space modded out by equivalence relations (e.g., F and R moves in $D = 3$ UBFC),

$$\mathcal{V}(M^D; c) := \mathcal{C}(M^D; c)/\sim . \tag{3.8}$$

The path integral $\mathcal{Z}(M^{D+1})$ is a map from $\mathcal{V}(\partial M^{D+1})$ to a number,

$$\mathcal{Z}(M^{D+1}): \quad \mathcal{V}(\partial M^{D+1}) \mapsto \mathbb{C}. \tag{3.9}$$

We will write this as $\mathcal{Z}(M^{D+1})[c]$, for $c \in \mathcal{V}(\partial M^{D+1})$. The inner product in $\mathcal{V}(M^D; c)$ is defined via bulk partition function as

$$\langle x|y\rangle_{\mathcal{V}(M^D;c)} := \mathcal{Z}(M^D \times I)[\overline{x} \cup y], \tag{3.10}$$

where $M^D \times I$ is a D+1-manifold pinched at $\partial M^D \times I$ by identification $(b, s) \sim (b, t)$ for $b \in \partial M^D$ and $s, t \in I$, so that $\partial(M^D \times I) = M \cup -M$. $\overline{x}$, y specify boundary conditions on $-M$, M respectively, where $\overline{x}$ denotes the field configuration on $-M$ given by reversing orientation of x. Finally, we describe gluing relations for $D + 1$-manifolds. Let M^{D+1} be a $D + 1$-manifold whose boundary is $\partial M^{D+1} = M^D \cup -M^D \cup W$, and M^{D+1}_{gl} be a $D+1$-manifold which is given by gluing the boundary of M^{D+1} along M^D and $-M^D$. Then, the partition function $\mathcal{Z}(M^{D+1}_{\mathrm{gl}})[c]$ on M^{D+1}_{gl} with boundary condition $c \in \mathcal{V}(W)$ on $W = \partial M^{D+1}_{\mathrm{gl}}$ is evaluated via the following gluing relation,

$$\mathcal{Z}(M^{D+1}_{\mathrm{gl}})[c] = \sum_{e_i} \frac{\mathcal{Z}(M^{D+1})[c_{\mathrm{cut}} \cup e_i \cup \overline{e}_i]}{\langle e_i|e_i\rangle_{\mathcal{V}(M^D;c^{D-1}_{\mathrm{cut}})}}, \tag{3.11}$$

where c_{cut} is boundary condition inherited from c after the cut, and $c^{D-1}_{\mathrm{cut}})$ is restriction of c_{cut} to ∂M^D. $\{e_i\}$ is an orthonormal basis of $\mathcal{V}(M^D; c^{D-1}_{\mathrm{cut}})$. We illustrate the gluing relation in Fig.3.3.

3.1.2 $\mathcal{Z}(\mathbb{RP}^4)$: (2+1)d R anomaly

Let us turn to explicit computation of $\mathcal{Z}(\mathbb{RP}^4)$. We can compute the partition function on $\mathbb{RP}^4$ via gluing relations, by decomposing $\mathbb{RP}^4$ into simpler manifolds which are easier to evaluate. To do this, we employ handle decomposition on $\mathbb{RP}^4$, which takes $\mathbb{RP}^4$ apart into 4-balls.

For $1 \le k \le d$, k-handle in d dimension is defined as a pair $(D^k \times D^{d-k}, S^{k-1} \times D^{d-k})$. $S^{k-1} \times D^{d-k} \subset \partial(D^k \times D^{d-k})$ is called an attaching region of k-handle. 0-handle is defined as D^d. We think of attaching k-handle to d-manifold M_0 with boundary, by an embedding of attaching region $\phi : S^{k-1} \times D^{d-k} \mapsto \partial M_0$ such that the image of ϕ is contained in ∂M_0. It is known that every compact d-manifold M without boundary allows handle decomposition, i.e., M is developed from a 0-handle by successively attaching to it handles of dimension d.

We can see that $\mathbb{RP}^4$ is decomposed into single k-handles for each $k = 0, 1, 2, 3, 4$ by the following steps.

1. To see this, it is convenient to think of $\mathbb{RP}^4$ as D^4 with its boundary $\partial D^4 = S^3$ identified by antipodal map. First, we begin with locating a small 0-handle containing the center of D^4.

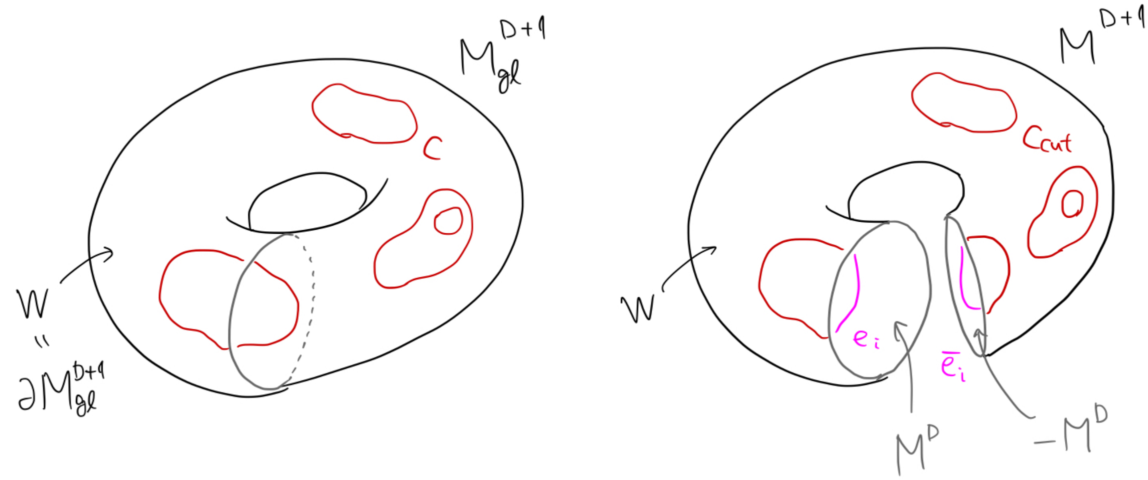

Figure 3.3: Illustration of gluing relation.

2. Next, we attach a 1-handle $(D^1 \times D^3, S^0 \times D^3)$ to the 0-handle. The attaching region of a 1-handle consists of two 3-balls, $S^0 \times D^3 = D^3 \cup D^3$. We attach one of these D^3s to the boundary S^3 of 0-handle, by identifying with a small D^3 in S^3. Then, we radially extend a 1-handle from the attached D^3, which tunnels through antipodal map and returns to 0-handle again. Eventually, we attach the other D^3 of 1-handle to 0-handle. We denote the composition of $0, 1, \dots k$ handle in $\mathbb{RP}^4$ as $\mathbb{RP}^4_k$. At this point, we have constructed $\mathbb{RP}^4_1$. See Fig.3.4 (2) in one dimensional lower case.

3. Then, we attach a 2-handle $(D^2 \times D^2, S^1 \times D^2)$ to $\mathbb{RP}^4_1$. We note that $\mathbb{RP}^4_1 = (D^3 \times S^1)/\sigma$, where σ is $\mathbb{Z}_2$ action on $D^3 \times S^1$ as composite of antipodal maps $\sigma : (x, \theta) \mapsto (-x, \theta + \pi)$, with $D^3 : |x| \le 1$ in $\mathbb{R}^3$ and $\theta \in \mathbb{R}/2\pi\mathbb{Z}$ is a coordinate in S^1. The attaching region $D^2 \times S^1$ is embedded in $\partial(\mathbb{RP}^4_1) = (S^2 \times S^1)/\sigma$, via embedding a small D^2 in S^2.

4. Likewise, we attach a 3-handle $(D^3 \times D^1, S^2 \times D^1)$ to $\mathbb{RP}^4_2 = (D^2 \times S^2)/\sigma$ by embedding the attaching region in $\partial(\mathbb{RP}^4_2) = (S^1 \times S^2)/\sigma$, [3] via embedding a small D^1 in S^1.

5. Finally, we complete $\mathbb{RP}^4$ with attaching a 4-handle (D^4, S^3) to $\mathbb{RP}^4_3 = (D^1 \times S^3)/\sigma$, by identifying the attaching region with $\partial(\mathbb{RP}^4_3) = (S^0 \times S^3)/\sigma = S^3$.

In general, $\mathbb{RP}^n$ is decomposed into single k-handles for each $k = 0, 1, \dots n$ in a similar way. Namely, we sequently attach $k+1$-handle $(D^{k+1} \times D^{d-k-1}, S^k \times D^{d-k-1})$ to $\mathbb{RP}^n_k = (D^{d-k} \times S^k)/\sigma$ to construct $\mathbb{RP}^n_{k+1}$, by embedding the attaching region $D^{d-k-1} \times S^k$ to $\partial(\mathbb{RP}^n_k) = (S^{d-k-1} \times S^k)/\sigma$, via embedding a small D^{d-k-1} in S^{d-k-1}. The handle decomposition for real projective space is shown in Fig.3.4, in the case of $\mathbb{RP}^3$.

Now we can compute $\mathcal{Z}(\mathbb{RP}^4)$ by successively applying gluing relations in each process of handle decomposition, assuming that the surface 3d topological phase is described by the data of UMTC. The computation is performed as follows.

[3] We note the abuse of notation; σ always denotes composite of antipodal maps in this context.

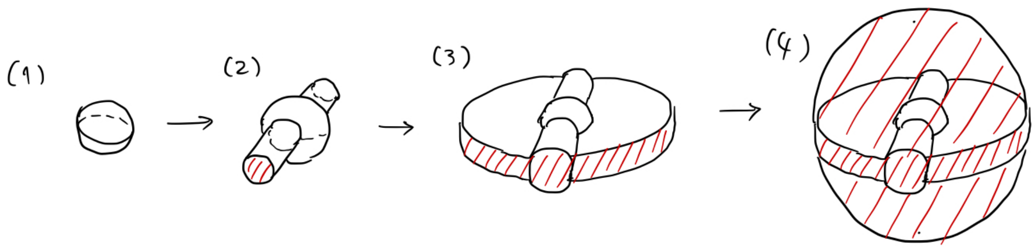

Figure 3.4: Developing $\mathbb{RP}^3$ by attaching handles sequently. (4) Finally, we can construct $\mathbb{RP}^3$, which is shown as D^3 with its boundary S^2 identified by antpiodal map. (In this picture, the red hatched area is identified with the opposite one by antipodal map.) (1) First, we put a 0-handle at the center of D^3. (2) We extend a 1-handle from a 0-handle, which tunnels through antipodal map and returns to 0-handle again. (3) We extend a 2-handle from $\mathbb{RP}^3_1$, whose attaching region is $D^1 \times S^1$. (4) We attach a 3-handle D^3 to $\mathbb{RP}^3_2$ along S^2, completing $\mathbb{RP}^3$.

1. First, we decompose $\mathbb{RP}^4$ into $\mathbb{RP}^4_3$ and a 4-handle, along the attaching region S^3. Since there is no nontrivial anyon diagram on S^3 up to equivalence relations, only empty diagram ϕ contributes to the boundary condition. Hence, the gluing relation becomes

$$\mathcal{Z}(\mathbb{RP}^4) = \frac{\mathcal{Z}(\mathbb{RP}^4_3)[\phi]\mathcal{Z}(D^4)[\phi]}{\langle\phi|\phi\rangle_{\mathcal{V}(S^3)}}. \tag{3.12}$$

In appendix C, we have $\mathcal{Z}(D^4)[\phi] = 1/\mathcal{D}$ and $\langle\phi|\phi\rangle_{\mathcal{V}(S^3)} = \mathcal{Z}(S^3 \times D^1)[\phi] = 1/\mathcal{D}^2$. Thus,

$$\mathcal{Z}(\mathbb{RP}^4) = \frac{\mathcal{Z}(\mathbb{RP}^4_3)[\phi] \cdot 1/\mathcal{D}}{1/\mathcal{D}^2} = \mathcal{D} \cdot \mathcal{Z}(\mathbb{RP}^4_3)[\phi]. \tag{3.13}$$

2. Next, we decompose $\mathbb{RP}^4_3$ into $\mathbb{RP}^4_2$ and a 3-handle, along the attaching region $S^2 \times D^1$. Similarly, only empty diagram ϕ contributes to the bounndary condition on the cut $S^2 \times D^1$. Gluing relation becomes

$$\mathcal{Z}(\mathbb{RP}^4_3)[\phi] = \frac{\mathcal{Z}(\mathbb{RP}^4_2)[\phi]\mathcal{Z}(D^4)[\phi]}{\langle\phi|\phi\rangle_{\mathcal{V}(S^2\times D^1;\phi)}}. \tag{3.14}$$

In appendix C, we have $\mathcal{Z}(D^4)[\phi] = 1/\mathcal{D}$ and $\langle\phi|\phi\rangle_{\mathcal{V}(S^2\times D^1;\phi)} = \mathcal{Z}(S^2 \times D^2)[\phi] = 1$. Thus,

$$\mathcal{Z}(\mathbb{RP}^4_3)[\phi] = 1/\mathcal{D} \cdot \mathcal{Z}(\mathbb{RP}^4_2)[\phi]. \tag{3.15}$$

Combining this expression with (3.13), we have

$$\mathcal{Z}(\mathbb{RP}^4) = \mathcal{Z}(\mathbb{RP}^4_2)[\phi]. \tag{3.16}$$

3. Then, we decompose $\mathbb{RP}^4_2$ into $\mathbb{RP}^4_1$ and a 2-handle, along the attaching region $S^1 \times D^2$. The boundary condition on the cut $S^1 \times D^2$ is labeled by the loop l_a of anyon a going around the S^1. Gluing relation becomes

$$\mathcal{Z}(\mathbb{RP}^4_2)[\phi] = \sum_a \frac{\mathcal{Z}(\mathbb{RP}^4_1)[l_a^{(+1)}]\mathcal{Z}(D^4)[l_a]}{\langle l_a | l_a \rangle_{\mathcal{V}(S^1\times D^2;\phi)}}. \tag{3.17}$$

Here, we have a l_a line on $\partial(\mathbb{RP}^4_1) = (S^2 \times S^1)/\sigma$ going along $(\{p_\theta\} \times S^1)/\sigma$, where p_θ denotes some point of S^2. The notation $l_a^{(+1)}$ means that the l_a diagram has $+1$ framing. To see this, let us recall that $\partial(\mathbb{RP}^4_1) = (S^2 \times S^1)/\sigma$, where σ is combination of antipodal maps acting on S^2 and $S^1 = \mathbb{R}/2\pi\mathbb{Z}$; $\sigma : (x, \theta) \mapsto (-x, \theta + \pi) \in S^2 \times S^1$. This space is a fibre bundle on a base space $S^1 = [0, \pi)$ whose fibre is given by S^2, where fibers on $\theta = 0, \pi$ are identified by antipodal map. On each fiber S^2 at fixed θ, we have two anyons $a, \overline{a}$ on antipodal points $p_\theta, -p_\theta$. As θ increases from 0 to π, the configuration of anyons $p_\theta, -p_\theta$ are gradually moved (keeping antipodal positions), and eventually flipped from that $\theta = 0$ at $\theta = \pi$; $p_0 = -p_\pi$ (see Fig.3.5). This process half-braids a and $\bar{a}$ exactly once, counting $+1$ framing.

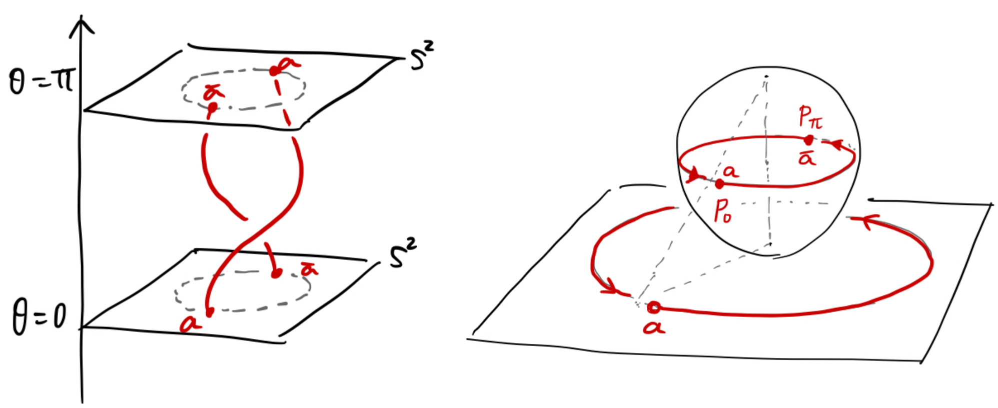

Figure 3.5: The contour of a line on $\partial(\mathbb{RP}^4_1) = (S^2 \times S^1)/\sigma$. We represent S^2 as a plane via stereograph mapping. If we regard the S^1 coordinate θ as time, we can see that a and $\overline{a}$ are half-braided, counting $+1$ framing. The configuration of quasiparticles at $\theta = 0, \pi$ are identified, via the action of R on anyon labels $\mathsf{R} : a \mapsto \overline{a}, \overline{a} \mapsto a$ when we have $\overline{a} = \mathsf{R}(a)$.

For $\mathcal{Z}(D^4)[l_a]$, we have a bubble of l_a loop on $S^3 = \partial D^4$ weighted by quantum dimension d_a. Hence, $\mathcal{Z}(D^4)[l_a] = d_a \mathcal{Z}(D^4)[\phi]$. In appendix C, we have $\mathcal{Z}(D^4)[\phi] = 1/\mathcal{D}$, $\langle l_a | l_a \rangle_{\mathcal{V}(S^1\times D^2;\phi)} = 1$. Therefore,

$$\mathcal{Z}(\mathbb{RP}^4_2)[\phi] = \frac{1}{\mathcal{D}} \sum_a d_a \cdot \mathcal{Z}(\mathbb{RP}^4_1)[l_a^{(+1)}]. \tag{3.18}$$

4. Finally, we evaluate $\mathcal{Z}(\mathbb{RP}^4_1)[l_a^{(+1)}]$. Similar to the previous step, we regard $\mathbb{RP}^4_1 = (D^3 \times S^1)/\sigma$ as a fibre bundle on $S^1 = [0, \pi)$, with fibre D^3. We apply gluing relation by cutting $\mathbb{RP}^4_1$ at

$\theta = \pi$. At $\theta = \pi$, R is acted on anyons $a, \overline{a}$ at $p, -p \in S^2 = \partial D^3$, together with the transition function given by antipodal map. Recall that we have defined η_a as the eigenvalue of R on the state with two anyons $a, \overline{a}$, so we count η_a on the Hilbert space of the cut $\mathcal{V}(D^3; a, \overline{a})$. After all, gluing relation becomes

$$\mathcal{Z}(\mathbb{RP}^4_1)[l_a^{(+1)}] = e^{\mathrm{i}\theta_a} \cdot \eta_a \cdot \sum_{e_i \in \mathcal{V}(D^3;a,\overline{a})} \frac{\mathcal{Z}(D^4)[\mathrm{arc}_a \cup e_i \cup \mathrm{arc}_{\overline{a}} \cup \mathsf{R}(e_i)]}{\langle e_i | e_i \rangle_{\mathcal{V}(D^3;a,\overline{a})}}, \tag{3.19}$$

where arc_a (resp. $\mathrm{arc}_{\overline{a}}$) denotes the line of a (resp. $\overline{a}$) after the cut. Framing $+1$ contributes as topological spin $e^{\mathrm{i}\theta_a}$ of a. The boundary condition on the cut e_i consists of an arc of anyon a connected with $\mathrm{arc}_a, \mathrm{arc}_{\overline{a}}$ at ∂D^3, making the diagram $(\mathrm{arc}_a \cup e_i \cup \mathrm{arc}_{\overline{a}} \cup \mathsf{R}(e_i))$ a closed loop on $S^3 = \partial D^4$ (see Fig.3.6).

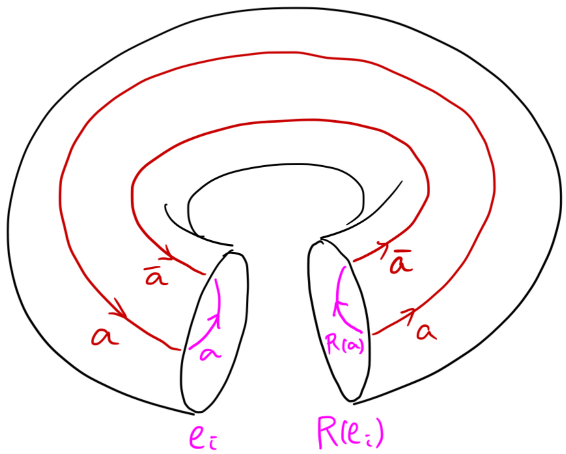

Figure 3.6: Anyon diagram $\mathrm{arc}_a \cup e_i \cup \mathrm{arc}_{\overline{a}} \cup \mathsf{R}(e_i)$ after cutting $\mathbb{RP}^4_1 = (D^3 \times S^1)/\sigma$, though we are showing $D^2 \times S^1$ instead of $D^3 \times S^1$ in this figure. R acts on the Hilbert space of the cut $\mathcal{V}(D^3; a, \overline{a})$.

This loop becomes a bubble of l_a loop on S^3 when we have $\overline{a} = \mathsf{R}(a)$, otherwise weights zero. Therefore, we have $\mathcal{Z}(D^4)[\mathrm{arc}_a \cup e_i \cup \mathrm{arc}_{\overline{a}} \cup \mathsf{R}(e_i)] = d_a \delta_{\overline{a},\mathsf{R}(a)} \mathcal{Z}(D^4)[\phi]$. Moreover, we have $\langle e_i | e_i \rangle_{\mathcal{V}(D^3;a,\overline{a})} = \mathcal{Z}(D^4)[l_a] = d_a \mathcal{Z}(D^4)[\phi]$. Hence, (3.19) becomes

$$\mathcal{Z}(\mathbb{RP}^4_1)[l_a^{(+1)}] = \eta_a e^{\mathrm{i}\theta_a} \delta_{\overline{a},\mathsf{R}(a)}. \tag{3.20}$$

Combining (3.16), (3.18) with (3.20), we eventually obtain anomaly indicator

$$\mathcal{Z}(\mathbb{RP}^4) = \frac{1}{\mathcal{D}} \sum_{\overline{a} = \mathsf{R}(a)} d_a \eta_a e^{\mathrm{i}\theta_a}. \tag{3.21}$$

The indicator formula (3.21) is also generalized for $\mathbb{Z}_{16}$ valued anomaly of fermionic topological phases with reflection symmetry such that $\mathsf{R}^2 = 1$ [20, 21] (known as class DIII in literature).

3.2 Rotation anomaly in (3+1)d topological order

In this section, we discuss anomaly of (3+1)d topological phases with C_k rotation symmetry. Similar to anyons in $(2+1)$d, (3+1)d topological phases also support quasiparticle excitations. The main difference of (3+1)d from (2+1)d is that there are two kinds of excitations in (3+1)d; point-like excitations and loop-like excitations, compared with (2+1)d where only point-like excitations exist.

Based on the observation in the case of reflection in (2+1)d, it is natural to expect that, in (3+1)d topological phases the anomaly is captured by symmetry properties of point-like and loop-like excitations. Concretely, we consider the anomaly of C_k rotation symmetry around some axis in (3+1)d untwisted discrete gauge theories (i.e., (3+1)d Dijkgraaf-Witten type gauge theory [7] with a trivial 4-cocycle).

The classification of (4+1)d C_k SPT phases that governs C_k anomalies in (3+1)d is again systematically provided by dimension reduction approach. Following the logic in Ref. [13], let us think of a small volume V in the spatial manifold of (4+1)d bulk away from the C_k rotation axis (in the 4d space, the C_k rotation axis is realized as a 2d plane). Then, we can act k local unitary operators $U_V, U_{C_k(V)}, \dots, U_{C_k^{k-1}(V)}$ related by C_k symmetry with each other, which are supported on $V, C_k(V), \dots, C_k^{k-1}(V)$ respectively. Acting these operators on the SPT state successively gives a C_k symmetric local unitary circuit. In (4+1)d, the bosonic topological phases without any symmetry are classified as $\mathbb{Z}_2$, which corresponds to the (4+1)d oriented bordism group $\Omega_5^{SO}(pt) = \mathbb{Z}_2$ [22]. If we do not have the nontrivial SPT phase corresponding to the generator of $\Omega_5^{SO}(pt) = \mathbb{Z}_2$ in the bulk, we can bring the C_k SPT state *away from the rotation axis* to the trivial product state by operating C_k symmetric unitary circuit.

Hence, apart from the nontrivial element of $\Omega_5^{SO}(pt) = \mathbb{Z}_2$, the (4+1)d C_k SPT phase reduces to the (2+1)d system supported on the rotation axis, where the C_k symmetry behaves as an onsite $\mathbb{Z}_k$ symmetry. On the (2+1)d rotation axis, there can be a single (2+1)d SPT phase protected by the onsite $\mathbb{Z}_k$ symmetry (classified as $\mathcal{H}^3(\mathbb{Z}_k, U(1)) = \mathbb{Z}_k$), or integer n_{E_8} copies of the E_8 state [23, 24] where the $\mathbb{Z}_k$ symmetry acts as an identity operator. From these states, we obtain $\mathbb{Z}_k \times \mathbb{Z}$ classification of the (2+1)d system on the rotation axis. However, it should be noted that the number of E_8 states on the rotation axis n_{E_8} can be changed by $\pm k$, by adjoining or annihilating k E_8 states with the same chirality in the C_k symmetric way. Thus, the classification of the E_8 part reduces from $\mathbb{Z}$ to $\mathbb{Z}/k\mathbb{Z} = \mathbb{Z}_k$. Eventually, we obtain $\mathbb{Z}_k \times \mathbb{Z}_k$ classification on the rotation axis.

The above discussion also gives the classification of C_k anomaly in the (3+1)d surface. In this thesis, we focus on the $\mathbb{Z}_k$ SPT ($\mathcal{H}^3(\mathbb{Z}_k, U(1)) = \mathbb{Z}_k$) part of the total $\mathbb{Z}_k \times \mathbb{Z}_k$ anomaly on the C_k rotation axis. Namely, we consider the C_k anomaly in (3+1)d bosonic systems that is equivalent to the assignment of the (1+1)d boundary of the (2+1)d $\mathbb{Z}_k$ SPT phase located on the C_k rotation axis.

In the case of $\mathbb{Z}_N$ gauge theories, we propose the indicator formula that can diagnose the $\mathbb{Z}_k$ part of the total C_k anomaly in (3+1)d as

$$\exp\left(\frac{2\pi \mathrm{i}\nu}{k}\right) = \frac{1}{N}\sum_{n,m} \eta_{e_n}\tilde{\eta}_{q_m} \exp\left[-\frac{2\pi\mathrm{i}}{N}nm\right], \tag{3.22}$$

where $\nu \in \mathbb{Z}_k$ detects the anomaly. Here, $\eta_{e_n}, \tilde{\eta}_{q_m}$ characterize the symmetry fractionalization of the point-like excitation e_n and loop-like excitation (vortex line) q_m, respectively. Similar to the case of (2+1)d with R symmetry, $\eta_{e_n}, \tilde{\eta}_{q_m}$ are defined via locating excitations in symmetric fashion: η_{e_n} is the C_k eigenvalue of the state with k point-like excitations $e_n, C_k(e_n), \dots, C_k^{k-1}(e_n)$ located in C_k symmetric fashion (see Fig.3.7.(a)). $\tilde{\eta}_{q_m}$ is the C_k eigenvalue of the state with a single loop-like excitation q_m rounding the rotation axis, located in C_k symmetric fashion (see Fig.3.7.(b)). The sum in (3.22) runs over point-like excitations e_n such that k particles $e_n, C_k(e_n), \ldots, C_k^{k-1}(e_n)$ fuse into vacuum, and loop-like excitations q_m such that $q_m = C_k(q_m)$. We can read from the indicator formula that some C_k symmetry action on excitations are prohibited on a standalone (3+1)d system, i.e., realized only on the surface of a (4+1)d SPT phase.

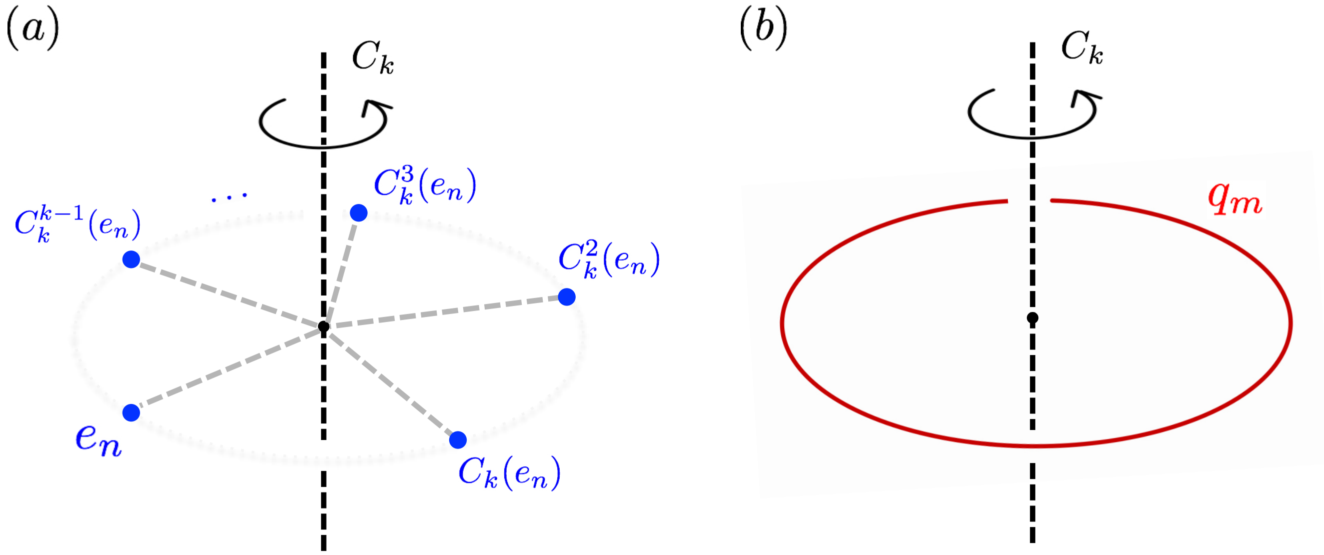

Figure 3.7: (a): C_k symmetric configuration of k point-like excitations. To ensure the existence of such state, we must require that k point-like excitations $e_n, C_k(e_n), \ldots, C_k^{k-1}(e_n)$ fuse into vacuum. (b): C_k symmetric configuration of a single loop-like excitation. To ensure the invariance of such state under C_k symmetry, we must require that $C_k(q_m) = q_m$.

3.2.1 anomalous toric code on the (3+1)d surface

Now, we examine the (3+1)d surface of the (4+1)d C_k SPT phase. Here, the surface can host the topological ordered phase enriched with C_k symmetry, where the C_k action is realized on the surface in an anomalous fashion. As we have seen in $eMmM$ fractionalization of reflection symmetry in (2+1)d toric code (see Table 3.1), we expect that we can detect anomaly of spatial symmetry in (3+1)d topological phase, from symmetry fractionalization on point-like and loop-like excitations. To see this, we begin with constructing the simplest lattice model of the (3+1)d toric code with anomalous C_2 symmetry ($k = 2$), which is a natural generalization of the $eMmM$ toric code in (2+1)d.

Let us consider the (3+1)d toric code on a cubic lattice with anomalous C_2 symmetry. As we have discussed above, the C_2 anomaly contains $\mathcal{H}^3(\mathbb{Z}_2, U(1)) = \mathbb{Z}_2$ part, which is equivalent to the assignment of the (1+1)d boundary of the (2+1)d $\mathbb{Z}_2$ SPT phase located on the C_2 rotation axis. The construction of anomalous lattice model is based on the effective theory on the boundary of the (2+1)d $\mathbb{Z}_2$ SPT phase, which is known as the CZX model in literature [9]: we construct the (3+1)d lattice model with anomalous symmetry action, by putting the boundary of the CZX model on the C_2 rotation axis. The similar construction of $eMmM$ toric code in (2+1)d based on dimensional reduction approach is found in Ref. [13].

For constructing lattice model, the rotation axis is defined such that the axis intersects edges of cubic lattice, see Fig.3.8. The symmetry action is realized on the rotation axis $x = y = 0$ as the boundary of CZX model [9],

$$C_2: X_z \mapsto Z_{z-1}X_zZ_{z+1}, \quad Y_z \mapsto -Z_{z-1}Y_zZ_{z+1}, \quad Z_z \mapsto -Z_z \qquad \text{at } x=y=0, \tag{3.23}$$

otherwise, we have non-anomalous symmetry action. For convenience, we define

$$C_2: X_{\vec{x}} \mapsto X_{-\vec{x}}, \quad Y_{\vec{x}} \mapsto -Y_{-\vec{x}}, \quad Z_{\vec{x}} \mapsto -Z_{-\vec{x}}, \qquad \text{otherwise.} \tag{3.24}$$

Namely, away from rotation axis C_2 symmetry acts as the π rotation around x axis on qubits. The anomalous nature of the model is encoded in the non-onsite symmetry action (3.23) realized on the axis. Now let us define the Hamiltonian which respects the C_2 symmetry defined above. The Hamiltonian of the conventional toric code has the form of

$$H = -\sum_s A_s - \sum_p B_p, \tag{3.25}$$

where $A_s := \prod_{s\in\partial i} X_i$ is the product of six X operators at edges touching a vertex s, and $B_p := \prod_{i\in\partial p} Z_i$ is the product of four Z operators at edges rounding a plaquette (2d square) p. Although the model (3.25) manifestly does not respect the C_2 symmetry (3.23), (3.24), one can construct the symmetric commuting projector model, just by slightly deforming local Hamiltonians touching the rotation axis. Let us modify the local Hamiltonian A_s adjacent to the rotation axis as

$$\begin{cases} A_s = \left[\prod'_{s\in\partial i} X_i\right] Y_{s-\vec{z}/2} Z_{s+\vec{x}/2-\vec{z}}, & s_x = -1/2, s_y = 0, \\ A_s = -\left[\prod'_{s\in\partial i} X_i\right] Y_{s-\vec{z}/2} Z_{s-\vec{x}/2+\vec{z}}, & s_x = 1/2, s_y = 0, \end{cases} \tag{3.26}$$

where $\left[\prod'_{s\in\partial i} X_i\right]$ stands for product of X at five edges touching a vertex s, except for the edge below s. We illustrate the redefined operators in Fig.3.8 (a). We can see that the above modification provides a commuting projector model which respects the C_2 symmetry (3.23), (3.24).

Let us examine quasiparticle excitations in the (3+1)d toric code. The (3+1)d toric code has one point-like electric particle and one loop-like vortex line. Electric particle e violates the Gauss law; $A_s = -1$ if e lives at the vertex s. Electric particles are generated by acting 1d open line operator S_e, which is given by the product of Z operators along the line. A pair of particles is created at the ends of an open string. On the other hand, a loop-like vortex line is generated by acting 2d surface operator S_q with a boundary. A single vortex line is created at the boundary of an open surface (see Fig.3.9). One can also think of composite excitation of e and q.

How the C_2 symmetry acts on e and q particles? As introduced in Fig. 3.7, the symmetry fractionalization $\eta_e, \tilde{\eta}_q$ are defined via locating quasiparticles in a C_2 symmetric fashion. This is performed by acting a line operator S_e and a surface operator S_q as illustrated in Fig. 3.9. S_e creates two e particles in a rotation symmetric way (in this model we have $C_2(e) = e$), and S_q creates a single q vortex line rounding the rotation axis. We can read the symmetry fractionalization η_e and $\tilde{\eta}_q$ by the symmetry action on S_e and S_q operators, $C_2:\ S_e \mapsto \eta_e S_e,\ S_q \mapsto \tilde{\eta}_q S_q$. In the case of our toric code model with anomalous C_2 symmetry, we can show that S_e and S_m acts under C_2 as

$$C_2: \quad S_e \mapsto -S_e, \quad S_q \mapsto -S_q, \tag{3.27}$$

hence we have $\eta_e = \tilde{\eta}_q = -1$. Among the four choices of symmetry fractionalization $\eta_e = \pm 1, \tilde{\eta}_q = \pm 1$, the three other than $\eta_e = \tilde{\eta}_q = -1$ are easily shown to be realized in a standalone (3+1)d system. According to the above observation that $\eta_e = \tilde{\eta}_q = -1$ fractionalization is realized on surface of the (4+1)d C_2 SPT phase, we expect that $\eta_e = \tilde{\eta}_q = -1$ fractionalization pattern is anomalous, otherwise non-anomalous. This prediction is immediately confirmed by computing the

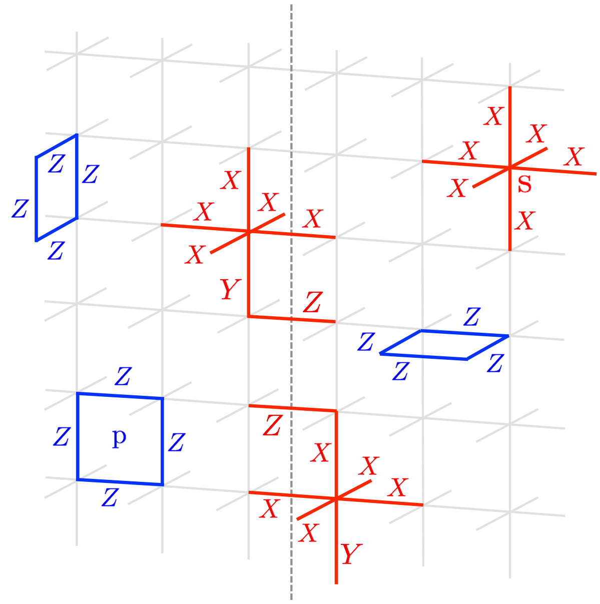

Figure 3.8: 3d toric code on a cubic lattice. Qubits on the C_2 rotation line (gray dotted line) transform in anomalous way (3.23) under C_2 symmetry. To respect symmetry, A_s operators (red operators) touching the reflection line are modified. B_p operators (blue operators) need not be modified.

anomaly indicator (3.22), which will be derived in Section 3.3. For instance, for $\eta_e = \tilde{\eta}_q = -1$, the indicator (3.22) for the $\mathbb{Z}_2$ gauge theory (toric code, $N = 2$) with C_2 rotation ($k = 2$) becomes,

$$\mathrm{e}^{\pi \mathrm{i}\nu} = \frac{1}{2}\sum_{n,m} \eta_{e_n}\tilde{\eta}_{q_m}\mathrm{e}^{-\pi i n m} = -1, \tag{3.28}$$

where e_0, q_0 are trivial excitation and $e_1 = e$, $q_1 = q$ in this expression. Hence, we read from the indicator that the anomaly is $\nu = 1 \bmod 2$.

3.3 Anomaly indicator in (3+1)d $\mathbb{Z}_N$ gauge theory

In this section, we derive anomaly indicator (3.22) for $G = \mathbb{Z}_N$ gauge theory in (3+1)d. After reviewing basic properties of $\mathbb{Z}_N$ gauge theory in Sec. 3.3.1, we justify that the partition function on the 5d lens space $\mathcal{Z}(L(k;1,1,1))$ detects the (partial) $\mathbb{Z}_k$ classification of C_k SPT phases in (4+1)d (Sec.3.3.2), by using the dimensional reduction. In Sec. 3.3.3, we derive the indicator formula (3.22) by explicit computation of $\mathcal{Z}(L(k;1,1,1))$, for given $\mathbb{Z}_N$ gauge theory on the (3+1)d surface. The computation of $\mathcal{Z}(L(k;1,1,1))$ is performed by applying gluing relation to the 5d path integral (Sec. 3.1.1).

3.3.1 $\mathbb{Z}_N$ gauge theories on lattice

Discrete gauge theory is formulated on a (3+1)d lattice, whose vertices are labeled by i. The degrees of freedom live on edges labeled by ij. On an oriented edge ij, such degrees of freedom are discrete G-gauge field $g_{ij} \in G$, which satisfies $g_{ij} = g_{ji}^{-1}$. Vacuum is given by an assignment of a flat G-gauge field $\{g_{ij}\}$ on the whole lattice, up to gauge equivalence. There are two kinds of extended operators

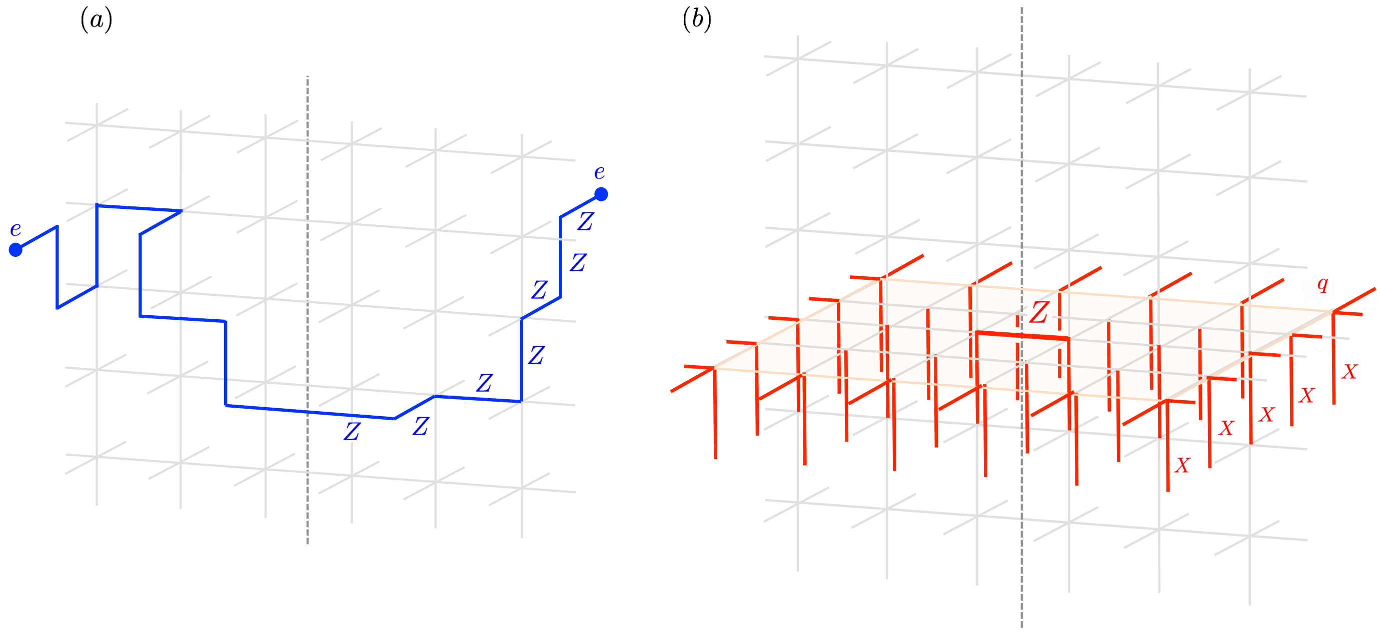

Figure 3.9: (a): S_e string operator which creates a pair of electric e particles at the ends of an open string. If two e particles are created in a C_2 respecting way, the length of S_e operators are always odd. Since we have $C_2 : Z \mapsto -Z$ everywhere, we have $S_e \mapsto -S_e$ under C_2. (b): S_q surface operator which creates a loop-like excitation q at the boundary of an open surface. S_q operator mostly consists of X operators, but we have a Z operator at the intersection between S_q surface and the C_2 axis. Thus, we have $S_q \mapsto -S_q$ under C_2 when q loop rounds the C_2 axis.

in (3+1)d discrete gauge theory: line operator and surface operator (which corresponds to S_e and S_q in the toric code, respectively).

In Appendix B, we also pose a conjecture for anomaly indicator for general (possibly non-abelian) gauge theories based on heuristic argument. In the case of $\mathbb{Z}_N$ gauge theories, both line and surface operators are labeled by group elements.

- The line operator $W_{A,n}(C)$ supported on a closed string on the lattice C, is labeled by a group element $n \in \mathbb{Z}_N$:

$$W_{A,n}(C) \left|\{g_{ij}\}\right\rangle = \exp\left[\frac{2\pi n \mathrm{i}}{N} \prod_{ij\in C} g_{ij}\right] \left|\{g_{ij}\}\right\rangle, \tag{3.29}$$

  i.e., a line operator is an Wilson line of electric charge labeled by $n \in \mathbb{Z}_N$. If supported on an open string, such line operator generates a pair of point-like electric excitations e_n, e_{-n} at the end of the string.

- The surface operator $W_{B,m}(S)$ supported on a face of the dual lattice S, is characterized by a group element $m \in \mathbb{Z}_N$:

$$W_{B,m}(S) = \prod_{ij\in S} \hat{B}_{ij}(m), \tag{3.30}$$

  where $\hat{B}_{ij}(m)$ is defined as

$$\hat{B}_{ij}(m) \left|g_{ij}\right\rangle = \left|m + g_{ij}\right\rangle, \tag{3.31}$$

where i is on one side of the surface, and j is on the other side of the surface. If supported on an open surface, such surface operator generates a loop-like excitation q_m at the boundary of the surface.

We denote quasiparticles created by $W_{A,n}, W_{B,m}$ as e_n, q_m respectively. The braiding between e_n and q_m is implemented by the correlator of the line and surface operators

$$\langle W_{A,n}(C) W_{B,m}(S) \rangle = \exp[-\mathrm{i}\frac{2\pi}{N} nm \cdot \mathrm{Lk}(C,S)], \tag{3.32}$$

where $\mathrm{Lk}(C,S)$ denotes the linking number between C and S.

C_k symmetry

Here, let us briefly refer to properties of C_k symmetry in (3+1)d topological ordered phases. In general, C_k symmetry can permute the label of quasiparticles. For (2+1)d, the symmetry action on anyon labels is defined such that the symmetry leaves the fusion and braiding data invariant, which is formulated as an automorphism of unitary braided fusion categories. [4] However, in (3+1)d we generally do not know how to characterize "automorphism", since we do not know what the complete input data is like that can characterize (3+1)d topological ordered phase. (For instance, diverse link invariants are known in (3+1)d topological ordered phase, see Ref. [25].)

If we limit ourselves to $\mathbb{Z}_N$ gauge theories, we just have to require that C_k leaves invariant the data of fusion, and the linking phase (3.32) between loop and point-like particles. Concretely, let us assume that C_k acts on the labels as

$$C_k : e_1 \mapsto e_r, \;\; q_1 \mapsto q_s. \tag{3.33}$$

Since C_k preserves the fusion of quasiparticles, the C_k action on any quasiparticles e_n, q_m are determined by (3.33),

$$C_k : e_n \mapsto e_{rn}, \;\; q_m \mapsto q_{sm}. \tag{3.34}$$

The above C_k action induces permutation of quasiparticle labels. Hence, we must have

$$\gcd(r,N) = \gcd(s,N) = 1. \tag{3.35}$$

In addition, C_k preserves the braiding between point and loop-like excitations (3.32). Thus, we must have

$$\exp[-\mathrm{i}\frac{2\pi}{N} \cdot \mathrm{Lk}(C,S)] = \exp[-\mathrm{i}\frac{2\pi}{N} rs \cdot \mathrm{Lk}(C,S)], \tag{3.36}$$

hence

$$rs = 1 \mod N. \tag{3.37}$$

Moreover, since $(C_k)^k = 1$ on labels, we must have

$$r^k = 1, \quad s^k = 1 \mod N. \tag{3.38}$$

[4]for orientation reversing symmetry such as R, we take symmetry as anti-automorphism instead, which operates on anyon diagrams as complex conjugate associated with usual automorphism.

3.3.2 topological invariant of bulk C_k SPT phases via partial rotation

In this subsection, we justify that $\mathcal{Z}(L(k;1,1,1))$ works as a topological invariant that diagnoses $\mathbb{Z}_k$-valued anomaly of C_k symmetry in (3+1)d. To do this, we first express the partition function $\mathcal{Z}(L(k;1,1,1))$ in terms of the ground state expectation value of the partial rotation operator $C_k[D^2\times D^2]$ [26],

$$\mathcal{Z}(L(k;1,1,1)) = \langle\Psi_{S^4}|\, C_{k;12}[D^2\times D^2]\cdot C_{k;34}[D^2\times D^2]\,|\Psi_{S^4}\rangle\,. \tag{3.39}$$

Let us explain the notations in (3.39). We prepare the Hilbert space on S^4, and the C_k SPT ground state on S^4 is expressed as $|\Psi_{S^4}\rangle$. We write the coordinate of S^4 as $(x,y,z,w)\in\mathbb{R}^4$, with infinite points identified. C_k transformations are defined as

$$C_{k;12} : ((x,y),(z,w)) \mapsto ((x,y), C_k(z,w))\,,\quad C_{k;34} : ((x,y),(z,w)) \mapsto (C_k(x,y),(z,w))\,. \tag{3.40}$$

We can think of acting the rotations "partially", on $D^2\times D^2 : x^2+y^2\le 1, z^2+w^2\le 1$ in S^4. Let us define the partial rotation operators supported on the $D^2\times D^2$ as $C_{k;34}[D^2\times D^2], C_{k;12}[D^2\times D^2]$ respectively. Then, the expectation value of the partial rotations on $D^2\times D^2$ (3.39) simulates the path integral on the 5d lens space, where inserting the partial rotation operator $C_{k;12}C_{k;34}$ on a time slice works as creating a "cross-cap" in the spacetime. Since the lens space $L(k;1,1,1)$ is defined as identifying two $D^4=D^2\times D^2$ on the boundary of D^5 ($S^4=D^4\cup D^4=\partial D^5$) by using the $C_{k;12}C_{k;34}$ transformation, inserting the cross-cap makes the spacetime the lens space $L(k;1,1,1)$. (The definition of the 5d lens space is illustrated in Sec. 3.3.3.)

Here, it should be emphasized that one of the C_k transformations $C_{k;34}, C_{k;12}$ is the C_k symmetry that is used to define the C_k SPT phase. The other one is rather taken as an *inherent* C_k symmetry which is the subgroup of $SO(d+1)$ Lorentz symmetry present in TQFT, which is not relevant to symmetry protection. Hence, we set the $C_{k;12}$ as a symmetry that protects our SPT phase, and the $C_{k;34}$ as an inherent one.

Next, let us perform the dimensional reduction in terms of the $C_{k;12}$ symmetry. As we have explained previously, one can trivialize the $C_{k;12}$ SPT phase away from the $C_{k;12}$ rotation axis, using the dimensional reduction by $C_{k;12}$ symmetric unitary circuits. In our case, the $C_{k;12}$ rotation axis is realized as $S^2 : z=w=0$ (xy-plane), and we are interested in the $C_{k;12}$ SPT phase that is equivalent to locating a (2+1)d onsite $\mathbb{Z}_k$ SPT phase on the xy-plane.

After the dimensional reduction, the rotation operator $C_{k;12}$ becomes the generator $U_{\mathbb{Z}_k}$ of the onsite $\mathbb{Z}_k$ symmetry in the reduced (2+1)d SPT phase. Thus, the partial rotation operator $C_{k;12}[D^2\times D^2]$ gives a partial onsite $\mathbb{Z}_k$ transformation $U_{\mathbb{Z}_k}[D^2]$ supported on $D^2 : x^2+y^2\le 1$ in the xy-plane, while $C_{k;34}[D^2\times D^2]$ still works as a partial rotation operator $C_k[D^2]$ supported on $D^2 : x^2+y^2\le 1$. Therefore, the expectation value in (4+1)d (3.39) reduces to

$$\mathcal{Z}(L(k;1,1,1)) = \langle\Psi_{S^2}|\,(U_{\mathbb{Z}_k}C_k)[D^2]\,|\Psi_{S^2}\rangle\,, \tag{3.41}$$

where $|\Psi_{S^2}\rangle$ is the ground state of the (2+1)d $\mathbb{Z}_k$ SPT phase, whose spatial manifold is taken as S^2. Now, the expectation value of the partial operation $U_{\mathbb{Z}_k}C_k$ simulates the partition function of the (2+1)d $\mathbb{Z}_k$ SPT phase on the 3d lens space $L(k;1,1)$, in the presence of the flat background $\mathbb{Z}_k$ gauge field;

$$\langle\Psi_{S^2}|\,(U_{\mathbb{Z}_k}C_k)[D^2]\,|\Psi_{S^2}\rangle = \mathcal{Z}(L(k;1,1))[A], \tag{3.42}$$

where A denotes the $\mathbb{Z}_k$ flat background gauge field that corresponds to the generator of $\mathrm{Hom}(\pi_1(L(k;1,1)),\mathbb{Z}_k)$. Here, inserting $C_k[D^2]$ creates a cross-cap to make the geometry of the spacetime the lens space

$L(k;1,1)$, and inserting the $\mathbb{Z}_k$ symmetry defect $U_{\mathbb{Z}_k}[D^2]$ on the cross-cap introduces a nontrivial $\mathbb{Z}_k$ flat connection A. Eventually, (3.42) gives the partition function of the (2+1)d $\mathbb{Z}_k$ SPT phase on a generator manifold $\mathcal{Z}(L(k;1,1))[A]$ [27], hence detects the distinct $\mathbb{Z}_k$ SPT phases characterized by $\mathcal{H}^3(\mathbb{Z}_k, U(1)) = \mathbb{Z}_k$. Therefore, $\mathcal{Z}(L(k;1,1,1))$ also diagnoses the $\mathbb{Z}_k$ classification of (4+1)d C_k SPT phases.

3.3.3 $\mathcal{Z}(L(k;1,1,1))$: (3+1)d C_k anomaly

In this section, we explicitly compute $\mathcal{Z}(L(k;1,1,1))$, based on (3+1)d discrete gauge theory on the surface. We pause here to mention that to construct (4+1)d SPT phases from given data of general (3+1)d surface theories. We should first generalize the construction of (3+1)d bulk TQFT from (2+1)d topological ordered phases known as Walker-Wang construction [28, 29], to one dimension higher. The authors plan to do so in the future; in the present paper, we just exploit some machinery required to evaluate anomalies.

First, let us recall the definition of the lens space. Let k, p_j for $j = 1, 2, \dots n$ be natural numbers such that $\gcd(k, p_j) = 1$ for all j. The lens space $L(k; p_1, \dots, p_n)$ in $(2n-1)$d is defined as the quotient space by a free linear acton of cyclic group $\mathbb{Z}_k$ on a sphere S^{2n-1}, considered as the unit sphere in $\mathbb{C}^n$. The $\mathbb{Z}_k$ action is generated by

$$(w_1, \dots, w_n) \mapsto (w_1 \cdot e^{2\pi \mathrm{i} p_1/k}, \dots, w_n \cdot e^{2\pi \mathrm{i} p_n/k}). \tag{3.43}$$

Especially, $L(k;1,1,1)$ is a quotient space of S^5 by $\mathbb{Z}_k$ action given by

$$(w_1, w_2, w_3) \mapsto (w_1 \cdot e^{2\pi \mathrm{i}/k}, w_2 \cdot e^{2\pi \mathrm{i}/k}, w_3 \cdot e^{2\pi \mathrm{i}/k}). \tag{3.44}$$

handle decomposition

For evaluating the partition function $\mathcal{Z}(L(k;1,1,1))$, we perform handle decomposition of $L(k;1,1,1)$, which takes $L(k;1,1,1)$ apart into 5-balls. We find that the 5d lens space $L(k;1,1,1)$ is decomposed into single m-handles for $m = 0,1,2,3,4,5$. We denote $L(k;1,1,1)_m$ as the composition of $0,1,2,\dots,m$ handles of $L(k;1,1,1)$.

For convenience, we sometimes regard $L(k;1,1,1)$ as a D^5, whose points on the boundary $S^4 = \partial D^5$ are identified by a certain rule. Concretely, we write D^5 as $D^4 \times I$ ($D^4 : |w_1|^2 + |w_2|^2 \le 1$, $I : \theta_3 \in [0, 2\pi/k]$), pinched at $\partial D^4 \times I$. Then, ∂D^5 consists of two D^4s at $\theta_3 = 0$ and $\theta_3 = 2\pi/k$, which is identified by the homeomorphism

$$(w_1, w_2) \mapsto (w_1 \cdot e^{2\pi \mathrm{i}/k}, w_2 \cdot e^{2\pi \mathrm{i}/k}). \tag{3.45}$$

We can obtain this picture, by seeing a D^5 as a subregion of S^5 such that $0 \le \arg(w_3) \le 2\pi/k$. If we define $\theta_3 := \arg(w_3)$, the D^4s at $\theta_3 = 0$ and $\theta_3 = 2\pi/k$ are indeed identified by (3.45). Now, the handle decomposition of $L(k;1,1,1)$ is performed by the following steps:

1. First, we decompose $L(k;1,1,1)$ into a 5-handle and $L(k;1,1,1)_4$. We denote $\theta_1 := \arg(w_1), \theta_2 := \arg(w_2), \theta_3 := \arg(w_3)$ for convenience. The 5-handle is given by the subspace of $L(k;1,1,1)$

specified as

$$
\begin{aligned}
&\left\{(w_1, w_2, \theta_3)\middle| |w_1| \geq \epsilon, \quad \epsilon \leq \theta_1 \leq \frac{2\pi}{k} - \epsilon\right\}, \\
&\left\{(w_1, w_2, \theta_3)\middle| |w_1| \geq \epsilon, \quad \frac{2\pi}{k} + \epsilon \leq \theta_1 \leq \frac{4\pi}{k} - \epsilon\right\}, \\
&\dots \\
&\left\{(w_1, w_2, \theta_3)\middle| |w_1| \geq \epsilon, \quad \frac{2(k-1)\pi}{k} + \epsilon \leq \theta_1 \leq 2\pi - \epsilon\right\},
\end{aligned}
\tag{3.46}
$$

where $0 < \epsilon \ll 1$ is a small positive constant. The above k regions are connected by the identification map (3.45) with the neighboring one at $\theta_3 = 0$ and $\theta_3 = 2\pi/k$, making a single connected space. This space is isomorphic to a subspace $0 \leq \theta_1 \leq 2\pi/k$ of the initial $S^5 = \{(w_1, w_2, w_3)||w_1|^2 + |w_2|^2 + |w_3|^2 = 1\}$, thus D^5, as described before.

2. Next, we decompose $L(k;1,1,1)_4$ into a 4-handle and $L(k;1,1,1)_3$. The 4-handle is given by connected k regions,

$$
\begin{aligned}
&\{(w_1, w_2, \theta_3)||w_1| \geq \epsilon, \quad -\epsilon \leq \theta_1 \leq \epsilon\}, \\
&\left\{(w_1, w_2, \theta_3)\middle| |w_1| \geq \epsilon, \quad \frac{2\pi}{k} - \epsilon \leq \theta_1 \leq \frac{2\pi}{k} + \epsilon\right\}, \\
&\dots \\
&\left\{(w_1, w_2, \theta_3)\middle| |w_1| \geq \epsilon, \quad \frac{2(k-1)\pi}{k} - \epsilon \leq \theta_1 \leq \frac{2(k-1)\pi}{k} + \epsilon\right\}.
\end{aligned}
\tag{3.47}
$$

For fixed θ_1, the above region looks like $\{|w_1| \geq \epsilon, \arg(w_1) = 0\}$ in the initial $S^5 = \{(w_1, w_2, w_3)||w_1|^2 + |w_2|^2 + |w_3|^2 = 1\}$, which specifies $D^4 : |w_2|^2 + |w_3|^2 \leq 1 - \epsilon^2$. Hence, we see that the subspace makes a 4-handle $(D^4 \times D^1, S^3 \times D^1)$, where $D^1 : \theta_1 \in [-\epsilon, \epsilon]$.

3. Let us examine what $L(k;1,1,1)_3$ looks like. $L(k;1,1,1)_3$ is a subspace of $L(k;1,1,1)$ specified as $|w_1| \leq \epsilon$. As we did for $L(k;1,1,1)$, we can also parameterize $L(k;1,1,1)_3$ by (w_1, w_2, θ_3) for $0 \leq \theta_3 \leq 2\pi/k$, embedded in $L(k;1,1,1)$. The subspace of $L(k;1,1,1)_3$ given by fixing θ_3 is a subregion $|w_1| \leq \epsilon$ in $D^4 : |w_1|^2 + |w_2|^2 \leq 1$, which is homeomorphic to $D^2 \times D^2$. Since we are pinching at $\partial D^4 \times I$ in $L(k;1,1,1)$, we also have to pinch at the subspace of $\partial(D^2 \times D^2)$ such that $|w_1|^2 + |w_2|^2 = 1$. This pinching region becomes $D^2 \times S^1 \in \partial(D^2 \times D^2)$, where $S^1 : \theta_2 \in [0, 2\pi]$. For convenience, we reparametrize $D^2 \times D^2$ by (z_1, z_2) such that $|z_1| \leq 1, |z_2| \leq 1$, where the pinching region is represented as $|z_2| = 1$.

   Thus, $L(k;1,1,1)_3$ is given by first preparing $(D^2 \times D^2) \times I : (z_1, z_2, \theta_3)$, pinched at $(D^2 \times S^1) \times I$. Then, we identify $D^2 \times D^2$s at $\theta_3 = 0$ and $\theta_3 = 2\pi/k$ by the map (3.45), which is represented by z_1, z_2 as

$$
(z_1, z_2) \mapsto (z_1 \cdot e^{2\pi \mathrm{i}/k}, z_2 \cdot e^{2\pi \mathrm{i}/k}). \tag{3.48}
$$

   If we forget about z_1, we can see that (z_2, θ_3) is essentially a parametrization of the 3D lens space $L(k;1,1)$. Namely, $L(k;1,1)$ is quotient space of $S^3 : |z_2|^2 + |z_3|^2 = 1$ by the $\mathbb{Z}_k$ action $(z_2, z_3) \mapsto (z_2 \cdot e^{2\pi \mathrm{i}/k}, z_3 \cdot e^{2\pi \mathrm{i}/k})$. If we pick up a subspace of S^3 specified by $0 \leq \theta_3 := \arg(z_3) \leq 2\pi/k$, we have $D^2 \times I$ pinched at $S^1 \times I$, with identification at $\theta_3 = 0$ and $\theta_3 = 2\pi/k$ by $z_2 \mapsto z_2 \cdot e^{2\pi \mathrm{i}/k}$, which corresponds to (3.48). Hence, we can see $L(k;1,1,1)_3$ as a fibre bundle whose base space is $L(k;1,1)$, with fibre D^2. Therefore, $L(k;1,1,1)_3$ is the quotient space of $D^2 \times S^3, \{(z_1,(z_2,z_3)) : |z_1| \le 1, |z_2|^2+|z_3|^2 = 1\}$ by the following $\mathbb{Z}_k$ action denoted by σ_k,

$$\sigma_k : (z_1, z_2, z_3) \mapsto (z_1 \cdot e^{2\pi \mathrm{i}/k}, z_2 \cdot e^{2\pi \mathrm{i}/k}, z_3 \cdot e^{2\pi \mathrm{i}/k}). \tag{3.49}$$

The handle decomposition of $L(k;1,1,1)_3$ is essentially given by decomposing the base space $L(k;1,1)$ into handles, which is shown in Fig.3.10. The 3-handle is given by the subspace of $(D^2 \times D^2) \times I : (z_1, z_2, \theta_3)$ $(I : 0 \le \theta_3 \le 2\pi/k)$, specified as

$$\begin{aligned}
&\left\{(z_1,z_2,\theta_3)\middle| |z_2| \ge \epsilon, \quad \epsilon \le \arg(z_2) \le \frac{2\pi}{k} - \epsilon\right\},\\
&\left\{(z_1,z_2,\theta_3)\middle| |z_2| \ge \epsilon, \quad \frac{2\pi}{k} + \epsilon \le \arg(z_2) \le \frac{4\pi}{k} - \epsilon\right\},\\
&\dots\\
&\left\{(z_1,z_2,\theta_3)\middle| |z_2| \ge \epsilon, \quad \frac{2(k-1)\pi}{k} + \epsilon \le \arg(z_2) \le \frac{2(k-1)\pi}{k} - \epsilon\right\},
\end{aligned} \tag{3.50}$$

which are connected with each other by identification map (3.48). This subspace gives a 3-handle (D^3, S^2) in the base space $L(k;1,1) : (z_2, \theta_3)$. Correspondingly, this gives a 3-handle $(D^3 \times D^2, S^2 \times D^2)$ in the total space $L(k;1,1,1)_3 = (D^2 \times S^3)/\sigma_k$.

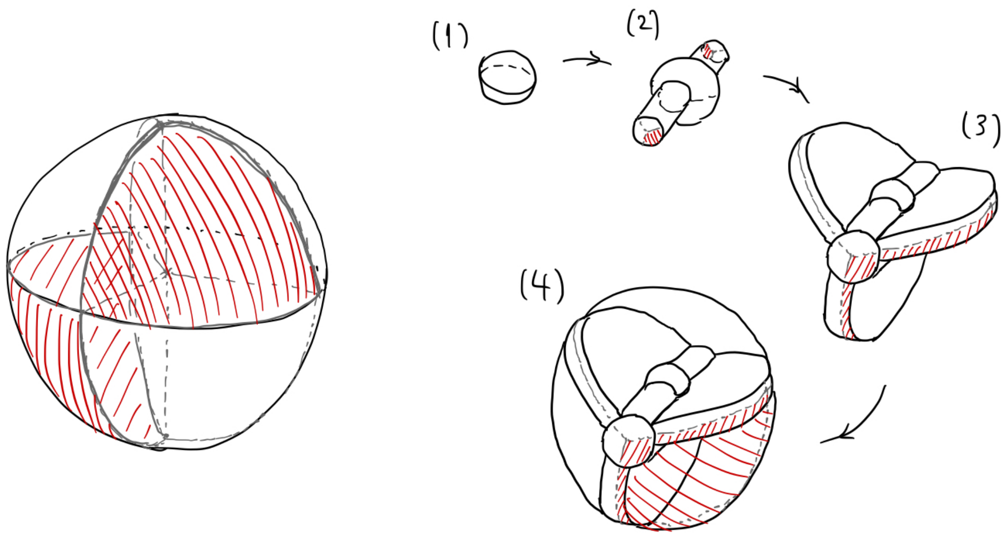

Figure 3.10: 3d Lens space $L(k;1,1)$ is obtained by identifying two D^2s on the boundary $\partial D^3 = D^2 \cup D^2$, by $2\pi/k$ rotation $z_2 \mapsto z_2 \cdot e^{2\pi \mathrm{i}/k}$. In the figure, we represent $L(k;1,1)$ for $k=3$, where the red regions are identified by this map. We can develop $L(3;1,1)$ by attaching handles successively.

4. Then, we decompose $L(k;1,1,1)_2$ into a 2-handle and $L(k;1,1,1)_1$. The 2-handle is given by

connected k regions in $(D^2 \times D^2) \times I$ parametrized by (z_1, z_2, θ_3) $(I: 0 \leq \theta_3 \leq 2\pi/k)$,

$$\begin{aligned}
&\{(z_1, z_2, \theta_3) | |z_2| \geq \epsilon, \quad -\epsilon \leq \arg(z_2) \leq \epsilon\}, \\
&\left\{(z_1, z_2, \theta_3) \middle| |z_2| \geq \epsilon, \quad \frac{2\pi}{k} - \epsilon \leq \arg(z_2) \leq \frac{2\pi}{k} + \epsilon\right\}, \\
&\ldots \\
&\left\{(z_1, z_2, \theta_3) \middle| |z_2| \geq \epsilon, \quad \frac{2(k-1)\pi}{k} - \epsilon \leq \arg(z_2) \leq \frac{2(k-1)\pi}{k} + \epsilon\right\}.
\end{aligned} \tag{3.51}$$

For the base space $L(k;1,1) : (z_2, \theta_3)$ of $L(k;1,1,1)_3 = (D^2 \times S^3)/\sigma_k$, the above subspace gives a 2-handle $(D^2 \times D^1, S^1 \times D^1)$. Correspondingly, this gives a 2-handle $(D^2 \times D^3, S^1 \times D^3)$ in $L(k;1,1,1)_3$.

Let us examine what $L(k;1,1,1)_1$ looks like. $L(k;1,1,1)_1$ is a subspace of $L(k;1,1,1)_3 = (D^2 \times S^3)/\sigma_k$, specified as $|z_2| \leq \epsilon$. In the base space $L(k;1,1)$, $\{(z_2, \theta_3), |z_2| \leq \epsilon\}$ gives a quotient space of $(D^2 \times S^1), \{(z_2, \theta_3), |z_2| \leq \epsilon, \theta_3 \in \mathbb{R}/2\pi\mathbb{Z}\}$ by the $\mathbb{Z}_k$ action σ_k,

$$\sigma_k : (z_2, \theta_3) \mapsto (z_2 \cdot e^{2\pi \mathrm{i}/k}, \theta_3 + 2\pi/k). \tag{3.52}$$

Then, $L(k;1,1,1)_1$ is a fibre bundle whose base space is given by $(D^2 \times S^1)/\mathbb{Z}_k$, with fibre D^2. Therefore, $L(k;1,1,1)_1$ is a quotient space of $(D^2 \times D^2 \times S^1), \{(z_1, z_2, \theta_3), |z_1| \leq 1, |z_2| \leq \epsilon, \theta_3 \in \mathbb{R}/2\pi\mathbb{Z}\}$ by the $\mathbb{Z}_k$ action σ_k,

$$\sigma_k : (z_1, z_2, \theta_3) \mapsto (z_1 \cdot e^{2\pi \mathrm{i}/k}, z_2 \cdot e^{2\pi \mathrm{i}/k}, \theta_3 + 2\pi/k). \tag{3.53}$$

computation of partition function

Based on handle decomposition discussed above, now we evaluate $\mathcal{Z}(L(k;1,1,1))$ via gluing relation. In our case where the surface theory is described by discrete gauge theory, the boundary condition $\mathcal{C}$ is an assignment of configuration of flat G-gauge field on boundaries.

1. First, we decompose $L(k;1,1,1)$ into a 5-handle and $L(k;1,1,1)_4$. The boundary condition on the attaching region S^4 is unique up to gauge equivalence, since no surface or line operator can wrap S^4 nontrivially. Thus, the gluing relation becomes

$$\begin{aligned}
\mathcal{Z}(L(k;1,1,1)) &= \frac{\mathcal{Z}(L(k;1,1,1)_4)[\phi]\mathcal{Z}(D^5)[\phi]}{\langle\phi|\phi\rangle_{\mathcal{V}(S^4)}} \\
&= \frac{\mathcal{Z}(L(k;1,1,1)_4)[\phi]\mathcal{Z}(D^5)[\phi]}{\mathcal{Z}(S^4 \times D^1)[\phi]},
\end{aligned} \tag{3.54}$$

where ϕ is the vacuum state on S^4. Similarly, for the decomposition of $L(k;1,1,1)_4$ into a 4-handle and $L(k;1,1,1)_3$, the gluing relation is expressed as

$$\mathcal{Z}(L(k;1,1,1)_4)[\phi] = \frac{\mathcal{Z}(L(k;1,1,1)_3)[\phi]\mathcal{Z}(D^5)[\phi]}{\langle\phi|\phi\rangle_{\mathcal{V}(S^3 \times D^1)}}. \tag{3.55}$$

Here, we have used again that no surface or line operator can wrap $S^3 \times D^1$ nontrivially. We can evaluate $\mathcal{Z}(S^4 \times D^1)[\phi]$ via gluing formula, by cutting $S^4 \times D^1$ into two D^5s along $S^3 \times D^1$,

$$\mathcal{Z}(S^4 \times D^1)[\phi] = \frac{\mathcal{Z}(D^5)[\phi]\mathcal{Z}(D^5)[\phi]}{\langle\phi|\phi\rangle_{\mathcal{V}(S^3 \times D^1)}}. \tag{3.56}$$

Combining (3.54), (3.55), with (3.56), we obtain

$$\mathcal{Z}(L(k;1,1,1)) = \mathcal{Z}(L(k;1,1,1)_3)[\phi]. \tag{3.57}$$

2. Next, we decompose $L(k;1,1,1)_3$ into a 3-handle and $L(k;1,1,1)_2$. Now the attaching region is $S^2\times D^2$, where a surface operator can wrap S^2. Therefore, the boundary condition is labeled by a surface operator $W_{B,m}$ for $0\leq m\leq N-1$ wrapping S^2,

$$\mathcal{Z}(L(k;1,1,1)_3)[\phi]=\sum_{0\leq m\leq N-1}\frac{\mathcal{Z}(L(k;1,1,1)_2)[W_{B,m}]\mathcal{Z}(D^5)[W_{B,-m}]}{\langle W_{B,m}|W_{B,m}\rangle_{\mathcal{V}(S^2\times D^2;\phi)}}. \tag{3.58}$$

Since a closed surface operator is a bubble on ∂D^5, we have $\mathcal{Z}(D^5)[W_{B,-m}]=\mathcal{Z}(D^5)[\phi]$, since bubbles of surface operator for $\mathbb{Z}_N$ gauge theory weights 1.

$\langle W_{B,m}|W_{B,m}\rangle_{\mathcal{V}(S^2\times D^2)}=\mathcal{Z}(S^2\times D^3)[W_{B,-m}\cup W_{B,m}]$ is evaluated via gluing relation by cutting $S^2\times D^3$ into two D^5s along $S^1\times D^3$, see Fig.3.11. Here, the boundary condition on the cut is labeled by a line operator $W_{A,n}$ rounding S^1 of $S^1\times D^3$. Hence, the gluing relation becomes

$$\mathcal{Z}(S^2\times D^3)[W_{B,-m}\cup W_{B,m}]=\sum_{0\leq n\leq N-1}\frac{\mathcal{Z}(D^5)[W_{A,-n},W_{B,-m}]\mathcal{Z}(D^5)[W_{A,n},W_{B,m}]}{\langle W_{A,n},e_{B,m}|W_{A,n},e_{B,m}\rangle_{\mathcal{V}(S^1\times D^3;q_m,q_{-m})}}. \tag{3.59}$$

By the cutting, the surface operators before the cut $W_{B,-m}$, $W_{B,m}$ are divided into two discs respectively. To make a membrane closed, the boundary condition $e_{B,m}$ on the cut $S^1\times D^3$ is introduced as a tube $S^1\times I$ connecting discs on ∂D^5 (see Fig.3.11). Since bubbles of line and surface operator for $\mathbb{Z}_N$ gauge theory weights 1, we have $\mathcal{Z}(D^5)[W_{A,-n},W_{B,-m}]=\mathcal{Z}(D^5)[\phi]$. [5] Moreover, by gluing relation, we can show that

$$\langle W_{A,n},e_{B,m}|W_{A,n},e_{B,m}\rangle_{\mathcal{V}(S^1\times D^3;q_m,q_{-m})}=1. \tag{3.60}$$

Therefore, we obtain

$$\langle W_{B,m}|W_{B,m}\rangle_{\mathcal{V}(S^2\times D^2;\phi)}=N\cdot\mathcal{Z}(D^5)[\phi]\mathcal{Z}(D^5)[\phi]. \tag{3.61}$$

Combined with (3.58), we have

$$\mathcal{Z}(L(k;1,1,1)_3)[\phi]=\frac{1}{N}\sum_{0\leq m\leq N-1}\frac{\mathcal{Z}(L(k;1,1,1)_2)[W_{B,m}]}{\mathcal{Z}(D^5)[\phi]}. \tag{3.62}$$

3. Then, we decompose $L(k;1,1,1)_2$ into a 2-handle and $L(k;1,1,1)_1$. Since the attaching region is $S^1\times D^3$, the boundary condition on the cut is labeled by a line operator rounding S^1. The gluing relation becomes

$$\mathcal{Z}(L(k;1,1,1)_2)[W_{B,m}]=\sum_{0\leq n\leq N-1}\frac{\mathcal{Z}(L(k;1,1,1)_1)[W_{A,n},W_{B,m}]\mathcal{Z}(D^5)[W_{A,-n},W_{B,-m}]}{\langle W_{A,n},e_{B,m}|W_{A,n},e_{B,m}\rangle_{\mathcal{V}(S^1\times D^3;q_m,q_{-m})}}, \tag{3.63}$$

Using (3.60), we obtain

$$\mathcal{Z}(L(k;1,1,1)_2)[W_{B,m}]=\sum_{0\leq n\leq N-1}\mathcal{Z}(L(k;1,1,1)_1)[W_{A,n},W_{B,m}]\mathcal{Z}(D^5)[W_{A,-n},W_{B,-m}]. \tag{3.64}$$

[5]When we have both line and surface operator on the boundary, one must care about linking of these two objects, since the correlator of these two objects has nontrivial phase (3.32) when the line and surface are linked. In our case, we can have nontrivial linking in $\mathcal{Z}(D^5)[W_{A,n},W_{B,m}]$ for some choice of configuration of operators. However, the linking in $\mathcal{Z}(D^5)[W_{A,n},W_{B,m}]$ and $\mathcal{Z}(D^5)[W_{A,n},W_{B,m}]$ cancels in the expression of (3.59), since the linking number is reversed for opposite orientation. In the main text, we are evaluating $\mathcal{Z}(D^5)[W_{A,n},W_{B,m}]$ by choosing trivially linked configurations.

$\partial(D^2 \times D^3) = S^4$

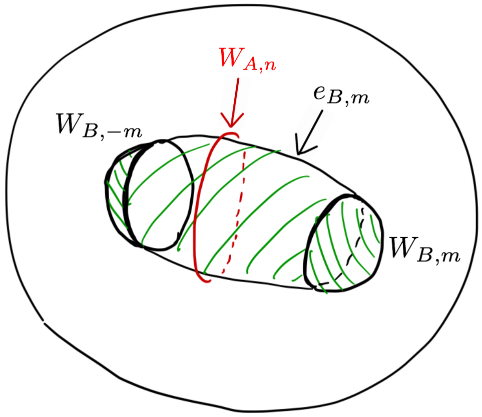

Figure 3.11: The configuration of line and surface operator on ∂D^5 after cutting $\mathcal{Z}(S^2 \times D^3)[W_{B,-m} \cup W_{B,m}]$ as (3.59). By the cutting, the surface operators before the cut $W_{B,-m}$, $W_{B,m}$ are divided into two discs respectively. To make a membrane closed, the boundary condition $e_{B,m}$ on the cut $S^1 \times D^3$ is introduced as a tube $S^1 \times I$ connecting discs on ∂D^5. Moreover, a line operator $W_{A,n}$ can round S^1 of the cut.

Combining (3.64) with (3.62), we have

$$\mathcal{Z}(L(k;1,1,1)_3)[\phi] = \frac{1}{N} \sum_{0 \leq n,m \leq N-1} \frac{\mathcal{Z}(L(k;1,1,1)_1)[W_{A,n}, W_{B,m}]\mathcal{Z}(D^5)[W_{A,-n}, W_{B,-m}]}{\mathcal{Z}(D^5)[\phi]}. \tag{3.65}$$

4. To evaluate $\mathcal{Z}(L(k;1,1,1)_1)[W_{A,n}, W_{B,m}]$, we should be careful about the configuration of line and surface operator, since the correlator of these two objects has nontrivial phase (3.32) when the line and surface are linked. To examine the configuration of these operators, we recall that $L(k;1,1,1)_1$ is a quotient space of $(D^2 \times D^2 \times S^1), \{(z_1, z_2, \theta_3), |z_1| \leq 1, |z_2| \leq 1, \theta_3 \in \mathbb{R}/2\pi\mathbb{Z}\}$ by the $\mathbb{Z}_k$ action σ_k,

$$\sigma_k : (z_1, z_2, \theta_3) \mapsto (z_1 \cdot e^{2\pi \mathrm{i}/k}, z_2 \cdot e^{2\pi \mathrm{i}/k}, \theta_3 + 2\pi/k). \tag{3.66}$$

We can choose the configuration of a surface operator $W_{B,m}$ as $(S^1 \times S^1)/\sigma_k$ given by $\{z_1 = 0, |z_2| = 1\}$. Recall that the cut of $L(k;1,1,1)_2$ into $L(k;1,1,1)_1$ and a 2-handle is the subregion of $\partial L(k;1,1,1)_1$ given by

$$\{(z_1, z_2, \theta_3) | |z_2| = 1, \quad -\epsilon \leq \arg(z_2) \leq \epsilon\}. \tag{3.67}$$

Then, we know that a line operator on the cut $W_{A,n}$ can be located on S^1 given by $(f(\theta_3), 1, \theta_3)$ for $\theta_3 \in \mathbb{R}/2\pi\mathbb{Z}$, where $f : S^1 \mapsto D^2$ is some function of $\theta_3 \in \mathbb{R}/2\pi\mathbb{Z}$.

Since we are putting a surface opeator $W_{B,m}$ at $z_1 = 0$, we must have $f \neq 0$ to make a line and surface operator dislocated (otherwise the linking number is ill-defined). We choose f as a constant function of θ_3; $f(\theta_3) = p_0 \neq 0$, so that the linking of $W_{A,n}$, $W_{B,m}$ on the boundary of a 2-handle ∂D^5 becomes trivial; $\mathcal{Z}(D^5)[W_{A,-n}, W_{B,-m}] = \mathcal{Z}(D^5)[\phi]$ in (3.65).

To visualize the configuration of operators on $\partial L(k;1,1,1)_1$, it is convenient to see $\partial L(k;1,1,1)_1 = (S^3 \times S^1)/\sigma_k$ as a fibre bundle on a base space $S^1 : 0 \le \theta_3 \le 2\pi/k$, with fibre S^3. At $\theta_3 = 2\pi/k$, we have a transition function on a fibre; $\sigma_k : (z_1, z_2) \mapsto (z_1 \cdot e^{2\pi \mathrm{i}/k}, z_2 \cdot e^{2\pi \mathrm{i}/k})$. If we regard θ_3 as time direction, at a fixed time θ_3 we have a loop-like excitation q_m at $S^1 : \{z_1 = 0, |z_2| = 1\}$ which corresponds to a time slice of $W_{B,m}$. We also have k point-like excitations $e_n, C_k(e_n), \dots C_k^{k-1}(e_n)$ at $(z_1, z_2) = (p_0, 1), (p_0 \cdot e^{2\pi \mathrm{i}/k}, e^{2\pi \mathrm{i}/k}), \dots, (p_0 \cdot e^{2(k-1)\pi \mathrm{i}/k}, e^{2(k-1)\pi \mathrm{i}/k})$ respectively, which correspond to time slice of $W_{A,n}$ (see Fig.3.12). Remark that the label of excitation is transformed by C_k associated with the transition function. Especially, loop-like excitations are counted only when $C_k(q_m) = q_m$.

We can see that $W_{A,n}$ and $W_{B,m}$ link exactly once; $\mathrm{Lk}(W_{A,n}, W_{B,m}) = 1$, which is explained in Fig.3.12.

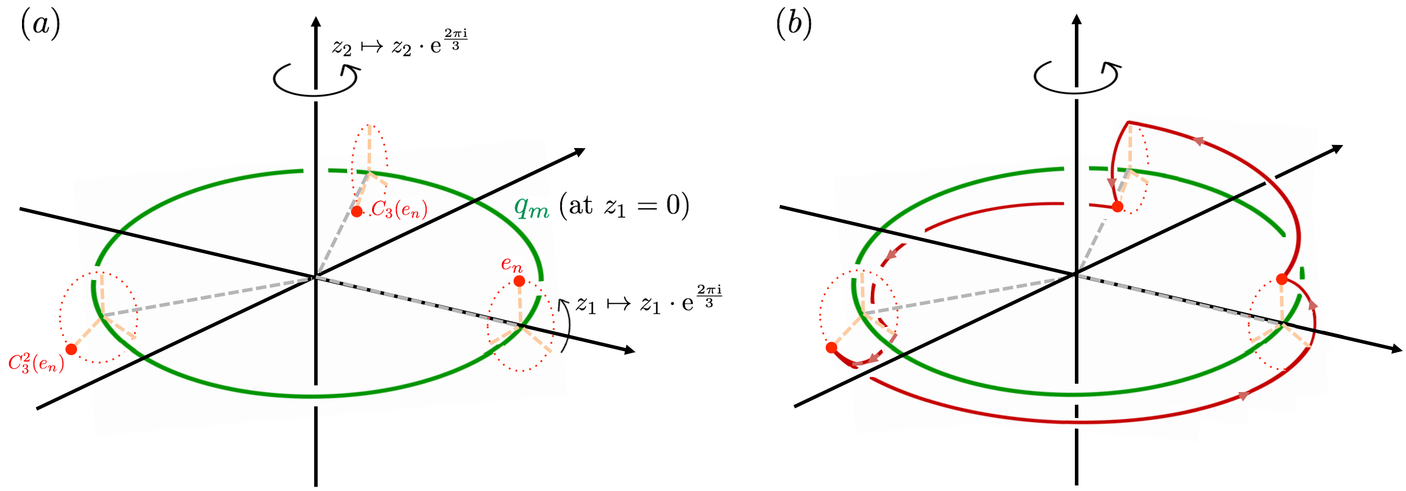

Figure 3.12: (a): The configuration of point-like and loop-like particles in S^3 is shown for $k = 3$, via mapping to a unit 3-sphere $(z_1, z_2) \mapsto \left(z_1, z_2\sqrt{1 - |z_1|^2}\right)$, and stereograph mapping of unit 3-sphere $S^3 \mapsto \mathbb{R}^3$. In the stereograph projected picture, the action $z_2 \mapsto z_2 \cdot e^{2\pi \mathrm{i}/k}$ is realized as $2\pi/k$ rotation around z axis in $\mathbb{R}^3$. A loop-like excitation q_m is located at S^1 given by $z_1 = 0$. In the vicinity of $z_1 = 0$, the action $z_1 \mapsto z_1 \cdot e^{2\pi \mathrm{i}/k}$ is realized as $2\pi/k$ rotation around S^1: $z_1 = 0$. For small p_0, the configuration of point-like excitations $e_n, C_k(e_n), \dots C_k^{k-1}(e_n)$ looks like red points, each of which is transformed to the neighboring one by acting $\sigma_k : (z_1, z_2) \mapsto (z_1 \cdot e^{2\pi \mathrm{i}/k}, z_2 \cdot e^{2\pi \mathrm{i}/k})$ associated with C_k on particle label. The configuration of these excitations are thus left invariant under the action of transition function σ_k, associated with C_k on labels. (b): To compute the linking number, it is convenient to think of the worldline of point-like particles (red line) transported gradually by the composite of $2\pi/k$ rotation, which finally amounts to the action of σ_k. As shown in the figure, the worldline links with a green loop of q_m exactly once. Since $\mathrm{Lk}(W_{A,n}, W_{B,m})$ corresponds to the linking number of a time-independent q_m loop and a world-line of e_n, we can see that $\mathrm{Lk}(W_{A,n}, W_{B,m}) = 1$.

Now, we have

$$
\begin{aligned}
\mathcal{Z}(L(k;1,1,1)_3)[\phi] &= \frac{1}{N}\sum_{0\le n,m\le N-1} \mathcal{Z}(L(k;1,1,1)_1)[\{W_{A,n},W_{B,m}\}^{+1}] \\
&= \frac{1}{N}\sum_{0\le n,m\le N-1} \exp\left[-\frac{2\pi \mathrm{i}}{N}nm\right]\cdot \mathcal{Z}(L(k;1,1,1)_1)[\{W_{A,n},W_{B,m}\}^{+0}],
\end{aligned}
\tag{3.68}
$$

where $+1$ means that $W_{A,n}, W_{B,m}$ are linked once. The linking between these operators counts the extra factor of braiding phase $\exp\left[-\frac{2\pi \mathrm{i}}{N}nm\right]$ (3.32), compared with the case where the line and surface operators are not linked, which is denoted as $\{W_{A,n},W_{B,m}\}^{+0}$.

Finally, let us consider gluing relation by cutting $L(k;1,1,1)_1 = (D^4\times S^1)/\sigma_k$ into a D^5 along D^4 at $\theta_3 = 2\pi/k$. The gluing relation becomes

$$
\begin{aligned}
&\mathcal{Z}(L(k;1,1,1)_1)[\{W_{A,n},W_{B,m}\}^{+0}] \\
&= \eta_{e_n}\tilde{\eta}_{q_m}\cdot \sum_{e_i} \frac{\mathcal{Z}(D^5)[\mathrm{arc}(W_{A,n})\cup \mathrm{arc}(W_{B,m})\cup e_i\cup \bar{e}_i]}{\langle e_i|e_i\rangle_{\mathcal{V}(D^4)}},
\end{aligned}
\tag{3.69}
$$

where $\mathcal{V}(D^4)$ is a shorthand notation of $\mathcal{V}(D^4; q_m, e_n, C_k(e_n), \dots C_k^{k-1}(e_n))$, which is a Hilbert space on the cut in the presence of excitations on its boundary ∂D^4, as shown in Fig.3.12. $\{e_i\}$ is the orthonormal basis in $\mathcal{V}(D^4)$ (it should not be confused with the notation of electric particle e_n). $\mathrm{arc}(W_{A,n}), \mathrm{arc}(W_{B,n})$ denotes open line or surface operator after the cut. Since we are acting C_k on the cut, we count C_k eigenvalues $\eta_{e_n}\tilde{\eta}_{q_m}$ on the Hilbert space of the cut $\mathcal{V}(D^4)$.

$\mathcal{Z}(D^5)[\mathrm{arc}(W_{A,n})\cup \mathrm{arc}(W_{B,m})\cup e_i\cup \bar{e}_i]$ contributes only when k point-like particles fuses into vacuum and $C_k(q_m) = q_m$, otherwise weights zero. Both $\mathcal{Z}(D^5)[\mathrm{arc}(W_{A,n})\cup \mathrm{arc}(W_{B,m})\cup e_i\cup \bar{e}_i]$, $\langle e_i|e_i\rangle_{\mathcal{V}(D^4)}$ reduces to evaluation of $\mathcal{Z}(D^5)$ with unlinked bubbles of line and surface operators if k point-like particles fuses into vacuum and $C_k(q_m) = q_m$, thus these factors become $\mathcal{Z}(D^5)[\phi]$. Therefore, we have

$$
\mathcal{Z}(L(k;1,1,1)_1)[\{W_{A,n},W_{B,m}\}^{+0}] = \eta_{e_n}\tilde{\eta}_{q_m}\delta_{C_k^j e_n}\delta_{q_m, C_k(q_m)},
\tag{3.70}
$$

where $\delta_{C_k^j e_n}$ is 1 when $e_n, C_k(e_n), \dots C_k^{k-1}(e_n)$ fuses into vacuum, otherwize zero.

Combining (3.57), (3.68) with (3.70), we finally obtain anomaly indicator

$$
\mathcal{Z}(L(k;1,1,1)) = \frac{1}{N}\sum_{n,m}\eta_{e_n}\tilde{\eta}_{q_m}\exp\left[-\frac{2\pi \mathrm{i}}{N}nm\right],
\tag{3.71}
$$

where the sum runs over n such that k particles $e_n, C_k(e_n), \dots C_k^{k-1}(e_n)$ fuse into vacuum, m such that $q_m = C_k(q_m)$.

3.3.4 Example of anomalous $\mathbb{Z}_N$ gauge theory

Based on the indicator formula (3.71), we provide several examples of anomalous $\mathbb{Z}_N$ gauge theories under C_k symmetry. First, let us think of the case where C_k does not permute the label of quasi-particles. In this case, the electric particle e_n contributes to the sum of the indicator (3.71), iff k e_n particles fuse into vacuum, i.e., $kn = 0 \bmod N$. Thus, we can set n as

$$
n = p\cdot \frac{N}{\gcd(k,N)},
\tag{3.72}
$$

where $p \in \mathbb{Z}_{\gcd(k,N)}$. Let us define $\eta_p := \eta_{e_{p\cdot N/\gcd(k,N)}}$. Since we have $(C_k)^k = 1$, η_p satisfies $(\eta_p)^k = 1$. In addition, η should be compatible with fusion of quasiparticles: $\eta_a \eta_b = \eta_c$ if $a+b=c$ mod $\gcd(k,N)$. Therefore, $(\eta_p)^{\gcd(k,N)} = \eta_{e_0} = 1$. To summarize, η_p must satisfy

$$(\eta_p)^{\gcd(k,N)} = 1. \tag{3.73}$$

On the other hand, all vortex line operators q_m contribute to the sum of (3.71), since $q_m = C_k(q_m)$ is always satisfied when C_k does not permute labels. Using the same logic as the case of η_p, we can see that $\tilde{\eta}$ satisfies $(\tilde{\eta}_{q_m})^k = 1, (\tilde{\eta}_{q_m})^N = 1$. Hence, $\tilde{\eta}_{q_m}$ must also satisfy

$$(\tilde{\eta}_{q_m})^{\gcd(k,N)} = 1. \tag{3.74}$$

Thus, we can set $\eta_p, \tilde{\eta}_{q_m}$ as

$$\eta_p = \exp\left[\frac{2\pi \mathrm{i}}{\gcd(k,N)}\alpha p\right], \quad \tilde{\eta}_{q_m} = \exp\left[\frac{2\pi \mathrm{i}}{\gcd(k,N)}\beta m\right], \tag{3.75}$$

where $\alpha, \beta \in \mathbb{Z}_{\gcd(k,N)}$. Then, the indicator formula (3.71) becomes

$$\exp\left(\frac{2\pi \mathrm{i}\nu}{k}\right) = \frac{1}{N}\sum_{p,m} \exp\left[\frac{2\pi \mathrm{i}}{\gcd(k,N)}(\alpha p + \beta m - pm)\right] = \exp\left[\frac{2\pi \mathrm{i}}{\gcd(k,N)}\alpha\beta\right], \tag{3.76}$$

where the sum is taken over $p \in \mathbb{Z}_{\gcd(k,N)}, m \in \mathbb{Z}_N$. We can read the $\mathbb{Z}_k$-valued anomaly from (3.76) as

$$\nu = \frac{k}{\gcd(k,N)}\alpha\beta \qquad \mathrm{mod}\ k. \tag{3.77}$$

Next, we illustrate the case where labels of quasiparticles are changed by C_k action. For instance, let us consider $\mathbb{Z}_9$ gauge theory with C_9 symmetry ($N = k = 9$), and C_k acts on quasiparticle labels as

$$C_9 : e_n \mapsto e_{4n}, \ q_m \mapsto q_{7m}, \tag{3.78}$$

i.e., we have $r = 4$, $s = 7$ in (3.33). We can check that the setup satisfies (3.35), (3.37), (3.38). For this C_9 action, we can check that 9 particles $e_n, C_k(e_n), \dots C_9^8(e_n)$ fuse into vacuum for all $n \in \mathbb{Z}_9$. Thus, all electric particles e_n contribute to the sum of the indicator formula (3.71). Since $\eta_{e_1} = \eta_{e_4} = (\eta_{e_1})^4$, η_{e_1} satisfies $(\eta_{e_1})^3 = 1$. Thus, we can express η_{e_1} as $\eta_{e_1} = \omega^\alpha$, where $\omega = \mathrm{e}^{2\pi \mathrm{i}/3}$.

On the other hand, vortex lines q_m contribute to the sum of (3.71) iff $q_m = C_k(q_m)$. In our case, we can see that only q_0, q_3, q_6 are fixed under C_k. Since $(\tilde{\eta}_{q_3})^3 = 1$, we can express $\tilde{\eta}_{q_3}$ as $\tilde{\eta}_{q_3} = \omega^\beta$. Then, the indicator formula (3.71) becomes

$$\exp\left(\frac{2\pi \mathrm{i}\nu}{9}\right) = \frac{1}{9}\sum_{\substack{1\le n\le 9,\\ 1\le m\le 3}} \omega^{n\alpha + m\beta - nm} = \omega^{\alpha\beta}. \tag{3.79}$$

Therefore, the anomaly is read as $\nu = 3\alpha\beta$ mod 9.

Chapter 4

Anomalies and topological phases based on generalized global symmetries

Inspired by the discovery of 't Hooft anomalies on boundaries of SPT phases in condensed matter literature, new types of 't Hooft anomalies involving various symmetries have been discovered. In this chapter, we review and discuss anomalies based on higher-form symmetry, which is a generalized concept of ordinary global symmetry.

Higher-form symmetry (p-form symmetry) is a global symmetry whose charged object has dimension p, e.g., lines for 1-form symmetry, membranes for 2-form symmetry, and so on [4, 30, 31]. Theories with higher-form symmetry are ubiquitous in diverse range of physics. For example, pure abelian gauge theories possess 1-form symmetry whose charged object is given by Wilson line operator. For $SU(N)$ gauge theory, 1-form symmetry appears as a center symmetry which shifts the holonomy by an element of the center $\mathbb{Z}_N$ of gauge group $SU(N)$. For discrete symmetries, their spontaneous symmetry breaking implies realization of topological ordered phase, where vacuums in distinct topological sectors are tunneled by acting symmetry generator which shifts the value of line operators.

Various important concepts in ordinary (0-form) global symmetries are naturally generalized for higher-form symmetries. For instance, spontaneous symmetry breaking (SSB) can also be formulated for higher-form symmetry [32]. Concretely, we say that the higher-form symmetry is spontaneously broken in the reference ground state $|0\rangle$, if there exists an operator $\mathcal{O}$ which is charged under the symmetry such that $\langle 0|\,\mathcal{O}\,|0\rangle \neq 0$.

We can also think of gauging p-form symmetry. This procedure is explicitly performed in Lagrangian formalism by coupling derivative of p-form matter field with $p+1$-form gauge field, which can be either classical (background) or dynamical. Accordingly, ordinary quantum anomaly can also be generalized for higher-form symmetries. Specifically, 't Hooft anomaly leads to SPT phases protected by higher-form symmetries [33–35]. The consequences of such anomalies have been extensively studied in hep-th literature and applied to constrain vacuum structures and phase structures of quantum field theories. [4, 36–48] For example, $SU(N)$ pure Yang-Mills theory in (3+1)d with $\theta = \pi$ is found to possess an 't Hooft anomaly involving CP symmetry and center symmetry, while at $\theta = 0$ is not anomalous. The 't Hooft anomaly provides strong constraint on spectral properties of low energy theory; in this case, we can claim the spontaneously breaking of CP symmetry at zero temperature of $\theta = \pi$.

In condensed matter literature, such constraint on spectral properties provided by 't Hooft anomalies appears as Lieb-Schultz-Mattis (LSM) mechanism. LSM mechanism is applied for quantum many-body system defined on a lattice, possessing both internal and lattice symmetries. Roughly speaking, LSM theorem prohibits a symmetric gapped phases without ground state degeneracy (i.e., trivial symmetric insulator) with input of combination of internal and lattice symmetries. Such theorem of LSM-type is empirically known to manifest itself as a consequence of 't Hooft anomaly in the continuum infrared limit. More concretely, in the IR theory where lattice symmetry such as translational symmetry can be treated as internal symmetry, LSM-type constraint is understood as a mixed 't Hooft anomaly involving internal and lattice symmetries. We will discuss in detail the generalization of LSM mechanism for higher-form symmetries and relation to anomalies in the next chapter.

4.1 Generalized global symmetries

In this section, we give a basic definition of higher-form symmetry. Let us start with recalling fundamental properties of ordinary global symmetries we are familiar with in $(d+1)$ dimension. For ordinary (0-form) global symmetries, charged object is 0 dimensional particle, i.e., there exists a local operator charged under the symmetry. Generator of symmetry is supported on a d-dimensional manifold. Specifically, for continuous symmetries, the conserved charge is given by integrating d-form Noether current j over a d-dimensional manifold M^d regarded as a space,

$$Q(M^d) = \int_{M^d} j. \tag{4.1}$$

Then, the generator is obtained by exponentiating the conserved charge; $U_g(M^d) := \exp[\mathrm{i}\alpha Q(M^d)]$, where $g \in G$ is an element of the symmetry group. The symmetry transformation on a charged operator is implemented via equal-time commutation relation,

$$U_g(M^d)V_i(p)U_g(M^d)^\dagger = R_i^j(g)V_j(p) \qquad \text{at equal time}, \tag{4.2}$$

where $V_i(p)$ is a charged operator which transforms as representation R of the symmetry group G under G-action. We recall that the equal-time commutation relation is understood as a time ordered product, where the generator acts on charged objects via canonical commutation relations. Thus, letting p be located at time t, two generators $U_g(M^d)$, $U_g(M^d)^\dagger$ in (4.2) sandwiching the charged object are supported on the whole space of time slice at $t+\epsilon, t-\epsilon$ respectively, where ϵ is an infinitesimal constant. Here, note that correlation function involving symmetry generators U_g is left invariant under deforming the configuration of a generator, as long as the manifold supporting the generator does not cross an operator V charged under symmetry. Thus, by deforming the configuration of generators at $t+\epsilon, t-\epsilon$ in (4.2), we obtain

$$U_g(S^d)V_i(p) = R_i^j(g)V_j(p), \tag{4.3}$$

where the generator is supported on a small sphere S^d surrounding p.

We can readily generalize the above properties of ordinary global symmetries for p-form symmetries. For general p-form symmetry, charged object $W(M^p)$ is supported on p-dimensional closed manifold M^p. Correspondingly, the generator is of dimension $d-p$. For continuous symmetries, the conserved charge is given by integrating $(d-p)$-form current j on a closed manifold N^{d-p},

$$W(M^p) = \int_{M^p} \mathcal{O}, \quad Q(N^{d-p}) = \int_{N^{d-p}} j. \tag{4.4}$$

Then, the generator is again obtained by exponentiating the conserved charge,

$$U_g(N^{d-p}) := \exp[\mathrm{i}\alpha Q(N^{d-p})], \tag{4.5}$$

where $g \in G$ is an element of symmetry group G and α is a transformation parameter. The generators respect the group law, $U_g(N^{d-p})U_{g'}(N^{d-p}) = U_{g''}(N^{d-p})$ for $gg' = g''$. The group multiplication of generators is again regarded as time ordered product. For $p \geq 1$, we note that the order of generators are permuted by continuously deforming the configuration of generators. Hence, we have $U_g U_{g'} = U_{g'} U_g$, i.e., the symmetry must be abelian for p-form symmetry of $p \geq 1$. The symmetry action on charged object is implemented by equal-time commutation relation,

$$U_g(N^{d-p})W(M^p)U_g(N^{d-p})^\dagger = g(V)^{\mathcal{I}[N^{d-p},M^p]}W(M^p), \tag{4.6}$$

where $g(V)$ is a representation of G (i.e., phase), and both manifolds are defined on spatial manifold whose intersection number is $\mathcal{I}[N^{d-p}, M^p]$. The interpretation for (4.6) is that a generator acts on a charged object as it crosses M^p (see Fig.4.1). By deforming generators sandwiching a charged object in (4.6), we obtain

$$U_g(S^{d-p})W(M^p) = g(V)^{\mathrm{Lk}[S^{d-p},M^p]}W(M^p), \tag{4.7}$$

where S^{d-p} is a sphere linking with M^p whose linking number is given by $\mathrm{Lk}[S^{d-p}, M^p]$.

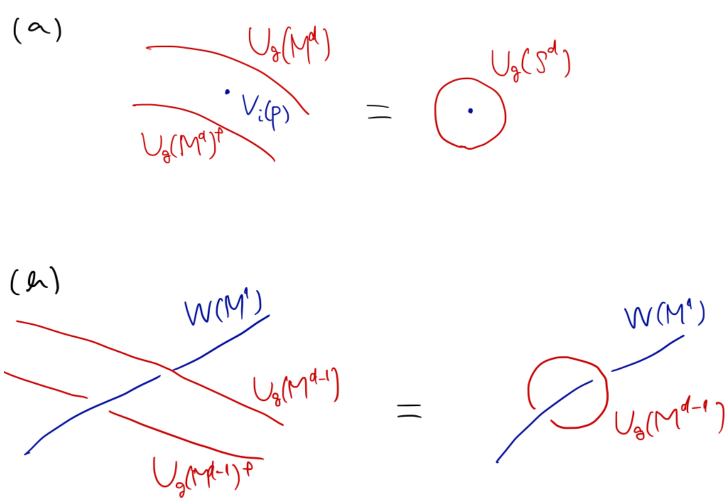

Figure 4.1: Generators in equal-time commutation relation are deformed to a sphere linking with a charged object. (a): 0-form symmetry in (1+1)d spacetime. (b): 1-form symmetry in (2+1)d spacetime.

1-form symmetries in (3+1)d Maxwell theory

As an example, let us consider the Maxwell theory in (3+1)d without matter, whose action is given by

$$S = \int_X F \wedge *F, \tag{4.8}$$

with $F = \mathrm{d}A$, where X is 4d spacetime manifold. Actually, we have two 1-form symmetries in the action (4.8). These symmetries correspond to conserved currents followed by equation of motion and Bianchi identity,

$$\mathrm{d} * F = 0, \quad \mathrm{d}F = 0, \tag{4.9}$$

respectively, whose integration over surfaces give rise to generators of 1-form symmetries,

$$U^{E}_{g=e^{\mathrm{i}\alpha_{\mathrm{e}}}}(M^2) = \exp\left(\frac{\mathrm{i}\alpha_{\mathrm{e}}}{2\pi}\int_{M^2} *F\right), \quad U^{M}_{g=e^{\mathrm{i}\alpha_{\mathrm{m}}}}(M^2) = \exp\left(\frac{\mathrm{i}\alpha_{\mathrm{m}}}{2\pi}\int_{M^2} F\right). \tag{4.10}$$

The first 1-form symmetry generated by $U^E_g(M^2)$ is referred to as electric. The electric symmetry shifts $U(1)$ gauge field $A \mapsto A + \lambda$, with $\lambda \in Z^1(X, \mathbb{R}/2\pi\mathbb{Z})$ a flat field. [1] The charged object under the electric symmetry is the Wilson line operator,

$$W(C^1) = \exp\left(\mathrm{i}\int_{C^1} A\right). \tag{4.13}$$

The symmetry action on the Wilson line is summarized in the equal-time commutation relation (4.7),

$$U^{E}_{g=e^{\mathrm{i}\alpha_{\mathrm{e}}}}(S^2)W(C^1) = \mathrm{e}^{\mathrm{i}\alpha_{\mathrm{e}}\mathrm{Lk}[S^2,C^1]}W(C^1). \tag{4.14}$$

The other symmetry generated by $U^M_g(M^2)$ is referred to as magnetic, which is related to electric symmetry by electromagnetic duality. Magnetic symmetry shifts the dual gauge field by a flat field $\widetilde{A} \mapsto \widetilde{A} + \widetilde{\lambda}$, where dual field $\widetilde{A}$ is locally defined via $*F = \mathrm{d}\widetilde{A}$. The charged object is the 't Hooft line operator,

$$T(C^1) = \exp\left(\int_{C^1} \widetilde{A}\right). \tag{4.15}$$

The combination of these two 1-form symmetries have a mixed 't Hooft anomaly. To see this, we introduce 2-form background gauge field $B_{\mathrm{e}}, B_{\mathrm{m}}$ for electric and magnetic symmetry, respectively. The gauge transformations are defined as

$$\begin{aligned} A &\mapsto A + \xi, \quad B_{\mathrm{e}} \mapsto B_{\mathrm{e}} + \mathrm{d}\xi, \\ \widetilde{A} &\mapsto \widetilde{A} + \eta, \quad B_{\mathrm{m}} \mapsto B_{\mathrm{m}} + \mathrm{d}\eta. \end{aligned} \tag{4.16}$$

First, we gauge magnetic symmetry by coupling the background field B_{m} to the conserved current F,

$$\mathcal{L} = F \wedge *F + \frac{1}{2\pi} F \wedge B_{\mathrm{m}}. \tag{4.17}$$

Next, we introduce background field B_{e} for electric symmetry,

$$\mathcal{L} = (F - B_{\mathrm{e}}) \wedge *(F - B_{\mathrm{e}}) + \frac{1}{2\pi}(F - B_{\mathrm{e}}) \wedge B_{\mathrm{m}}. \tag{4.18}$$

Then, we can see that the gauged action is no longer invariant under gauge transformation $B_{\mathrm{m}} \mapsto B_{\mathrm{m}} + \mathrm{d}\eta$,

$$S \mapsto S - \frac{1}{2\pi}\int_X B_{\mathrm{e}} \wedge \mathrm{d}\eta, \tag{4.19}$$

[1] Flat 1-form field λ is classified up to gauge transformations by the first cohomology group,

$$[\lambda] \in H^1(X, \mathbb{R}/2\pi\mathbb{Z}). \tag{4.11}$$

Here, the cohomology is generated by $[\omega] \in H^1(X, \mathbb{Z})$. Precisely, electric 1-form $U(1)$ symmetry is expressed as

$$A \mapsto A + \alpha_{\mathrm{e}}\omega, \quad \alpha_{\mathrm{e}} \in \mathbb{R}/2\pi\mathbb{Z}. \tag{4.12}$$

In the case of $\theta \in 2\pi\mathbb{Z}$, the above shift corresponds to large gauge transformation, which leaves the Wilson operator invariant.

which signals an 't Hooft anomaly involving two 1-form symmetries. This phase ambiguity is cancelled by gauge variation of the following 5d bulk topological action,

$$S_{\text{bulk}} = \frac{1}{2\pi} \int_Y B_{\text{m}} \text{d} B_{\text{e}} - B_{\text{e}} \text{d} B_{\text{m}}, \tag{4.20}$$

where $\partial Y = X$.

4.2 Anomalous 1-form symmetries of toric code

In condensed matter literature, topological ordered phases often possess higher-form symmetries, due to the existence of extended operators supported on a line, membrane, etc. Here, we examine topological phases with extended line operators from the viewpoint of generalized global symmetries. For instance, let us look at the toric code (untwisted $\mathbb{Z}_2$ gauge theory) in (2+1)d with two kinds of line operator, e and m. We can see that both line operators generate $\mathbb{Z}_2$ 1-form symmetries. Let us call these two symmetries as $\mathbb{Z}_2^e, \mathbb{Z}_2^m$, respectively. Reflecting braiding statistics between e and m, equal-time commutation relation for $\mathbb{Z}_2^e$ symmetry is expressed as

$$W_e(S^1) W_m(M^1) = (-1)^{\text{Lk}[S^1, M^1]} W_m(M^1), \tag{4.21}$$

where W_e (resp. W_m) is a line operator of e (resp. m). We also have commutation relation for $\mathbb{Z}_2^m$ with e and m exchanged,

$$W_m(S^1) W_e(M^1) = (-1)^{\text{Lk}[S^1, M^1]} W_e(M^1). \tag{4.22}$$

Thus, for e, m line operators, one operator generates $\mathbb{Z}_2$ 1-form symmetry whose charged object is the other. Interestingly, these two 1-form symmetries have a mixed 't Hooft anomaly. To see this, we introduce 2-form background field B_e, B_m for $\mathbb{Z}_2^e, \mathbb{Z}_2^m$ respectively. At Lagrangian level, gauge fields are introduced to (2+1)d BF theory by coupling with currents,

$$\mathcal{L} = \frac{2\text{i}}{2\pi} b \wedge \text{d}a + \frac{\text{i}}{2\pi} (a \wedge B_m + b \wedge B_e), \tag{4.23}$$

where B_m, B_e are understood as 2-form $\mathbb{Z}_2$ fields; $[B_e/2\pi], [B_m/2\pi] \in H^2(X, \mathbb{Z}_2)$. a, b are 1-form gauge fields whose integration on lines give W_e, W_m respectively. Because of Poincaré duality $H^2(X, \mathbb{Z}_2) \cong H_1(X, \mathbb{Z}_2)$, we can identify background gauge field as an assignment of line operators W_e, W_m on some 1-cycle $C_e, C_m \in H_1(X, \mathbb{Z}_2)$, by choosing B_e, B_m as a Poincaré dual of C_e, C_m. In this picture, there are many gauge equivalent configuration of line operators, since 1-form gauge transformation $B_e \mapsto B_e + \text{d}\xi, B_m \mapsto B_m + \text{d}\eta$ amounts to deforming the web of line operators. Here, due to nontrivial braiding statistics between e and m, the partition function $\mathcal{Z}(B_e, B_m)$ is no longer invariant for gauge equivalent configurations of background fields (see Fig.4.2). For example, under $\mathbb{Z}_2^e$ gauge transformation $a \mapsto a + \xi/2, B_e \mapsto B_e' = B_e - \text{d}\xi$, we observe phase ambiguity of partition function as

$$\mathcal{Z}(B_e, B_m) \mapsto \exp\left(\pi \text{i} \int_X \frac{\xi}{2\pi} \wedge \frac{B_m}{2\pi}\right) \mathcal{Z}(B_e, B_m) = (-1)^{\text{Lk}[C_e' - C_e, C_m]} \mathcal{Z}(B_e, B_m), \tag{4.24}$$

which signals a mixed 't Hooft anomaly involving $\mathbb{Z}_2^e$ and $\mathbb{Z}_2^m$ symmetries.

This phase ambiguity is cancelled by gauge variation of (3+1)d bulk topological action,

$$S_{\text{bulk}} = -\pi \text{i} \int_Y \frac{B_e}{2\pi} \wedge \frac{B_m}{2\pi}, \tag{4.25}$$

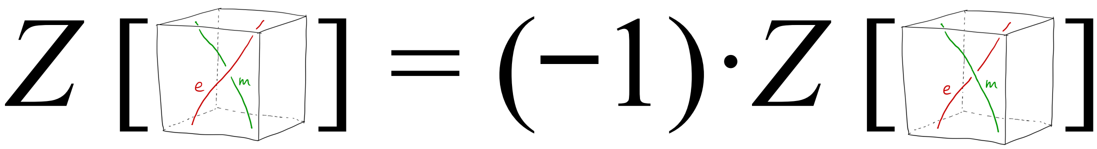

Figure 4.2: Background gauge fields of $\mathbb{Z}_2^e, \mathbb{Z}_2^m$ are specified by the web of line operators e (red), and m (green) respectively. Reflecting mutual statistics of e and m, the phase of partition function has ambiguity for gauge equivalent configurations of background fields.

where $\partial Y = X$. Here, we note that background gauge field of 1-form symmetry is generally expressed by assigning codimension 2 defects (which is supported on Poincaré dual of 2-form background field). In our case, the background field in the 4d bulk is an assignment of $(4-2)$d defects of $\mathbb{Z}_2 \times \mathbb{Z}_2$ 1-form symmetry, which become $(3-2)$d defects (supported on C_e, C_m) when restricted to 3d boundary. Our situation here is somewhat similar to (1+1)d Haldane chain introduced in Section 2.1, where we had a network of codimension 1 defect of $\mathbb{Z}_2 \times \mathbb{Z}_2$ 0-form symmetry on 2d bulk, cancelling anomaly on the boundary.

Let us explicitly see how symmetry defects on the (3+1)d bulk can cancel the anomaly, on a lattice model of the $(3+1)$d $\mathbb{Z}_2^e \times \mathbb{Z}_2^m$ SPT phase [33, 34]. We consider a lattice system of qubits in (3+1)d defined on a cubic lattice, where each edge (1-cell) and face (2-cell) contains one qubit. We label a face and edge by σ_2, σ_2^* respectively, where 1-cells are regarded as 2-cells on the dual lattice. We consider the following Hamiltonian (called RBH model [49]) known to simulate the SPT phase, which is given by

$$H_{\mathrm{RBH}} = -\sum_{\sigma_2} X(\sigma_2) Z(\partial\sigma_2) - \sum_{\sigma_2^*} X(\sigma_2^*) Z(\partial^*\sigma_2^*), \tag{4.26}$$

where $Z(\partial\sigma_2)$ is the product of Z operators on 1-cells contained in $\partial\sigma_2$, and $Z(\partial^*\sigma_2^*)$ is defined likewise on the dual lattice (see Fig.4.3). Like the Haldane chain Hamiltonian (2.1), the RBH Hamiltonian is also obtained by operating CZ circuits on the trivial Hamiltonian,

$$H_{\mathrm{RBH}} = \mathcal{U}_{CZ} H_0 \mathcal{U}_{CZ}^{\dagger}, \tag{4.27}$$

where

$$H_0 = -\sum_{\sigma_2} X(\sigma_2) - \sum_{\sigma_2^*} X(\sigma_2^*), \tag{4.28}$$

and

$$\mathcal{U}_{CZ} = \prod_{\sigma_2, \sigma_2^*} \left(\prod_{\sigma_1' \in \partial\sigma_2} (CZ)_{\sigma_2, \sigma_1'} \right) \left(\prod_{\sigma_1'^* \in \partial^*\sigma_2^*} (CZ)_{\sigma_2^*, \sigma_1'^*} \right). \tag{4.29}$$

This expression ensures that the ground state is unique and short-range entangled.

Let us refer to symmetries of the RBH Hamiltonian. We have two $\mathbb{Z}_2$ 1-form symmetries $\mathbb{Z}_2^e, \mathbb{Z}_2^m$ generated by

$$U_e(C_2) = \prod_{\sigma_2 \in C_2} X(\sigma_2), \quad U_m(C_2^*) = \prod_{\sigma_2^* \in C_2^*} X(\sigma_2^*), \tag{4.30}$$

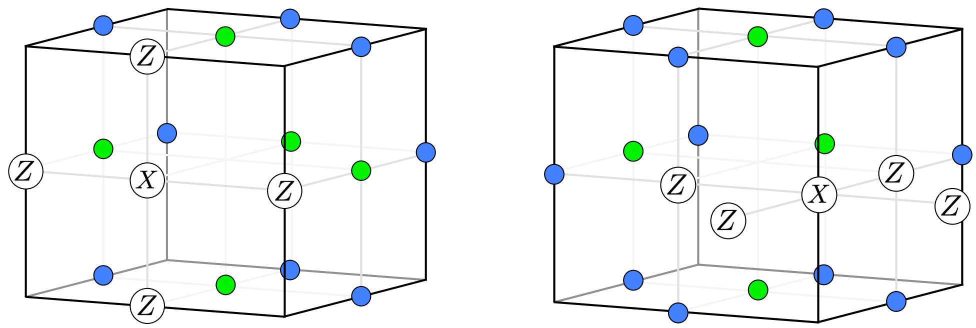

Figure 4.3: Local Hamiltonians of the RBH model. left: $X(\sigma_2)Z(\partial\sigma_2)$, right: $X(\sigma_2^*)Z(\partial^*\sigma_2^*)$.

for a 2-cycle C_2 and dual 2-cycle C_2^*. In Hamiltonian formalism, we can implement a symmetry defect by acting a symmetry generator at a certain time slice, as we did in the study of the Haldane chain. Charged objects are expressed as

$$W_e(C_1^*) = \prod_{\sigma_1^* \in C_1^*} Z(\sigma_1^*), \quad W_m(C_1) = \prod_{\sigma_1 \in C_1} X(\sigma_1). \tag{4.31}$$

In the presence of boundaries, we can actually see that these two symmetry defects are realized as line operators e, m of toric code on boundaies, respectively. Concretely, let us assume that 2-cycles C_2, C_2^* support symmetry defects, which intersect with the boundary on lines C_e, C_m. Then, symmetry generators $U_e(C_2), U_m(C_2^*)$ act only on boundary degrees of freedom on the ground state Hilbert space,

$$\begin{aligned} U_e(C_2) &= \prod_{\sigma_2 \in C_2} X(\sigma_2) = \prod_{\sigma_1 \in C_e} Z(\sigma_1), \\ U_m(C_2^*) &= \prod_{\sigma_2^* \in C_2^*} X(\sigma_2^*) = \prod_{\widetilde{\sigma_1} \in C_m} X(\widetilde{\sigma_1}) Z(\sigma_1^*), \end{aligned} \tag{4.32}$$

where we used $X(\sigma_2)Z(\partial\sigma_2) = X(\sigma_2^*)Z(\partial^*\sigma_2^*) = 1$ satisfied on the ground state. In this expression, $\sigma_1, \widetilde{\sigma_1}$ are contained in C_e, C_m defined on boundary, and σ_1^* denotes a 2-cell (dual 1-cell) in the bulk, neighboring $\widetilde{\sigma_1}$ (see Fig. 4.4). Here, we see that these generators simulate the braiding of line operators of toric code,

$$U_e(C_2) U_m(C_2^*) U_e(C_2)^\dagger = (-1)^{\mathcal{I}[C_e, C_m]} U_m(C_2^*), \tag{4.33}$$

which is consistent with cancellation of anomaly by the partition function on bulk, whose gauge variation is described by braiding phase of symmetry defects on the boundary.

4.3 Anomaly of $SU(N)$ pure Yang-Mills theory at $\theta = \pi$

In this section, we give a review on anomaly in (3+1)d pure $SU(N)$ Yang-Mills theory involving CP and center symmetry, to see how 't Hooft anomaly provides rigorous constraint on the vacuum structure of quantum field theories. We consider the 4d $SU(N)$ Yang Mills theory given by

$$S = -\frac{1}{2g^2} \int \mathrm{Tr}\,(F \wedge *F) + \frac{\mathrm{i}\theta}{8\pi^2} \int \mathrm{Tr}\,(F \wedge F)\,, \tag{4.34}$$

Since CP flips the sign of $\int F \wedge F$ term, CP symmetry exists only for $\theta = 0, \pi$.

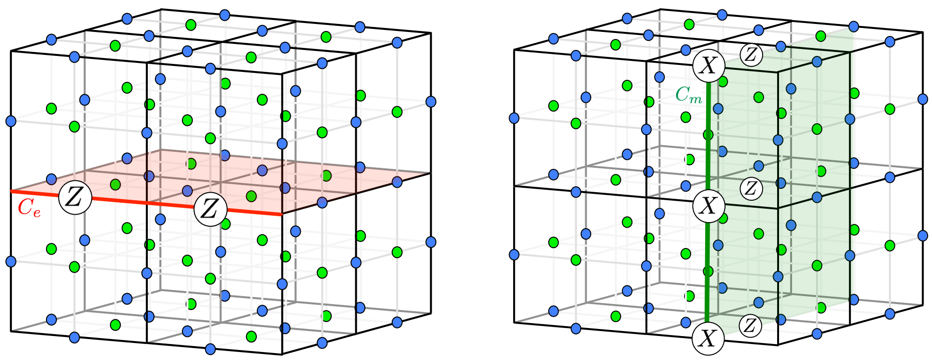

Figure 4.4: Symmetry defect of $\mathbb{Z}_2^e$ (left), $\mathbb{Z}_2^m$ (right) symmetry. These defects acts only on the boundary degrees of freedom, and behave as line operators of toric code.

center symmetry

Here we recall the center symmetry of $SU(N)$ Yang-Mills theory. Since gauge fields are left invariant under center $\mathbb{Z}_N$ in the gauge group $SU(N)$, the gauge transformation is determined only up to elements of $\mathbb{Z}_N$. Then, given a nontrivial cycle C in the spacetime, we can think of gauge transformation by $g \in SU(N)$, which is not single-valued along C parametrized by θ with $0 \leq \theta < 2\pi$,

$$g(2\pi) = \mathrm{e}^{2\pi \mathrm{i}/N} \cdot g(0). \tag{4.35}$$

This transformation leaves the action invariant, but we can see that the transformation (4.35) acts nontrivially on Wilson line operators

$$W(C) = \mathrm{Tr}\left[\mathcal{P}\exp\left(\mathrm{i}\oint_C a\right)\right]. \tag{4.36}$$

Under the transformation $a \mapsto a^g = gag^{-1} - \mathrm{i}g\mathrm{d}g^{-1}$ with (4.35), $W(C)$ transforms as

$$\begin{aligned}
W^g(C) = \mathrm{Tr}\left[\mathcal{P}\exp\left(\mathrm{i}\oint_C a^g\right)\right] &= \mathrm{Tr}\left[\prod_{i=0}^{n-1}\exp\left(\mathrm{i}\int_{x_i}^{x_{i+1}} a^g\right)\right] \\
&= \mathrm{Tr}\left[\mathcal{P}\prod_{i=0}^{n-1}(1+\mathrm{i}\Delta x a^g + \mathcal{O}(\Delta x^2))\right] \\
&= \mathrm{Tr}\left[\mathcal{P}\prod_{i=0}^{n-1} g_i(1+\mathrm{i}\Delta x a)(g_i^{-1} + \Delta x \mathrm{d}g^{-1}) + \mathcal{O}(\Delta x^2)\right] \\
&= \mathrm{Tr}\left[\mathcal{P}\prod_{i=0}^{n-1} g_i \exp\left(\mathrm{i}\int_{x_i}^{x_{i+1}} a\right) g_{i+1}^{-1} + \mathcal{O}(\Delta x^2)\right] \\
&= \mathrm{Tr}\left[g(0)\mathcal{P}\exp\left(\mathrm{i}\oint_C a\right) g(2\pi)\right] \\
&= \mathrm{e}^{2\pi\mathrm{i}/N} W(C).
\end{aligned} \tag{4.37}$$

Namely, the transformation shifts the Wilson line operator along C by $\mathbb{Z}_N$ phase, and is called the center transformation. It should be emphasized that the center symmetry associated with this transformation is interpreted as a $\mathbb{Z}_N$ 1-form symmetry shifting a by flat connection, $a \mapsto a + \epsilon/N$, where $\epsilon \in Z^1(X, \mathbb{R}/2\pi\mathbb{Z})$.

gauging center symmetry

To detect the anomaly, we introduce 2-form $\mathbb{Z}_N$ background gauge field coupled with the center symmetry. The $\mathbb{Z}_N$ background field is represented in the continuum theory by the pair (B, C), where B is a $U(1)$ 2-form field, C is a $U(1)$ 1-form field with the relation $NB = \mathrm{d}C$ satisfied. Such relation is incorporated by adding a multiplier term to the Lagrangian as $\frac{1}{2\pi} u \wedge (NB - \mathrm{d}C)$, which makes B into a $\mathbb{Z}_N$ field by integrating the multiplier u [5, 31].

To couple the $U(1)$ 2-form field B to center symmetry in $SU(N)$ gauge theory, we extend the gauge group from $SU(N)$ to $U(N) = [SU(N) \times U(1)] / \mathbb{Z}_N$, and gauge the $U(1)$ 1-form symmetry of the extended group by coupling to B. Let us denote the extended $U(N)$ gauge field as a'. Here, we postulate the invariance under $U(1)$ 1-form gauge transformation,

$$B \mapsto B + \mathrm{d}\lambda, \quad a' \mapsto a' + \lambda \mathbf{1}_N, \quad C \mapsto C + N\lambda, \tag{4.38}$$

where λ is a $U(1)$ 1-form field, and $\mathbf{1}_N$ denotes an identity matrix of size N. From now on, we sometimes omit $\mathbf{1}_N$ from the expression of gauge fields. We can check that the relation $NB = \mathrm{d}C$ is invariant under the gauge transformation.

To eliminate $U(1)$ photon, we introduce a $U(1)$ 2-form field u' as a multiplier and add to the Lagrangian the following term

$$\frac{1}{2\pi} u \wedge (\mathrm{Tr} F' - \mathrm{d}C), \tag{4.39}$$

where we denote the field strength of a' as F'. If we decompose the $U(1)$ gauge field a' into $SU(N)$ part and $U(1)$ part as

$$a' = a + \frac{1}{N} \hat{A} \cdot \mathbf{1}_N \tag{4.40}$$

with $\hat{A}$ a $U(1)$ gauge field, integrating the multiplier u' sets $\hat{A} \sim C$ up to gauge transformation. Especially, we recover the original $SU(N)$ gauge theory in the absence of background field $(B, C) = (0, 0)$, since one can eliminate the $U(1)$ part of $U(N)$ gauge field by the gauge transformation (4.38).

Now we couple background field to the Yang-Mills theory with extended gauge group in gauge invariant fashion, as

$$S = -\frac{1}{2g^2} \int \mathrm{Tr}\left((F' - B) \wedge *(F' - B)\right) + \frac{\mathrm{i}\theta}{8\pi^2} \int \mathrm{Tr}\left((F' - B) \wedge (F' - B)\right), \tag{4.41}$$

where we omitted multiplier terms. Here, the mixed anomaly between CP and center symmetry appears as the violation of CP symmetry, in the presence of background gauge field B. Since CP flips the sign of θ term and leaves the kinetic term unchanged, only θ term contributes to the variation. Thus, for $\theta = 0$ there is no mixed anomaly. For $\theta = \pi$, the change of the action $\mathsf{CP} : \theta \mapsto -\theta$ is given by

$$\begin{aligned}
\Delta S &= -\frac{\mathrm{i}}{4\pi} \int \mathrm{Tr}\left((F' - B) \wedge (F' - B)\right) \\
&= -\frac{\mathrm{i}}{4\pi} \int \left[\mathrm{Tr}(F' \wedge F') - 2B \cdot \mathrm{Tr} F' + N \cdot B \wedge B\right] \\
&= -\frac{\mathrm{i}}{4\pi} \int \mathrm{Tr}(F' \wedge F') + \frac{\mathrm{i}}{4\pi N} \int \mathrm{d}C \wedge \mathrm{d}C,
\end{aligned} \tag{4.42}$$

where we used $\mathrm{Tr}F' = NB = \mathrm{d}C$ in the third line of the equation. Since the first term takes the value in $2\pi\mathrm{i}\mathbb{Z}$ on spin manifolds due to index theorem, the variation of partition function becomes

$$\mathcal{Z}[B,C] \mapsto \exp\left[\frac{\mathrm{i}}{4\pi N}\int \mathrm{d}C \wedge \mathrm{d}C\right] \cdot \mathcal{Z}[B,C]. \tag{4.43}$$

We are tempted to deduce the presence of anomaly just by observing phase ambiguity (4.43). However, the theory is free of 't Hooft anomaly if one can eliminate the ambiguity by adding local counterterms. In this case, we can think of a counterterm in the form of

$$\frac{\mathrm{i}p}{4\pi N}\int \mathrm{d}\hat{A} \wedge \mathrm{d}\hat{A}. \tag{4.44}$$

Under $U(1)$ 1-form gauge transformation $\hat{A} \mapsto \hat{A} + N\lambda$ (4.38), the counterterm shifts by

$$\frac{\mathrm{i}p}{2\pi}\int \mathrm{d}\lambda \wedge \mathrm{d}\hat{A} + \pi\mathrm{i}pN\int \frac{\mathrm{d}\lambda}{2\pi} \wedge \frac{\mathrm{d}\lambda}{2\pi}. \tag{4.45}$$

The first term is quantized as $2\pi\mathrm{i}\mathbb{Z}$ for arbitrary integer p. On spin manifolds, the second term also becomes $2\pi\mathrm{i}\mathbb{Z}$ for $p \in \mathbb{Z}$ due to index theorem (for non-spin manifolds, we must require $Np/2 \in \mathbb{Z}$). We can restore CP symmetry at $\theta = \pi$ even in the presence of background field, by choosing p properly. Actually, with the counterterm (4.44) the variation of the action under CP becomes

$$\mathcal{Z}[B,C] \mapsto \exp\left[\frac{(-2p+1)\mathrm{i}}{4\pi N}\int \mathrm{d}C \wedge \mathrm{d}C\right] \cdot \mathcal{Z}[B,C], \tag{4.46}$$

since CP flips the counterterm. Hence, the action at $\theta = \pi$ is CP-invariant on spin manifolds, when

$$-2p + 1 \equiv 0 \qquad \mathrm{mod}\ N. \tag{4.47}$$

Next, let us take a look at $\theta = 0$. The variation at $\theta = 0$ becomes

$$\mathcal{Z}[B,C] \mapsto \exp\left[\frac{-2p\mathrm{i}}{4\pi N}\int \mathrm{d}C \wedge \mathrm{d}C\right] \cdot \mathcal{Z}[B,C], \tag{4.48}$$

Thus, anomaly-free condition at $\theta = 0$ on spin manifolds is

$$-2p \equiv 0 \qquad \mathrm{mod}\ N. \tag{4.49}$$

We can obatin the following consequences from the anomaly-free conditions (4.47), (4.49);

- For even N, we immediately see from (4.47) that the Yang-Mills theory suffers from 't Hooft anomaly at $\theta = \pi$ for arbitrary integer p.

- For odd N, the theory at $\theta = \pi$ is anomaly-free by setting the counterterm $p = (-N+1)/2$. However, this p manifestly violate CP at $\theta = 0$. We observe that there is no integer p which satisfies anomaly-free conditions at both $\theta = 0, \pi$ (4.47), (4.49). It is known that $\theta = 0$ has trivially gapped spectrum with unique ground state (i.e., non-anomalous), hence we conclude that the theory again suffers from 't Hooft anomaly at $\theta = \pi$.

  Further, if we assume that $0 \leq \theta < \pi$ realizes gapped trivial spectrum with no first order transition, we can conclude the first order transition occurs exactly at $\theta = \pi$.

In conclusion, we deduce that the Yang-Mills theory is anomalous at $\theta = \pi$ for arbitrary N. Reflecting 't Hooft anomaly in infrared, the theory at $\theta = \pi$ must have low energy degrees of freedom which accounts for violation of CP symmetry after coupling to background fields. We list possible fates of low energy spectrum here:

1. CP or center symmetry is spontaneously broken. Here, we note it is widely believed that the Wilson line is confined for all θ at zero temperature. Confinement of the Wilson line means that the center symmetry is unbroken, since charged object under center symmetry has exponentially decaying expectation value according to its length. Therefore, we conclude that broken symmetry must be CP, which leads to two-fold degeneracy of ground states.

2. The low-energy theory is described by TQFT with nontrivial topological order.

3. The spectrum is gapless.

Chapter 5

Lieb-Schultz-Mattis type theorem

In Chapter 4, we have observed an 't Hooft anomaly involving center symmetry and CP symmetry in $SU(N)$ pure Yang-Mills theory, where the anomaly provides a rigorous constraint on low energy spectrum of the IR theory, dictating spontaneous breaking of CP symmetry. In this chapter, we examine the spectral constraint thanks to the 't Hooft anomaly in condensed matter literature, which is celebrated as the Lieb-Schultz-Mattis (LSM) type theorem [50–52].

Historically, the LSM theorem was originally constructed for (1+1)d quantum spin chains [50]. Roughly speaking, the LSM theorem states that quantum spin chains with half-odd integer spin per unit cell cannot be trivial symmetric insulator; the ground state must spontaneously break the lattice translational symmetry. In higher dimensions, the LSM constraint is also accounted by the spontaneous breaking of $SO(3)$ spin rotation symmetry, or by nontrivial topological order [53]. Such obstruction to opening trivial gap is reminiscent of 't Hooft anomalies that appear on the boundary of SPT phases, as we have seen in the previous chapter. Actually, it was proposed that the half-odd integer spin systems are equivalent to the surface state of SPT phases protected by spin rotation and lattice translational symmetry. For instance, a (2+1)d $S = 1/2$ spin system is regarded as boundary of a (3+1)d system composed of an array of Haldane chains placed in translation symmetric fashion [54]. Based on these observations, we expect that the LSM constraint is understood as an 't Hooft anomaly in continuum field theory description, which is accounted by an SPT phase (as a conceptual tool) in the bulk. In recent years, the LSM theorem has been generalized for various combination of internal and spatial symmetries [55–66].

Although anomalies involving onsite symmetry solely are well understood as we have seen in Chapter 2, understanding for the anomalies involving crystal symmetries are still under development, mainly because crystal symmeties on a lattice cannot be gauged, due to their non-onsite nature. However, it should be noted that crystal symmetries like lattice translational symmetries can reduce to *internal* symmetries after taking continuum IR limit, allowing us to discuss 't Hooft anomalies in continuum field theory by introducing standard background fields. In this chapter, we explicitly see that the LSM constraint manifests itself as a mixed 't Hooft anomaly involving internal symmetry (e.g., $SO(3)$ spin rotation symmetry, charge $U(1)$ symmetry...), and internal version of lattice symmetry. [61–63, 67] Moreover, recent developments of anomalies based on higher-form symmetries implies the existence of LSM-type constraints involving higher-form symmetries. Actually, we can explicitly construct the LSM-type theorems on lattice systems which relies on lattice translational symmetry and higher-form symmetry, which are applied, for example, to pure abelian gauge theory constructed on a lattice. Concretely, the generalized Lieb-Schultz-Mattis theorem for p-form symmetries dictates the impossibility of having trivial gapped state without breaking p-form $U(1)$ and lattice translational symmetries, when the "filling factor" of the p-form symmetry is fractional (see Section 5.3).

Here, the filling for the charge of p-form symmetry is defined as follows: the $(d-p)$-dimensional hyperplane $M_{(d-p)}$ that supports the generator of the n-form symmetry is chosen so that $M_{(d-p)}$ is extended by $(d-p)$ unit lattice vectors among the d lattice vectors that constitute the whole system. With such choice, the filling is just defined as the charge per $(d-p)$-dimensional unit cell, measured on the hyperplane $M_{(d-p)}$.

The proof of the generalized theorem is in parallel with that of the original theorem by Oshikawa [51]: we first introduce the background gauge field coupled with the $U(1)$ global symmetry and consider the "adiabatic insertion" of the unit background magnetic flux, respecting the translation symmetry in the system. The unit magnetic flux can be eliminated by the homotopically non-trivial gauge transformation (the large gauge transformation), which can change the lattice momentum of the ground state depending on the filling of the 1-form charge of the ground state. This leads to the degeneracy of the ground states with different momentum.

As an interesting example that demonstrates the theorem, we consider the lattice gauge theory that simulates the dynamics of the (2+1)-dimensional quantum dimer model (QDM) on a bipartite lattice. This theory is a pure $U(1)$ lattice gauge theory whose Hamiltonian is analogous to the familiar compact quantum electrodynamics (CQED), but its Gauss law is modified from that of CQED due to the presence of background staggered charge density. This theory has a 1-form $U(1)$ global symmetry, which leads to the conservation of the number of dimers on a certain one dimensional closed string in the QDM. Then, the LSM theorem based on the 1-form symmetry and the lattice translation symmetry, implies that the system cannot be trivially gapped if the filling of the dimer on a deliberately chosen string is fractional. This result is explicitly demonstrated on the phase diagram of the QDM on the honeycomb and square lattice. For example, the filling of the 1-form symmetry is calculated as $\nu = 1/3$ in two neighboring gapped crystal (columnar and plaquette) phases of the QDM on the honeycomb lattice. In these phases the lattice translation symmetry is spontaneously broken, and the 3-fold degenerate ground states appear accordingly, which are related by the lattice translation to each other. A more interesting case is the incommensurate crystal found between two distinct crystal (plaquette and staggered) phases, where the gapless excitation called phason emerges. This gapless spectrum is enforced by the irrational filling of the 1-form charge realized in the incommensurate crystal.

A remarkable feature of the QDM is the existence of the special point called the Rokhsar-Kivelson (RK) point, where the exact ground state wavefunction can be obtained by the equal weight superposition of all dimer configuration states. When the lattice is bipartite, the RK point appears as a quantum criticality between the plaquette crystal and incommensurate ordered phase. The RK critical point on a bipartite lattice is described in the continuum by the quantum Lifshitz model, which is dual to a $U(1)$ gauge theory by the standard boson-vortex duality. In the continuum description, the LSM constraint is manifested in the form of the mixed 't Hooft anomaly afflicting the symmetries, by treating the lattice translation as an internal symmetry. We diagnose the 't Hooft anomaly for the 1-form $U(1)$ symmetry and the effective internal version of lattice translation, in the field theory which reproduces the vicinity of the RK critical point.

5.1 Oshikawa's argument

Here we recall a heuristic proof of Lieb-Schultz-Mattis theorem in general $(d+1)$ dimension by Oshikawa [51], which is a generalized version of Laughlin's argument. Namely, the argument proceeds by piercing unit flux of $U(1)$ background gauge field through the cylinder adiabatically, and looking at spectral flow of the system according to flux insertion.

Setup

- General quantum many-body system on $(d+1)$ dimensional lattice.
- $\mathcal{T}_x$: lattice translational operator in x-direction, s.t. $(\mathcal{T}_x)^L = 1$, i.e., periodic boundary condition with size L.
- Particle number conservation associated to global $U(1)$ symmetry.
- Given a "cross section" $C = \prod_{i(i\neq x)} L_i$, total volume is CL. Filling ν is fractional, $\nu = p/q$, s.t. $\gcd(p,q) = \gcd(C,q) = 1$.

Then, the proof proceeds as follows:

1. <u>$U(1)$ flux insertion</u>

   We introduce background $U(1)$ gauge field A for charge $U(1)$ global symmetry. Let us consider the time-dependent configuration of A that corresponds to "adiabatic flux insertion";

$$\begin{cases} A_x = 0 & t < 0, \\ A_x(\vec{r},t) = 2\pi t/LT & 0 \leq t \leq T, \\ A_x(\vec{r},t) = 2\pi/L & t > T, \end{cases} \tag{5.1}$$

   and $A_t = 0, A_j = 0$ for $x \neq j$. This configuration corresponds to threading flux $\Phi := \int_x A_x \mathrm{d}x$ from 0 to 2π,

$$\Phi_{t=0} = 0 \mapsto \Phi_{t=T} = 2\pi. \tag{5.2}$$

   Let us assume that the system is always gapped during the adiabatic flux insertion. Then, the ground state changes according to adiabatic process as

$$|\Psi_0\rangle \mapsto |\Psi_0'\rangle\,, \tag{5.3}$$

   The initial ground state is taken to be an eigenstate of $\mathcal{T}_x$, $\mathcal{T}_x |\Psi_0\rangle = e^{\mathrm{i}p_x} |\Psi_0\rangle$. We remark that the initial and final state possess identical momentum $\mathcal{T}_x |\Psi_0'\rangle = e^{\mathrm{i}p_x} |\Psi_0'\rangle$, since the adiabatic process (5.1) is performed in translational invariant fashion.

2. <u>Spectral flow</u>

   It should be emphasized that the adiabatic process is not gauge transformation, and hence the Hamiltonian is not invariant,

$$H_{\Phi=0} \neq H_{\Phi=2\pi}. \tag{5.4}$$

   However, the initial and final Hamiltonian are connected by large gauge transformation, which shifts the holonomy in x direction Φ by 2π. The generator of large gauge transformation is expressed as

$$U := \exp\left[\sum_x \frac{2\pi \mathrm{i}}{L} \sum_{\vec{r}} x \hat{n}_{\vec{r}}\right], \tag{5.5}$$

   where $\hat{n}_{\vec{r}}$ is the generator of $U(1)$ symmetry on a vertex $\vec{r}$. We have

$$U H_{\Phi=2\pi} U^\dagger = H_{\Phi=0}. \tag{5.6}$$

Therefore, we obtain a ground state of $H_{\Phi=0}$ by acting U on the ground state of $H_{\Phi=2\pi}$; $U\,|\Psi'_0\rangle$ is a ground state of H_0. What we have done is summarized as follows:

$$\begin{array}{ccccc} H_0 & \xrightarrow{\text{flux insertion}} & H_{2\pi} & \xrightarrow{U} & H_0 \\ |\Psi_0\rangle & \xrightarrow{\text{flux insertion}} & |\Psi'_0\rangle & \xrightarrow{U} & U|\Psi'_0\rangle. \end{array} \tag{5.7}$$

Now we have constructed two (possibly different) ground states of H_0, $|\Psi_0\rangle$ and $U|\Psi'_0\rangle$.

A crucial observation is that the momentum eigenvalue of the final state is different from the initial one. Recall that

$$P_x|\Psi_0\rangle = p_x|\Psi_0\rangle, \quad P_x|\Psi'_0\rangle = p_x|\Psi'_0\rangle, \tag{5.8}$$

where P_x is momentum in x direction. Also notice the following commutation relation,

$$[P_x, U] = [P_x, \mathrm{e}^{\frac{2\pi\mathrm{i}}{L}\sum_{\vec{r}} x\hat{n}_{\vec{r}}}] = \left(2\pi\frac{Q}{L}\right)U = \left(2\pi\frac{Q}{LC}C\right)U = \left(2\pi\frac{p}{q}C\right)U, \tag{5.9}$$

where $[x, P_x] = \mathrm{i}$, $Q = \sum_{\vec{r}}\hat{n}_{\vec{r}}$, and filling fraction $p/q = Q/(LC)$. Then, we observe the following

$$P_x U|\Psi'_0\rangle = UP_x|\Psi'_0\rangle + [P_x, U]|\Psi'_0\rangle = \left(p_x + 2\pi\frac{p}{q}C\right)U|\Psi'_0\rangle \tag{5.10}$$

Hence, the momentum eigenvalue of $U|\Psi'_0\rangle$ is different from that of $|\Psi_0\rangle$, and hence, different ground state. Particularly, the condition that $\gcd(p,q) = \gcd(C,q) = 1$ tells us that there is at least q-fold degeneracy in the ground states if the finite excitation gap exists as we assumed. Invalidation of the assumption means the gapless ground state. Therefore, we proved the LSM theorem.

5.2 LSM theorem and 't Hooft anomaly

5.2.1 (1+1)d spinless fermion system

Let us first illustrate the connection of LSM-type constraint to 't Hooft anomaly in continuum description with a simple example [61]. We begin with considering a chain of spinless complex fermions in (1+1) dimension with length L,

$$H = -t\sum_j (c_x^\dagger c_{x+1} + \text{h.c.}) - \mu\sum_j c_x^\dagger c_x \tag{5.11}$$

with the periodic boundary condition $c_{L+1} = c_1$. The system has $U(1)$ symmetry and lattice translation symmetry $\mathcal{T}$

$$\begin{aligned} U(1): &\quad c_x \mapsto e^{\mathrm{i}\phi}c_x, \\ \mathcal{T}: &\quad c_x \mapsto c_{x+1}. \end{aligned} \tag{5.12}$$

The ground state of the system is given by filling single particle states under the Fermi sea $|\text{GS}\rangle = \prod_{|k|\le k_\text{F}} c_k^\dagger\,|\text{vac}\rangle$, where $|\text{vac}\rangle$ denotes the Fock vacuum. The filling ν of the ground state $\nu = k_\text{F}/\pi$ is fractional, where the LSM theorem prohibits trivial symmetric insulator.

We would like to see the counterpart of LSM constraint in continuum description. To this end, we expand the fermion operator in the vicinity of Fermi points,

$$c_x \approx \psi^{\mathrm{R}}(x)\mathrm{e}^{\mathrm{i}k_{\mathrm{F}}x} + \psi^{\mathrm{L}}(x)\mathrm{e}^{-\mathrm{i}k_{\mathrm{F}}x}. \tag{5.13}$$

The gapless excitation is captured by the following continuum theory

$$H = \int \mathrm{d}x \Psi^{\dagger}(x)(-\mathrm{i}v_{\mathrm{F}}\partial_x)\sigma_z\Psi(x), \tag{5.14}$$

with $\Psi(x) := (\psi_R(x), \psi_L(x))^T$. It is noted that Ψ is a coarse-grained field in the sense that it is not sensitive to microscopic lattice scale, i.e., $\Psi(x+1) \approx \Psi(x)$. The transformation law of Ψ under the symmetries can be read off as

$$U(1) : \Psi(x) \mapsto \mathrm{e}^{\mathrm{i}\phi}\Psi(x), \tag{5.15}$$

$$\mathcal{T} : \Psi(x) \mapsto \mathrm{e}^{\mathrm{i}k_{\mathrm{F}}\sigma_z}\Psi_x = \mathrm{e}^{\mathrm{i}\pi\frac{p}{q}\sigma_z}\Psi_x, \tag{5.16}$$

where we have used $\nu = p/q = k_{\mathrm{F}}/\pi$. The translational symmetry is converted to internal $\mathbb{Z}_q$ chiral symmetry. Hence, the conflict between $\mathcal{T}$ and $U(1)$ on a lattice manifests itself as chiral anomaly in the continuum description.

To make the connection between the lattice and continuum descriptions even clearer let us remind ourselves the 't Hooft anomaly and anomaly matching condition briefly. A quantum field theory (QFT) with a global symmetry G and its background gauge field A is described by a partition function $\mathcal{Z}[A]$. We say that there is G-'t Hooft anomaly if the partition function is not invariant under the background gauge transformation,

$$\mathcal{Z}[A] \mapsto \mathcal{Z}[A + \mathrm{d}\lambda] = \mathcal{Z}[A]\mathrm{e}^{\mathrm{i}\mathcal{A}[\lambda, A]}. \tag{5.17}$$

We sometimes call $\mathcal{A}[\lambda, A]$ an anomaly or an anomalous phase. 't Hooft anomalies is invariant under renormalization group flow, which leads to the celebrated 't Hooft's anomaly matching. Provided the G-'t Hooft anomaly, the anomaly matching condition imposes constraints on the ground state of the QFT that it must be either of

- gapless,
- gapped with degenerate ground states,
- spontaneously G-broken.

5.3 LSM theorem based on generalized global symmetries

In this section, we discuss the generalization of the LSM type theorem based on $U(1)$ 1-form symmetry and lattice translation symmetry, which are found in pure $U(1)$ lattice gauge theory. The proof of the generalized theorem runs in parallel with Oshikawa's argument for the original one: we introduce background gauge field coupled with 1-form symmetry, and perform "adiabatic insertion" of unit flux for background field. It turns out that the generalized theorem also has a continuum description in terms of 't Hooft anomaly involving 1-form symmetry. The LSM theorem for most general p-form $U(1)$ symmetry is constructed in Appendix E.

We begin with summarizing briefly how to formulate 1-form symmetry and its background gauge field on lattice systems. Lattice formulation is most easily done on a simplical complex obtained by triangulating a spacetime manifold M. 1-form field configuration is set up by assigning $a \in \mathbb{R}/2\pi\mathbb{Z}$ on each 1-simplex (edge), satisfying the following properties:

$$a_{(ij)} = -a_{(ji)} \quad \text{on a edge } (ij), \tag{5.18}$$
$$(\mathrm{d}a)_{(ijkl)} = a_{(ij)} + a_{(jk)} + a_{(ki)} \quad \text{lattice differential on a 2-simplex } (ijk), \tag{5.19}$$
$$a_{(ij)} \mapsto a_{(ij)} + \omega_{(ij)}, \quad \mathrm{d}\omega = 0, \quad U(1) \text{ 1-form transformation.} \tag{5.20}$$

Then, we introduce 2-form background gauge field B of 1-form symmetry (5.20), assigned on each 2-simplex (face). Gauge transformation is defined as

$$a_{(ij)} \mapsto a_{(ij)} + \lambda_{(ij)}, \quad B_{(ijk)} \mapsto B_{(ijk)} - (\mathrm{d}\lambda)_{(ijk)}. \tag{5.21}$$

5.3.1 1-form LSM theorem

Now we are ready to formulate the LSM theorem involving 1-form symmetry and lattice translation symmetry in $(d+1)$-dimensional lattice. Below we describe the setup for constructing the generalized theorem.

setup

- d-dimensional spatial hypercubic lattice labeled as

$$(x_1, x_2, \cdots, x_d) \in \mathbb{Z}_{L_1} \times \mathbb{Z}_{L_1} \times \cdots \times \mathbb{Z}_{L_d}. \tag{5.22}$$

- $U(1)$ 1-form gauge field $a_j(\vec{x})$ defined on each edge. In the previous notation, $a_j(\vec{x}) := a_{(\vec{x}, \vec{x}+\vec{e}_j)}$ with a unit lattice vector $\vec{e}_j$ in the j-th direction.

- Global symmetries: lattice translational symmetry $\mathcal{T}_l = \mathrm{e}^{\mathrm{i}P_l}$ in the l-th direction and $U(1)$ 1-form symmetry $U(1)_{[1]}$,

$$\mathcal{T}_l : a_j(\vec{x}) \mapsto a_j(\vec{x} + \vec{e}_l), \tag{5.23}$$
$$U(1)_{[1]} : a_j(\vec{x}) \mapsto a_j(\vec{x}) + \omega_j(\vec{x}). \tag{5.24}$$

  In particular, we can prepare ground states $|\Psi_0\rangle$ such that

$$P_l|\Psi_0\rangle = p_l|\Psi_0\rangle, \tag{5.25}$$

  which should also be invariant under $U(1)_{[1]}$ transformation.

- The filling is interpreted as $U(1)_{[1]}$ charge per unit area of hypersurface on which the generator of $U(1)_{[1]}$ symmetry is supported. More precisely, the charge here is defined to be the intersection number between Wilson lines and a generator supported on $(d-1)$ dimensional hypersurface which is set at $x_m = 0$ with $l \neq m$ here. Accordingly, we define a cross section by $C = \prod_{i \neq l,m} L_i$ so that CL_l gives an area of the hypersurface (See Fig. 5.1).

Let us show that the low-energy spectrum is necessarily nontrivial if we have the filling $\nu = p/q$ for $U(1)_{[1]}$ charge measured on $x_m = 0$ at the ground state, based on the above setup. To this end, we first perform adiabatic insertion of 2-form background gauge field $B_{lm}(\vec{x})$, which is defined by $B_{ij}(\vec{x}) := B_{(\vec{x}, \vec{x}+\vec{e}_i, \vec{x}+\vec{e}_i+\vec{e}_j, \vec{x}+\vec{e}_j)}$ on each face of the lattice. Namely, the configuration of B gradually changes as time proceeds,

$$\begin{cases} B_{lm}(\vec{x}) = 0 & t < 0, \\ B_{lm}(\vec{x}) = \delta(x_m) \cdot 2\pi t / L_l T & 0 \leq t < T, \\ B_{lm}(\vec{x}) = \delta(x_m) \cdot 2\pi / L_l & T \leq t, \end{cases} \tag{5.26}$$

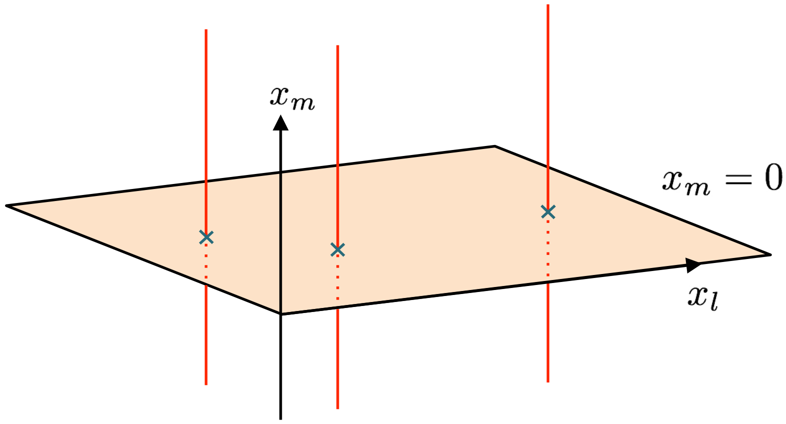

Figure 5.1: filling of $U(1)_{[1]}$ symmetry for (3+1)-dimensional systems. Charged objects of $U(1)_{[1]}$ symmetry are Wilson loops (red line), which are charged by a generator supported on a 2d surface $x_m = 0$ (orange plane). Filling is defined as the number of intersections (green dots) per unit area of the surface $x_m = 0$.

and other components are 0. We note that the holonomy of 2-form gauge field is given by integrating the 2-form field on a closed surface, and the final configuration at $t = T$ realizes "unit flux" of 2-form field B measured on lm-plane

$$\sum_{lm\text{-plane}} B_{lm} = \frac{2\pi t}{T} \qquad 0 \leq t \leq T. \tag{5.27}$$

Suppose that the spectrum is gapped at $t = 0$, and the gap does not close during the adiabatic process $0 \leq t \leq T$. Then, the initial state $|\Psi_0\rangle$ evolves into some ground state $|\Psi_0'\rangle$ at the end of the process $t = T$. Since the lattice translational symmetry is respected during the adiabatic process, the initial and final state share the identical momentum $P_l|\Psi_0\rangle = P_l\,|\Psi_0'\rangle = p_l|\Psi_0\rangle$.

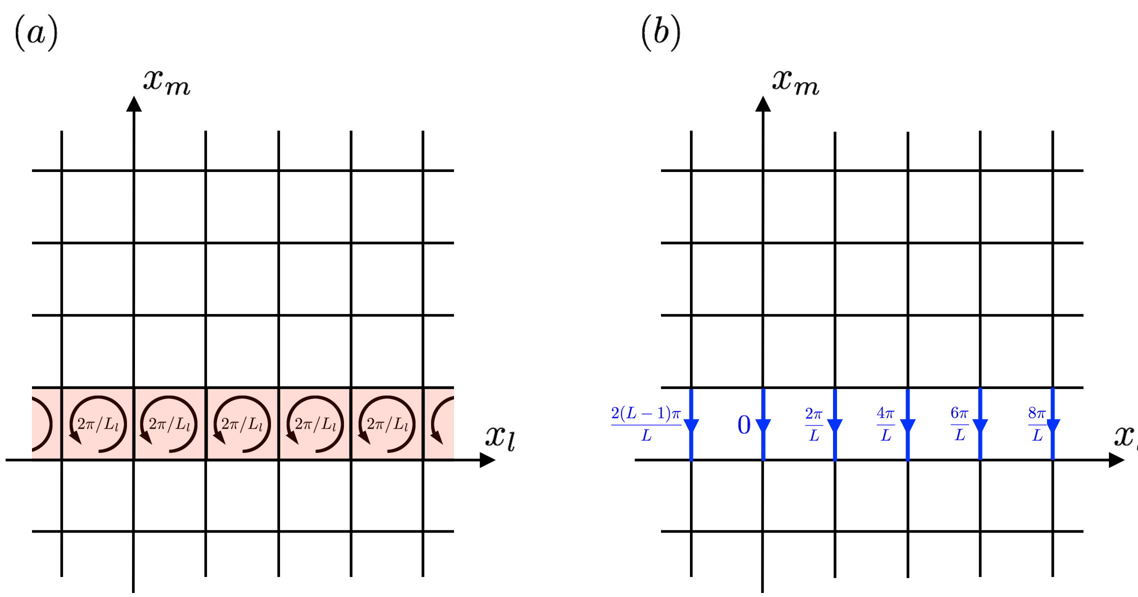

Figure 5.2: (a) Configuration of 2-form field B on lm-plane. (b) A large gauge transformation.

The final configuration of background field at $t = T$ is gauge equivalent to the initial one at $t = 0$ by the following $U(1)_{[1]}$ large gauge transformation

$$a_m(\vec{x}) \mapsto a_m(\vec{x}) + \delta(x_m)\frac{2\pi x_l}{L_l}, \tag{5.28}$$

$$B_{lm}(\vec{x}) \mapsto a_m(\vec{x}) - \delta(x_m)\frac{2\pi}{L_l}, \tag{5.29}$$

as shown in Fig. 5.2 (b). We write the generator of the above large gauge transformation (5.28) as U_{lm}. Then, $U_{lm}\,|\Psi'_0\rangle$ is also a ground state of the system before the adiabatic process (with $B = 0$ everywhere). To prove the ground states are degenerate it suffices to show that $|\Psi_0\rangle$ and $U_{lm}\,|\Psi'_0\rangle$ are orthogonal with each other. It can be seen by measuring the momentum eigenvalue of $U_{lm}\,|\Psi'_0\rangle$,

$$P_l U_{lm}|\Psi'_0\rangle = \left(p_l + 2\pi\frac{pC}{q}\right) U_{lm}|\Psi'_0\rangle, \tag{5.30}$$

where we have used a crucial relation

$$[P_l, U_{lm}] = \left(2\pi\frac{Q_m}{CL_l}C\right) U_{lm} = \left(2\pi\frac{pC}{q}\right) U_{lm}, \tag{5.31}$$

with the total $U(1)_{[1]}$ charge Q_m measured on $x_m = 0$ and filling fraction $p/q = Q_m/CL_l$. With an assumption $\gcd(pC, q) = 1$, we have found that $U_{lm}\,|\Psi'_0\rangle$ and $|\Psi_0\rangle$ are orthogonal with distinct momentum eigenvalues. Hence, we have proven that

Theorem 5.3.1 (LSMOH theorem for 1-form symmetry)
Consider a quantum many-body system defined on a d-dimensional periodic lattice, in the presence of a global 1-form $U(1)$ symmetry and a translation symmetry along the l-th primitive lattice vector, and assume that both symmetries are not broken. Then, if the $U(1)$ charge (measured on a $(d-1)$-dimensional hyperplane characterized by $x_m = 0$ for $m \neq l$) per unit cell is $\nu = p/q$ at the ground state, there are only two possibilities for the low energy spectrum:

1. *The system is gapped, and the ground states are at least q-fold degenerate, or*

2. *The system is gapless.*

5.3.2 LSM constraint on the quantum dimer model

In this section, we apply the generalization of the LSM theorem based on $U(1)_{[1]}$ symmetry to the quantum dimer model (QDM) on a honeycomb lattice. Previous applications of the original LSM theorem to the QDM are found in Refs. [68, 69]. The QDM describes the dynamics of dimers defined on each edge of a lattice. A dimer variable $l_{(ij)}$ takes a value in $\{0, 1\} \cong \mathbb{Z}_2$ representing the presence or absence of a dimer. They are subject to the geometric constraint called dimer constraint,

$$l_{(01)} + l_{(02)} + l_{(03)} = 1, \tag{5.32}$$

that the dimer variables emanating from each vertex sum to unit (see Fig.5.3).

The Hilbert space of the QDM is identified with the set of possible configurations of dimer variables on a lattice. Namely, we define a quantum state $|\mathcal{C}_{\text{dimer}}\rangle$ corresponding to each dimer configuration $\mathcal{C}_{\text{dimer}}$. The set of quantum states $\{|\mathcal{C}_{\text{dimer}}\rangle\}$ are orthogonal with each other

$$\langle\mathcal{C}_{\text{dimer}}|\,\mathcal{C}'_{\text{dimer}}\rangle = \delta_{\mathcal{C}_{\text{dimer}},\mathcal{C}'_{\text{dimer}}}. \tag{5.33}$$

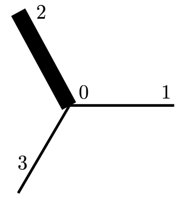

Figure 5.3: Dimer configuration around a vertex. Dimer variables $l_{(0i)} = 0$ (resp. 1) when the dimer is absent (resp. present) on an edge $(0i)$ for $i = 1, 2, 3$. The sum of dimer variables emanating from each vertex is 1.

and complete. The Hilbert space for the QDM is extended by $\{|\mathcal{C}_{\text{dimer}}\rangle\}$.

Here, we consider the QDM on a honeycomb lattice described by the Hamiltonian,

$$H_{\text{QDM}} = -t \underbrace{\sum_{\{\hexagon\}} \Big(|\hexagon\rangle\langle\hexagon| + |\hexagon\rangle\langle\hexagon| \Big)}_{\text{diagonal}} + v \underbrace{\sum_{\{\hexagon\}} \Big(|\hexagon\rangle\langle\hexagon| + |\hexagon\rangle\langle\hexagon| \Big)}_{\text{resonance (hopping)}}. \tag{5.34}$$

Remarkably, the QDM on a bipartite lattice can be rigorously converted to $U(1)$ lattice gauge theory that in turn makes it easier to apply the 1-form LSM theorem to constrain its ground state. With the parameter $v/t = 1$, known as the Rokhsar-Kivelson(RK) point, the ground state is expressed as the equal-weight superposition of possible dimer configurations. Moreover, the field theoretical description is known in the vicinity of the RK point. We shall find an 't Hooft anomaly and its constraint via anomaly matching, and make a connection to the LSM theorem.

Let us rewrite the Hamiltonian (5.34) in the form of $U(1)$ lattice gauge theory by the following procedure [70].

1. Lift the dimer variable from $\mathbb{Z}_2$ to $\mathbb{Z}$.

   Let $L_{(ij)}$ be an operator defined on a link (ij) whose eigenvalue is $l_{(ij)} \in \mathbb{Z}$ and $\Theta_{(ij)}$ be an conjugate momentum operator with eigenvalues in $[0, 2\pi)$. Then we add to the QDM Hamiltonian the following term

   $$H_K := K \sum_{(ij)} \left(L_{(ij)} - \frac{1}{2} \right)^2, \tag{5.35}$$

   which restricts $l_{(ij)}$ to take values $\{0, 1\}$ by taking a limit $K \to \infty$ and restore the original theory.

2. Express the QDM Hamiltonian (5.34) in terms of $L_{(ij)}$ and $\Theta_{(ij)}$.

   Provided an eigenstate of $L_{(ij)}$ by $|l_{(ij)}\rangle$,[1] the operator $\mathrm{e}^{\mathrm{i}\Theta_{(ij)}}$ plays a role of a ladder operator,

   $$L_{(ij)}|l_{(ij)}\rangle = l_{(ij)}|l_{(ij)}\rangle, \tag{5.36}$$
   $$L_{(ij)}\mathrm{e}^{\mathrm{i}\Theta_{(ij)}}|l_{(ij)}\rangle = (l_{(ij)} + 1)\mathrm{e}^{\mathrm{i}\Theta_{(ij)}}|l_{(ij)}\rangle. \tag{5.37}$$

[1] Precisely speaking, an eigenstate is given by dimer configuration covering the whole lattice, and hence, should be denoted as $|\{l_{(ij)}\}\rangle := \otimes_{(ij)}|l_{(ij)}\rangle$ with the dimer constraint.

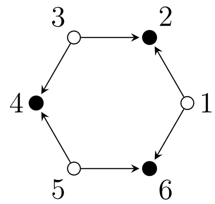

Figure 5.4: Numbering and sublattice assigning of each vertex on a hexagon. White circle represents a vertex contained in sublattice A, and black circle for sublattice B.

- Diagonal term
  Assigning a number for each vertex of a hexagon as shown in Fig. 5.4, the diagonal term of the QDM Hamiltonian can be written as follows,

$$
\begin{aligned}
&-t\sum_{\{\hexagon\}}\Big(|\hexagon\rangle\langle\hexagon| + |\hexagon\rangle\langle\hexagon|\Big)\\
&= -t\sum_{\{\hexagon\}}\big(L_{(12)}L_{(34)}L_{(56)} + L_{(23)}L_{(45)}L_{(61)}\big).
\end{aligned}
\tag{5.38}
$$

- Resonance term
  Using the ladder operator $\mathrm{e}^{\mathrm{i}\Theta_{(ij)}}|l_{(ij)}$ the resonance term is expressed as

$$
\begin{aligned}
&v\sum_{\{\hexagon\}}\Big(|\hexagon\rangle\langle\hexagon| + |\hexagon\rangle\langle\hexagon|\Big)\\
&= v\sum_{\{\hexagon\}}\big(\mathrm{e}^{\mathrm{i}(\Theta_{(12)}-\Theta_{(23)}+\Theta_{(34)}-\Theta_{(45)}+\Theta_{(56)}-\Theta_{(61)})} + \mathrm{h.c.}\big)\\
&= 2v\sum_{\{\hexagon\}}\cos(\Theta_{(12)}-\Theta_{(23)}+\Theta_{(34)}-\Theta_{(45)}+\Theta_{(56)}-\Theta_{(61)}).
\end{aligned}
\tag{5.39}
$$

3. Assign orientation to each link and introduce gauge fields.

   Dividing each lattice vertices into A- and B-sublattices as shown in Fig. 5.4, we assign a positive orientation to an edge (a,b) with $a \in \mathsf{A}$ and $b \in \mathsf{B}$, and a negative one to an edge (b,a).[2] We define "gauge fields" A and E by

$$
A_{(ab)} = -A_{(ba)} := \Theta_{(ab)}, \quad E_{(ab)} = -E_{(ba)} := L_{(ab)}. \tag{5.40}
$$

   In terms of these fields, the QDM hamiltonian is further converted into the following form:

- Diagonal term

$$
-t\sum_{\{\hexagon\}}\big(E_{(12)}E_{(34)}E_{(56)} - E_{(23)}E_{(45)}E_{(61)}\big). \tag{5.41}
$$

- Resonance term

$$
2v\sum_{\{\hexagon\}}\cos(\mathrm{rot}A), \tag{5.42}
$$

[2] Assignment of consistent orientation is possible only in bipartite lattices. A triangle lattice is not bipartite and cannot be assigned an orientation.

with

$$\mathrm{rot}A := A_{(12)} + A_{(23)} + A_{(34)} + A_{(45)} + A_{(56)} + A_{(61)}. \tag{5.43}$$

- Dimer constraint

$$(\mathrm{div}E - \rho)_{(i)}|\mathrm{Phys}\rangle = 0, \tag{5.44}$$

which is obtained from (5.32) via the following observations. Under the assignment of number on each vertex shown in 5.3, $\mathrm{div}E$ is given as follows,

$\underline{\text{vertex } 0 \in \mathsf{A}}$

$$(\mathrm{div}E)_{(0)}|\mathrm{Phys}\rangle = (E_{(01)} + E_{(02)} + E_{(03)})|\mathrm{Phys}\rangle = (L_{(01)} + L_{(02)} + L_{(03)})|\mathrm{Phys}\rangle$$
$$= |\mathrm{Phys}\rangle, \tag{5.45}$$

$\underline{\text{vertex } 0 \in \mathsf{B}}$

$$(\mathrm{div}E)_{(0)}|\mathrm{Phys}\rangle = (E_{(01)} + E_{(02)} + E_{(03)})|\mathrm{Phys}\rangle = -(L_{(01)} + L_{(02)} + L_{(03)})|\mathrm{Phys}\rangle$$
$$= -|\mathrm{Phys}\rangle. \tag{5.46}$$

Accordingly, ρ is given by

$$\underline{\text{On } \mathsf{A}} \quad \rho_{(0)} = 1, \tag{5.47}$$
$$\underline{\text{On } \mathsf{B}} \quad \rho_{(0)} = -1. \tag{5.48}$$

Therefore, the dimer constraint (5.32) yields the Gauss law constraint (5.44) with static staggered charges.

As the Gauss law constraint generates the $U(1)$ gauge transformation,[3] the resultant theory is interpreted as $U(1)$ lattice gauge theory described by the total Hamiltonian,

$$\begin{aligned} H_{\mathrm{gauge}} = K &\sum_{\substack{(ij) \\ i\in\mathsf{A}, j\in\mathsf{B}}} \left(E_{(ij)} - \frac{1}{2}\right)^2 \\ &- t \sum_{\{\hexagon\}} \left(E_{(12)}E_{(34)}E_{(56)} - E_{(23)}E_{(45)}E_{(61)}\right) + 2v \sum_{\{\hexagon\}} \cos(\mathrm{rot}A). \end{aligned} \tag{5.52}$$

This expression of the Hamiltonian (5.52) with the Gauss law (5.44) gives faithful representation of the QDM (5.32), (5.34) by taking a limit $K \to \infty$.

---

[3] We consider

$$U_\lambda := \exp\Big[\mathrm{i}\sum_{(ij)} (\mathrm{d}\lambda)_{(ij)} E_{(ij)} + \mathrm{i}\sum_i \lambda_{(i)}\rho_{(i)}\Big] = \exp\Big[-\mathrm{i}\sum_i \lambda_{(i)} (\mathrm{div}E - \rho)_{(i)}\Big] \tag{5.49}$$

up to surface term. Due to the commutation relation

$$[E_{(ij)}, A_{(kl)}] = \mathrm{i}(\delta_{ik}\delta_{jl} - \delta_{il}\delta_{jk}), \tag{5.50}$$

U_λ induces a transformation of A. As ρ_i is a c-number, it does not act on A. On the other hand, U_λ acts on the physical state as

$$U_\lambda|\mathrm{Phys}\rangle = |\mathrm{Phys}\rangle, \tag{5.51}$$

owing to the Gauss law constraint (5.44). Hence, it does not act on physical state (Hilbert space) and we identify it with the gauge transformation with a gauge parameter λ.

[4]

LSM theorem

Besides the lattice translational symmetry, the Hamiltonian (5.52) is invariant under a $U(1)$ 1-form transformation,

$$A_{(ij)} \mapsto A_{(ij)} + \omega_{(ij)}, \quad \mathrm{d}\omega = \mathrm{rot}\omega = 0, \tag{5.53}$$

which is generated by

$$U_\omega(M^1) = \mathrm{e}^{\mathrm{i}Q_\omega(M^1)}, \quad Q_\omega(M^1) = \sum_{\substack{(ij)\\ i\in\mathsf{A},j\in\mathsf{B}}} \omega_{(ij)} E_{(ij)} - \sum_i \omega_{(i)}\rho_{(i)}, \tag{5.54}$$

where ω is supported on a closed line M^1 (see Fig. 5.5) and ω is supported on a closed line Σ^2 such that $\partial\Sigma^2 = M^1$. The attachment of the surface Σ^2 makes the operator topological, i.e., invariant under deformation of the line M^1. [5] However, the surface term does not affect how it acts on the charged objects as ρ is a c-number. In terms of the original dimer variables, the charge operator takes the form of

$$Q(M^1) = \sum_{\substack{(ij)\in M^1\\ i\in\mathsf{A},j\in\mathsf{B}}} E_{(ij)} - \sum_{i\in\Sigma^2} \rho_{(i)} = \sum_{(ij)\in M^1} L_{(ij)} - \sum_{i\in\Sigma^2}\rho_{(i)}, \tag{5.56}$$

which counts the number of dimers intersecting the charge surface M^1.

Now we can apply the LSM theorem for the gauge theory Hamiltonian (5.52), based on lattice translational symmetry and $U(1)_{[1]}$ symmetry. [6] Let us check the consistency of the LSM theorem with several ordered phases in the QDM [71]. As shown in Fig. 5.6, it is known that in the columner and staggered phases the charge (5.56) per length is 1/3 and in the incommensurate phase the filling is irrational. Consequently, the LSM theorem claims the degenerate ground state in those phases because the spontaneous breaking of $U(1)$ 1-form symmetry is forbidden in $(2+1)$-dimensional spacetime by Coleman-Mermin-Wagner's theorem for 1-form symmetries.

We remark that the 1-form filling ν is allowed to take distinct values for different phases of the QDM. This should be contrasted with the 0-form filling of lattice models which preserve the particle number. [7] The LSM theorem is applied to each sector of the Hilbert space with the specific 1-form

[4] One may worry that the LSMOH constraint becomes unavailable in the limit $K \to \infty$ in (5.52): It is good to prove that the energy splitting of two states, which decays in the thermodynamic limit at finite K, still decays even if we first take the limit $K \to \infty$ and then the thermodynamic limit. This can be actually done in (2+1) dimensions rigorously as discussed in Appendix D.

[5] The charge (5.56) without ρ would not be well-defined topological operator because if we change its support from M^1 to N^1 the difference is

$$Q(N^1) - Q(M^1) = \sum_{(i)\in N^1 - M^1} (\mathrm{div}E)_{(i)} = \sum_{(i)\in N^1-M^1} \rho_{(i)} \tag{5.55}$$

which does not vanish due to the staggered charges.

[6] To apply LSM theorem for (5.52), we have to ensure that the LSM constraint is also applicable even after taking the limit $K \to \infty$, before taking the thermodynamic limit. Namely, we have to rule out the possibility that the energy splitting of the low-energy states would diverge, or converge to finite value by taking the limit $K \to \infty$. Such subtle problems are discussed in Appendix D.

[7] Thus, one may vary the filling ν at the ground state by introducing a kind of chemical potential term in the QDM Hamiltonian like

$$H_{\mathrm{chem}} = \mu \sum_{x_2} Q_2(x_2) = \mu \sum_{\mathbf{x}} n_\alpha(\mathbf{x}).$$

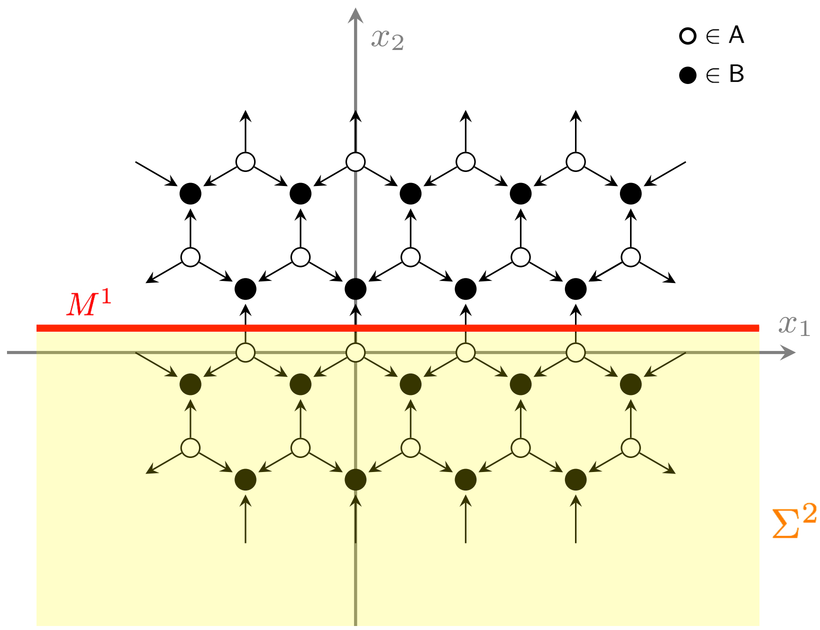

Figure 5.5: $U(1)_{[1]}$ gauge transformation and charge operator. ω_{ij} has finite value only on a line M^1. We choose a (x_1, x_2)-coordinate $i = (i_1, i_2)$ such that $\omega_{(ij)} \propto \delta_{i_2,0}\delta_{j_2,1}$ with unit lattice constant. On the links intersecting with M^1 the gauge field A transforms as (5.53).

charge. More generally, in gauge theories we usually sum over all configurations of gauge fields in path integral, without fixing specific topological sector.

5.3.3 't Hooft anomaly at RK point

We present a continuum description of the QDM in the vicinity of the quantum critical point, Rokhsar-Kivelson (RK) point [72, 73], realized in the quantum dimer model and discuss the consequences of anomaly matching. The degree of freedom in the effective field theory is a bosonic scalar field ϕ with compactification radius 2π, which is introduced as a height field. The underlying theory

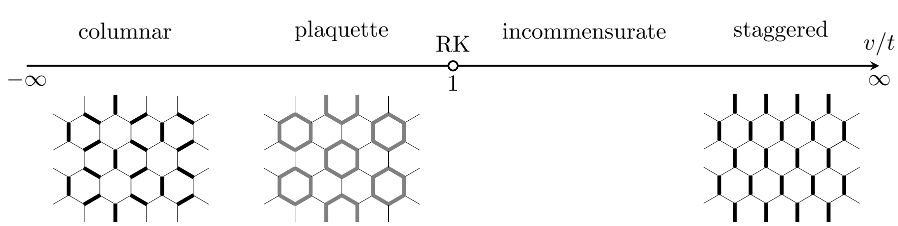

Figure 5.6: The schematic phase diagram of the QDM on the honeycomb lattice. The 1-form filling $\nu = 1$ in the staggered phase. $\nu = 1/3$ in the columnar and plaquette phase, which terminate at the RK critical point. There is a sequence of the incommensurate crystal and commensurate ordered phase between the RK point and the staggered phase, where ν increases continuously from $1/3$ to 1.

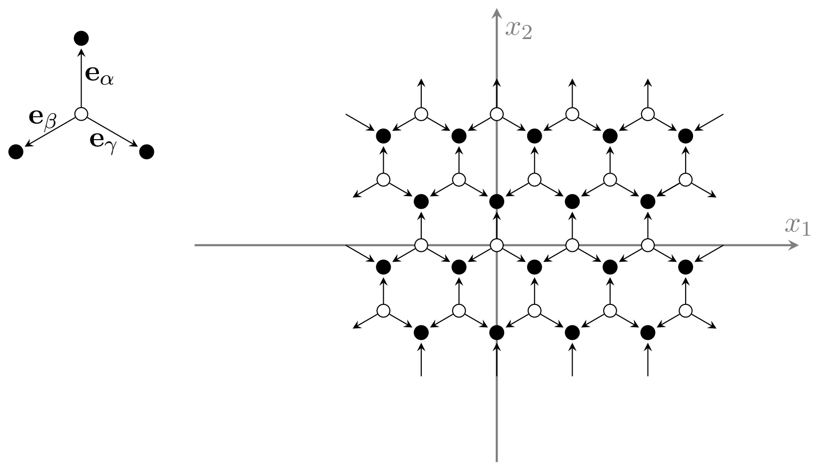

Figure 5.7: Cartesian coordinate on the honeycomb lattice. Lattice vectors connecting two neighboring vertices are labeled as $\mathbf{e}_\alpha, \mathbf{e}_\beta$ and $\mathbf{e}_\gamma$ respectively.

is given by the following Lagrangian [73],

$$\begin{aligned}\mathcal{L} &= \frac{1}{2}\partial_t\phi\partial_t\phi - \frac{\rho}{2}\nabla_i\phi\nabla_i\phi - \frac{\kappa^2}{2}\nabla^2\phi\nabla^2\phi \\ &= \frac{1}{2}\partial_\mu\phi\partial^\mu\phi - \frac{\tilde{\kappa}^2}{2}\partial_i\partial^i\phi\partial_j\partial^j\phi \\ &= \mathrm{d}\phi\wedge *\mathrm{d}\phi - \frac{\tilde{\kappa}^2}{2}(\Delta\phi)^2,\end{aligned} \tag{5.57}$$

with $\partial_\mu := (\partial_0, \sqrt{\rho}\nabla_i)$, $\Delta = \partial_i\partial^i$, and $\tilde{\kappa} := \kappa/\rho$.

An identification of dimer variables L and scalar field ϕ is given by [74, 75]

$$\begin{aligned} L_\alpha - \frac{1}{3} &= \frac{1}{2\pi}\partial_1\phi + \frac{1}{2}\left[e^{\mathrm{i}\phi+\mathrm{i}\frac{4\pi}{3}x_1} + \text{h.c.}\right], \\ L_\beta - \frac{1}{3} &= \frac{1}{2\pi}\left(-\frac{1}{2}\partial_1 + \frac{\sqrt{3}}{2}\partial_2\right)\phi + \frac{1}{2}\left[e^{\mathrm{i}\phi+\mathrm{i}\frac{4\pi}{3}(x_1+1)} + \text{h.c.}\right], \\ L_\gamma - \frac{1}{3} &= \frac{1}{2\pi}\left(-\frac{1}{2}\partial_1 - \frac{\sqrt{3}}{2}\partial_2\right)\phi + \frac{1}{2}\left[e^{\mathrm{i}\phi+\mathrm{i}\frac{4\pi}{3}(x_1-1)} + \text{h.c.}\right]. \end{aligned} \tag{5.58}$$

See Fig. 5.7 for coordinate we are using. One can read off the action of the translation symmetry in x_1 direction (denoted by $\mathcal{T}_1$) on ϕ from (5.58) and $\mathcal{T}_1 : L(x) \mapsto L(x+1)$. Then, in the continuum limit $\mathcal{T}_1$ acts on ϕ as an internal $\mathbb{Z}_3$ symmetry

$$\mathcal{T}_1 : \quad \phi \mapsto \phi - \frac{2\pi}{3}. \tag{5.59}$$

Besides the $\mathcal{T}_1$ symmetry (5.59), this theory has a $U(1)$ 1-form symmetry, whose generator is given by (5.56) in the lattice model. The continuum description of the charge operator of $U(1)_{[1]}$

(5.56) in the QDM is expressed as

$$
\begin{aligned}
Q_2 &= \sum_{x_1=0}^{L_1-1} n_\alpha(x_1, 0) \\
&= \sum_{x_1=0} \frac{1}{2\pi}\partial_1\phi(x_1,0) + \frac{1}{2}\left[e^{i\phi(x_1,0)}e^{\frac{4\pi i x_1}{3}} + \text{h.c.}\right] + \frac{L_1}{3} \\
&\approx \int_{x_2=0} dx_1 \partial_1\phi + \frac{L_1}{3},
\end{aligned}
\tag{5.60}
$$

where we used the identification (5.58) and dropped the summation of the staggered part in the last equation.

Equations of motion are read off from the Lagrangian (5.57),

$$
\begin{aligned}
&\partial_\mu\partial^\mu\phi + \tilde{\kappa}^2\Delta\Delta\phi = 0, \\
&\epsilon^{\mu\nu\rho}\partial_\nu\partial_\rho\phi = 0.
\end{aligned}
\tag{5.61}
$$

Conserved currents for 0-form and 1-form $U(1)$ symmetries are respectively given by

$$
\mathrm{d}j_A = 0, \quad (*j_A)^\mu = (\partial^0\phi,\, \partial^i\phi + \tilde{\kappa}^2\Delta\Delta\phi), \tag{5.62}
$$

$$
\mathrm{d}j_B = 0, \quad (*j_B)^{\mu\nu} = \epsilon^{\mu\nu\rho}\partial_\rho\phi. \tag{5.63}
$$

$\mathbb{Z}_3$ translation symmetry is a subgroup of the $U(1)$ 0-form symmetry. Then, (5.60) is identified as a generator of 1-form symmetry given by integrating the current on a line up to constant,

$$
Q_2 = \int_{x_2=0} j_B + \frac{L_1}{3}. \tag{5.64}
$$

On the other hand, $\mathbb{Z}_3$ translation symmetry (5.59) is a subgroup of the $U(1)$ 0-form symmetry.

According to (5.60), the filling measured relative to 1/3 is identified as the gradient of the height ϕ measured in x_1 direction per unit lattice,

$$
\nu - \frac{1}{3} = \frac{Q_2 - L_1/3}{L_1} \approx \int_{x_2=0} dx_1\partial_1\phi \tag{5.65}
$$

which is sometimes called "tilt". [76] The flat tilt is observed in the columnar and plaquette phase reflecting $\nu = 1/3$, while the staggered phase is fully tilted. On the tilted side of the RK transition $v/t > 1$, it is argued [74, 77, 78] that the tilt increases in the "incomplete devil's staircase" fashion. Namely, the increase of the tilt is continuous at least in the vicinity of the RK point on the tilted side, and there is a sequence of commensurate gapped crystal and incommensurate points. It is also argued [74] that the incommensurate region has finite measure in the parameter space. Here, the incommensurate region is characterized as the irrational tilt, which corresponds to the limit $q \to \infty$ for $\nu = p/q$. We remark that in the incommensurate region it is guaranteed non-perturbatively to have gapless spectrum by the LSM theorem based on $U(1)_{[1]}$ symmetry.

To diagnose the anomaly, we introduce a background $U(1)_{[1]}$-gauge field B by coupling to the conserved current $j_B = \mathrm{d}\phi$,

$$
\mathcal{L} = \mathrm{d}\phi \wedge *\mathrm{d}\phi + \mathrm{d}\phi \wedge B - \frac{\tilde{\kappa}^2}{2}(\Delta\phi)^2, \tag{5.66}
$$

which is invariant under a 1-form gauge transformation

$$B \mapsto B + \mathrm{d}\lambda. \tag{5.67}$$

Next, we introduce a background $U(1)$-gauge fields (A, C) to gauge $\mathbb{Z}_3$ symmetry by forming the covariant derivative $\mathrm{d}\phi + A$,

$$S = \int (\mathrm{d}\phi - A) \wedge *(\mathrm{d}\phi - A) + (\mathrm{d}\phi - A) \wedge B - \frac{\tilde{\kappa}^2}{2}(\partial_i(\partial^i\phi - A^i))^2 \mathrm{d}^2x + F \wedge (3A - \mathrm{d}C). \tag{5.68}$$

is not invariant under the 1-form gauge transformation (5.67) but

$$S \mapsto S - \frac{2\pi}{3}k \pmod{2\pi}, \tag{5.69}$$

with $k \in \mathbb{Z}$.

Dual gauge theory

Let us try to derive the dual gauge theory.

$$S = \int (\Phi + A) \wedge *(\Phi + A) + (\Phi + A) \wedge B - \frac{\tilde{\kappa}^2}{2}(\partial_i(\Phi^i + A^i))^2 \mathrm{d}^2x + \Phi \wedge \mathrm{d}a, \tag{5.70}$$

where a constraint $3A = \mathrm{d}C$ is understood. We perform the Gauss integral with respect to Φ by solving equation of motion and plugging the solution back into the action. The equation of motion is

$$2(\Phi^0 + A^0) = -\frac{1}{2}\epsilon^{0ij}(f_{ij} + 2B_{ij}), \tag{5.71}$$

$$2(\Phi^i + A^i) - \tilde{\kappa}^2\partial^i(\partial_j(\Phi^j + A^j)) = -\epsilon^{ij0}(f_{j0} + 2B_{j0}). \tag{5.72}$$

Assuming B is a flat two-form gauge field, the solution takes the form of [8]

$$\Phi + A = -\frac{1}{2} * (\mathrm{d}a + B). \tag{5.73}$$

Hence, the dual action is

$$S = \int \frac{1}{4}(\mathrm{d}a + B) \wedge *(\mathrm{d}a + B) - \frac{\tilde{\kappa}^2}{16}(\epsilon^{ij}\partial_i(e_j + 2B_{j0}))^2 \mathrm{d}^2x - A \wedge \mathrm{d}a. \tag{5.74}$$

In the dual gauge theory, the 1-form gauge transformation is

$$B \mapsto B + \mathrm{d}\lambda, \quad a \mapsto a + \lambda, \tag{5.75}$$

which does not leave the last term invariant but yields $\mathbb{Z}_3$ anomalous phase due to the constraint $3A = \mathrm{d}C$.

[8] It is interesting to observe that both hand sides of equality is invariant under $U(1)$ and $U(1)_{[1]}$ symmetries. Thus, it is understandable that the transformation law of $\mathrm{d}\phi \sim \Phi$ under $U(1)$ has nothing to do with that of a and a is indeed unchanged, and vice versa.

Chapter 6

Conclusion

In conclusion, we have observed several aspects of 't Hooft anomalies that appear in condensed matter literature. First of all, via the anomaly inflow assumption, the 't Hooft anomalies are regarded as the boundaries of SPT phases in one more dimension. The 't Hooft anomalies provide strong constraints on low energy effective theory. In particular, the trivial gapped symmetric phases are strictly forbidden on the boundary of SPT phases. Even in the presence of such spectral constraints required by anomalies, the boundaries can still host symmetric gapped states that is described by nontrivial TQFT with topological order. By focusing on such gapped boundaries governed by TQFT, we have seen that the symmetry properties in TQFT are controlled by the data of symmetry fractionalization of quasiparticle excitations. Some choices of symmetry fractionalization turn out to be anomalous, which are only realized as the boundaries of SPT phases in one dimension higher. For reflection in (2+1)d and rotation in (3+1)d, we have provided the indicator formulae which immediately tell us the presence or absence of anomalies in TQFT, from given input data of symmetry fractionalization. Some future generalizations would be to examine the generalization for anomalies based on other point group symmetries. Another possible generalization is to look for the indicator formula of anomalies in (3+1)D that correspond to $\Omega_5^{SO}(pt) = \mathbb{Z}_2$. It would also be interesting to see the generalization for fermionic topological phases.

Next, we have observed intimate relation between Lieb-Schultz-Mattis (LSM) mechanism and 't Hooft anomalies. Lieb-Schultz-Mattis (LSM) mechanism provides spectral constraint on lattice systems with both internal and lattice symmetries, reminiscent in anomalous states on boundaries of SPT phases. Actually, the nontrivial states due to LSM mechanism are equivalent to boundaries of SPT phases protected by both internal and lattice symmetries. The LSM mechanism is nothing but anomaly constraints in lattice systems: we have seen that the anomalies manifests itself as mixed 't Hooft anomaly between (internal version of) lattice and internal symmetries. We have revealed that pure lattice gauge theories can host the LSM mechanism based on the lattice symmetry and a 1-form symmetry, which is understood as anomalies involving the 1-form symmetry in continuum limit. One direction to extend the studies here is to apply our results to the QDM on a bipartite lattice in higher dimensions, which can be realized, for example, as an effective model of the spin-1/2 anti-ferromagnetic Heisenberg model on a pyrochlore lattice. [79] It would be interesting to look for the possibility of the deconfined phase enforced by the fractional 1-form filling in such systems, which is left for future investigation. Finally, in this work we have not considered spatial symmetries other than simple lattice translation and reflection, so we leave the refinement of our result for additional crystal symmetries for future work.

Appendix A

Group cohomology

In this appendix, we briefly summarize basic properties of group cohomology [6, 27] exploited in the main text.

Let $\omega_n(g_1, g_2, \dots g_n)$ be a function of G^n which takes the value in an Abelian group M; $\omega_n : G^n \mapsto M$. Any function $\omega_n : G^n \mapsto M$ is called a n-cochain. The space of n-cochains form a group $\mathcal{C}^n(G, M)$, whose group structure is given via group operation in M. In the main text, M is mostly set as $M = U(1)$. Next, we define coboundary operator d as a map $\mathrm{d} : \mathcal{C}^n(G, M) \mapsto \mathcal{C}^{n+1}(G, M)$ given by

$$\mathrm{d}\omega_n(g_1, \dots, g_{n+1}) = \omega_n(g_2, \dots, g_{n+1})\omega_n(g_1, \dots, g_n)^{(-1)^{n+1}} \cdot \prod_{i=1}^{n} \omega_n(g_1, \dots, g_{i-1}, g_i g_{i+1}, g_{i+1}, \dots, g_{n+1}). \tag{A.1}$$

Then, we define the cocycle condition as

$$\mathrm{d}\omega_n = 1. \tag{A.2}$$

Here, we can check that operating coboundary operator twice becomes null; $\mathrm{d}^2\omega_n = 1$ for any $\omega_n \in \mathcal{C}^n(G, M)$, which allows us to define cohomology algebraic structure. Let us define an n-cocycle as an n-cochain which satisfies the cocycle condition (A.2). The space of n-cocycles form a group $\mathcal{Z}^n(G, M)$,

$$\mathcal{Z}^n(G, M) = \{\omega_n | \mathrm{d}\omega_n = 1, \omega_n \in \mathcal{C}^n(G, M)\}. \tag{A.3}$$

Furthermore, an n-cocycle ω_n is called an n-coboundary if it is written as $\omega_n = \mathrm{d}\omega_{n-1}$ by some $n-1$-cochain $\omega_{n-1} \in \mathcal{C}^{n-1}(G, M)$. The space of n-coboundaries also form a group $\mathcal{B}^n(G, M)$,

$$\mathcal{B}^n(G, M) = \{\omega_n | \omega_n = \mathrm{d}\omega_{n-1}, \omega_{n-1} \in \mathcal{C}^{n-1}(G, M)\}. \tag{A.4}$$

The equivalence class of n-cocycles up to n-coboundary forms an n-th cohomology group $\mathcal{H}^n(G, M)$,

$$\mathcal{H}^n(G, M) = \mathcal{Z}^n(G, M)/\mathcal{B}^n(G, M). \tag{A.5}$$

Appendix B

C_k anomaly in (3+1)d non-abelian discrete gauge theory

In this appendix, we pose a conjecture on C_k anomaly indicator of (3+1)d for non-abelian discrete gauge group. We consider (3+1)d untwisted Dijkgraaf-Witten theory, which supports both point-like and loop-like excitations;

- Point-like excitations

  Point-like excitations are electric particles which can be created at the ends of an open line operator (Wilson line),

$$W_{R_i}(C) := R_i \left(\prod_{ij \in C} g_{ij} \right), \tag{B.1}$$

  where C is an open line. An electric charge is labeled by an irreducible representation $R_i \in \mathrm{Rep}(G)$ of gauge group G, with quantum dimension $d_i = \dim[R_i]$.

- Loop-like excitations

  A single loop-like excitation can be created at the boundary of an open surface operator. In (3+1)d gauge theory, a vortex line excitation exists as a loop-like excitation. A vortex line is characterized by a holonomy measured on a closed loop which rounds a vortex, which is labeled by a conjugacy class χ of G, since holonomy $h \in G$ is mapped $h \mapsto ghg^{-1}$ for some $g \in G$ under gauge transformation. A single vortex line is created by the following operator,

$$M_\chi(S) := \sum_{h \in \chi} \left(\prod_{ij \in S} B_{ij}(h) \right), \tag{B.2}$$

  where S is an open surface on a dual lattice, and B_{ij} is an operator which transforms a link variable $g_{ij} \mapsto hg_{ij}$. This operator implements a defect along S, and violates flatness at the boundary of S. Quantum dimension can be defined as weight of a bubble of a surface operator $d_\chi := \langle M_\chi(S) \rangle$, where S is taken as a small sphere. Thus, we have $d_\chi = |\chi|$, where $|\chi|$ is the number of elements in χ.

  We can further think of attaching a charge on a vortex line labeled by χ, defined as an irreducible representation $\mathrm{Rep}_i(G_\chi)$ of G_χ, where G_χ is a centralizer of χ [80–82]. Although we cannot explicitly write down the operator which creates such loop-like excitation associated with charge, we push on heuristic argument based on the conjecture that charged loop-like excitation is generated by a composite object of Wilson line and surface operator. By including the effect of charge, the quantum dimension becomes

$$d_{\chi;i} = |\chi| \cdot \dim[\mathrm{Rep}_i(G_\chi)]. \tag{B.3}$$

For example, let us consider S_3 gauge theory. S_3 is classified by three conjugacy classes; $\chi_1 = ((1)), \chi_2 = ((1,2),(2,3),(3,1)), \chi_3 = ((1,2,3),(1,3,2))$. For each conjugacy class, there are charged excitations labeled by irreducible representation of $G_{\chi_1} = S_3, G_{\chi_2} = \mathbb{Z}_2, G_{\chi_3} = \mathbb{Z}_3$ respectively. χ_1 corresponds to point-like excitations $p_1 = (\chi_1, R_0(S_3)), p_2 = (\chi_1, R_1(S_3)), p_3 = (\chi_1, R_2(S_3))$ with quantum dimensions $d_{1;0} = 1, d_{1;1} = 1, d_{1;2} = 2$. χ_2, χ_3 corresponds to vortex lines, $s_{10} = (\chi_1, R_0(\mathbb{Z}_2)), s_{11} = (\chi_1, R_1(\mathbb{Z}_2)), s_{20} = (\chi_2, R_0(\mathbb{Z}_3)), s_{21} = (\chi_2, R_1(\mathbb{Z}_3)), s_{22} = (\chi_2, R_2(\mathbb{Z}_3))$. Among them, $s_{10} = (\chi_1, R_0(\mathbb{Z}_2))$ and $s_{20} = (\chi_2, R_0(\mathbb{Z}_3))$ create "pure" vortex lines without charge, which are generated by (B.3). The rest corresponds to bound states of electric charge and vortex line. Fusion rules of these excitations are controlled by fusion rule of quantum double $D(G)$ [83, 84] (i.e., inherit the fusion rules of anyons in (2+1)d G-gauge theory).

B.1 partition functions

We want to evaluate partition function $\mathcal{Z}(L(k;1,1,1))$ based on (3+1)d G-gauge theory, as we did for $\mathbb{Z}_k$ gauge theory in the main text. As exercise, let us first try to compute partition function on a sphere, $\mathcal{Z}(S^5)$.

B.1.1 $\mathcal{Z}(S^5)$

First, we apply gluing relation by cutting S^5 along S^4 into two D^5s,

$$\mathcal{Z}(S^5) = \frac{\mathcal{Z}(D^5)[\phi]\mathcal{Z}(D^5)[\phi]}{\mathcal{Z}(S^4 \times D^1)[\phi]}. \tag{B.4}$$

Similarly, by cutting $S^4 \times D^1$ along $S^3 \times D^1$ into two D^5, we have

$$\mathcal{Z}(S^4 \times D^1) = \frac{\mathcal{Z}(D^5)[\phi]\mathcal{Z}(D^5)[\phi]}{\mathcal{Z}(S^3 \times D^2)[\phi]}. \tag{B.5}$$

Combining these relations gives

$$\mathcal{Z}(S^5) = \mathcal{Z}(S^3 \times D^2)[\phi]. \tag{B.6}$$

$S^3 \times D^2$ can be decomposed into two D^5s by cutting along $S^2 \times D^2$. Now, the boundary condition on the cut $S^2 \times D^2$ is labeled by a surface operator wrapping S^2. Since no line operator can round $S^2 \times D^2$ nontrivially, these surface operators cannot carry electric charge. Thus, the boundary condition is characterized by "pure" surface operators without charge, $s_{\chi;0}$ wrapping S^2. Therefore, by the gluing relation

$$\mathcal{Z}(S^3 \times D^2)[\phi] = \sum_{\chi} \frac{\mathcal{Z}(D^5)[s_{\chi;0}]\mathcal{Z}(D^5)[s_{\chi;0}]}{\langle s_{\chi;0}|s_{\chi;0}\rangle_{\mathcal{V}(S^2\times D^2;\phi)}}. \tag{B.7}$$

Since the configuration of $s_{\chi;0}$ of $\mathcal{Z}(D^5)[s_{\chi;0}]$ is a bubble in ∂D^5, it follows that $\mathcal{Z}(D^5)[s_{\chi;0}] = |\chi|\mathcal{Z}(D^5)[\phi]$. For $\langle s_{\chi;0}|s_{\chi;0}\rangle_{\mathcal{V}(S^2\times D^2;\phi)}$, we have

$$\langle s_{\chi;0}|s_{\chi;0}\rangle_{\mathcal{V}(S^2\times D^2;\phi)} = \mathcal{Z}(S^2 \times D^3)[s_{\chi;0} \cup s_{\overline{\chi};0}]. \tag{B.8}$$

We have two pure surface operators on the boundary. $\mathcal{Z}(S^2\times D^3)$ is evaluated by cutting along $S^1\times D^3$. Now the boundary condition on the cut contains a line operator rounding S^1, together with a tube $e_{\chi;0}$ of surface operator $s_{\chi;0}$ supported on $S^1\times I$ (see Fig.3.11). Such configuration of surface operators attached to a line operator are labeled by $(\chi, R_i(G_\chi))$. Thus, the gluing relation becomes

$$\mathcal{Z}(S^2\times D^3)[s_{\chi;0}\cup s_{\overline{\chi};0}] = \sum_{R_i\in\mathrm{Rep}(G_\chi)} \frac{\mathcal{Z}(D^5)[s_{\chi;i}]\mathcal{Z}(D^5)[s_{\chi;i}]}{\langle e_{\overline{\chi};\overline{i}}|e_{\chi;i}\rangle_{\mathcal{V}(S^1\times D^3;(\chi;R_i)\cup\overline{(\chi,R_i)})}}, \tag{B.9}$$

where $e_{\chi;i}$ denotes a tube of surface operator attached to a line operator with irreducible representation $R_i(G_\chi)$. We find by gluing relation that $\langle e_{\overline{\chi};\overline{i}}|e_{\chi;i}\rangle_{\mathcal{V}(S^1\times D^3;(\chi;R_i)\cup\overline{(\chi,R_i)})}=1$, hence

$$\begin{aligned}\mathcal{Z}(S^2\times D^3)[s_{\chi;0}\cup s_{\overline{\chi};0}] &= \sum_{R_i\in\mathrm{Rep}(G_\chi)} (|\chi|\cdot\dim[R_i(G_\chi)])^2\cdot\mathcal{Z}(D^5)[\phi]\mathcal{Z}(D^5)[\phi] \\ &= |G_\chi|\cdot(|\chi|\mathcal{Z}(D^5)[\phi])^2.\end{aligned} \tag{B.10}$$

Combining (B.10) with (B.7), we obtain

$$\mathcal{Z}(S^5) = \sum_\chi \frac{1}{|G_\chi|} = \sum_\chi \frac{|\chi|}{|G|} = 1. \tag{B.11}$$

Thus, we have $\mathcal{Z}(S^5)=1$, which is required for cobordism invariance of (4+1)d path integral.

B.1.2 Digression: impossibility of "loop only" topological order in (3+1)d

In Ref. [80], it is proposed that $(3+1)$d topological ordered phase whose excitations are all loop-like excitations cannot exist as a standalone (3+1)d system. In this section, we claim the result which supports the impossibility of "only loop-like excitation" topological order in Ref. [80], based on analysis of path integral of SPT phases in (4+1)d bulk. Our computation implies that such "only loop-like excitation" topological order cannot exist even as a surface state of (4+1)d invertible topological phases, strengthening the result in Ref. [80].

For odd dimensional invertible topological phases, it is known that the partition function on a sphere must be fixed to unit; $\mathcal{Z}(S^d)=1$ when d is odd. [11] [1] Here, we will show that $\mathcal{Z}(S^5)>1$ when the surface topological order in (3+1)d has only loop-like excitations. We note that "loop only" topological ordered phase supports only 2d surface operator as extended operators, where loop-like excitations are created by open surface operators. Let us assume we have N surfece operators, and label surface operators as $\{s_l\}$ for $1\le l\le N$. Line operators are absent since we have no point-like excitations. According to (B.6), it follows that $\mathcal{Z}(S^5)=\mathcal{Z}(S^3\times D^2)[\phi]$. Using gluing relation via cutting S^3 along S^2 into two D^3s, we obtain

$$\mathcal{Z}(S^3\times D^2)[\phi] = \sum_l \frac{\mathcal{Z}(D^5)[s_l]\mathcal{Z}(D^5)[\overline{s}_l]}{\langle s_l|s_l\rangle_{\mathcal{V}(S^2\times D^2;\phi)}}. \tag{B.12}$$

For $\langle s_l|s_l\rangle_{\mathcal{V}(S^2\times D^2;\phi)}$, we have

$$\langle s_l|s_l\rangle_{\mathcal{V}(S^2\times D^2;\phi)} = \mathcal{Z}(S^2\times D^3)[\overline{s}_l\cup s_l]. \tag{B.13}$$

[1] If d is even, we can add Euler term to shift the value of $\mathcal{Z}(S^d)$. In odd dimension, Euler term does not exist and $\mathcal{Z}(S^d)$ is fixed to unit. In any dimension we can have $\mathcal{Z}(S^d)=1$ by normalization using Euler term, which is required for cobordism invariance of SPT partition function. See Ref. [11] for detail.

Then, we use gluing relation by cutting S^2 into two D^2s along S^1. Then, we have

$$\mathcal{Z}(S^2 \times D^3)[\overline{s}_l \cup s_l] = \frac{\mathcal{Z}(D^5)[s_l]\mathcal{Z}(D^5)[\overline{s}_l]}{\langle e_l|e_l\rangle_{\mathcal{V}(S^1\times D^3;l\cup\bar{l})}}, \tag{B.14}$$

where e_l denotes a tube of surface operator which makes surface operators on boundaries closed. We remark that the boundary condition is unique on $S^1 \times D^3$ due to the absence of line operators. We use gluing relation by cutting S^1 at a point, then we obtain $\langle e_l|e_l\rangle_{\mathcal{V}(S^1\times D^3;l\cup\bar{l})} = 1$. Combining the above results, we have

$$\mathcal{Z}(S^3 \times D^2)[\phi] = \sum_l \frac{\mathcal{Z}(D^5)[s_l]\mathcal{Z}(D^5)[\overline{s}_l]}{\mathcal{Z}(D^5)[s_l]\mathcal{Z}(D^5)[\overline{s}_l]} = \sum_l 1 = N, \tag{B.15}$$

where N is a number of surface operators (including a trivial surface operator). Thus, if there exists a nontrivial surface operator, we have

$$\mathcal{Z}(S^5) = \mathcal{Z}(S^3 \times D^2)[\phi] = N > 1, \tag{B.16}$$

which implies that the bulk (4+1)d TQFT cannot be an invertible topological phase.

B.1.3 $\mathcal{Z}(L(k;1,1,1))$

Next, we evaluate partition function on the 5d lens space. Using the logic of 3.3.3, we obtain (3.57),

$$\mathcal{Z}(L(k;1,1,1)) = \mathcal{Z}(L(k;1,1,1)_3)[\phi]. \tag{B.17}$$

Next, we do handle decomposition for $L(k;1,1,1)_3$,

$$\begin{aligned}\mathcal{Z}(L(k;1,1,1)_3)[\phi] &= \sum_\chi \frac{\mathcal{Z}(L(k;1,1,1)_2)[s_{\chi;0}]\mathcal{Z}(D^5)[s_{\chi;0}]}{\langle s_{\chi;0}|s_{\chi;0}\rangle_{\mathcal{V}(S^2\times D^2;\phi)}} \\ &= \sum_\chi \frac{\mathcal{Z}(L(k;1,1,1)_2)[s_{\chi;0}]}{|G_\chi|\cdot|\chi|\mathcal{Z}(D^5)[\phi]} \\ &= \frac{1}{|G|}\sum_\chi \frac{\mathcal{Z}(L(k;1,1,1)_2)[s_{\chi;0}]}{\mathcal{Z}(D^5)[\phi]},\end{aligned} \tag{B.18}$$

where we used (B.10). For $L(k;1,1,1)_2$,

$$\begin{aligned}\mathcal{Z}(L(k;1,1,1)_2)[s_{\chi;0}] &= \sum_{R_i\in\mathrm{Rep}_i(G_\chi)} \frac{\mathcal{Z}(L(k;1,1,1)_1)[s^{(+1)}_{\chi;i}]\mathcal{Z}(D^5)[s_{\chi;i}]}{\langle e_{\overline{\chi};\bar{i}}|e_{\chi;i}\rangle_{\mathcal{V}(S^1\times D^3;(\chi;R_i)\cup\overline{(\chi,R_i)})}} \\ &= \sum_{R_i\in\mathrm{Rep}_i(G_\chi)} \mathcal{Z}(L(k;1,1,1)_1)[s^{(+1)}_{\chi;i}]\cdot d_{\chi;i}\cdot\mathcal{Z}(D^5)[\phi],\end{aligned} \tag{B.19}$$

where we choose the configuration of surface and line operator of $s_{\chi;i}$ in $\mathcal{Z}(L(k;1,1,1)_1)[s^{(+1)}_{\chi;i}]$, such that these operators link exactly once on the surface of $L(k;1,1,1)_1$, as explained in the main text (see the step 4 of Section 3.3.3, and Fig.3.12).

Therefore, using the logic in the final step of Section 3.3.3, we have

$$\mathcal{Z}(L(k;1,1,1)_1)[s^{(+1)}_{\chi;i}] = \sum_{\chi,i}\Theta_{\chi;i}\eta_{\chi;i}, \tag{B.20}$$

where $\eta_{\chi;i}$ is an eigenvalue of C_k for the state with a single vortex line χ and k charges R_i located in rotation symmetric manner. Θ denotes a phase by linking between a line and a surface; $\Theta_{\chi;i} := R_i(h)$, where $h \in \chi$ and we define G_χ as a centralizer of h. Then, $R_i(h)$ becomes a scalar because of Schur's lemma [83]. The sum runs over χ such that $C_k(\chi) = \chi$ for a vortex line, and R_i such that $R_i, C_k(R_i), \ldots, C_k^{k-1}(R_i)$ can fuse into vacuum. Finally, we obtain

$$\mathcal{Z}(L(k;1,1,1)) = \frac{1}{|G|} \sum_{\chi,i} d_{\chi;i} \Theta_{\chi;i} \eta_{\chi;i}. \tag{B.21}$$

Appendix C

Partition function on various 4d spaces

In this appendix, we compute partition function on various spaces of 4 dimension required to evaluate $\mathcal{Z}(\mathbb{RP}^4)$.

- $\langle l_a|l_b\rangle_{\mathcal{V}(S^1\times D^2;\phi)} = \mathcal{Z}(S^1\times D^3)[l_{\overline{a}}\cup l_b] = \delta_{a,b}$.

  To see this, we apply gluing relation by cutting $S^1\times D^3$ along $\{p\}\times D^3$, where p denotes some point in S^1. Gluing relation becomes

$$\mathcal{Z}(S^1\times D^3)[l_{\overline{a}}\cup l_b] = \sum_{e_i\in\mathcal{V}(D^3;\overline{a},b)} \frac{\mathcal{Z}(D^4)[\mathrm{arc}_{\overline{a}}\cup\overline{e}_i\cup\mathrm{arc}_b\cup e_i]}{\langle e_i|e_i\rangle_{\mathcal{V}(D^3;\overline{a},b)}}. \tag{C.1}$$

  The boundary condition on the cut e_i consists of an arc of anyon a connected with $\mathrm{arc}_{\overline{a}}, \mathrm{arc}_b$ at ∂D^3, making the diagram $(\mathrm{arc}_{\overline{a}}\cup\overline{e}_i\cup\mathrm{arc}_b\cup e_i)$ a closed loop on $S^3=\partial D^4$. This loop becomes a bubble of l_a loop on S^3 when we have $a=b$, otherwise weights zero. Therefore, we have $\mathcal{Z}(D^4)[\mathrm{arc}_{\overline{a}}\cup\overline{e}_i\cup\mathrm{arc}_b\cup e_i] = d_a\delta_{a,b}\mathcal{Z}(D^4)[\phi]$. Moreover, for $a=b$ we have

$$\langle e_i|e_i\rangle_{\mathcal{V}(D^3;\overline{a},b)} = \mathcal{Z}(D^4)[l_a] = d_a\mathcal{Z}(D^4)[\phi]. \tag{C.2}$$

  Therefore,

$$\mathcal{Z}(S^1\times D^3)[l_{\overline{a}}\cup l_b] = \delta_{a,b}. \tag{C.3}$$

- $\langle\phi|\phi\rangle_{\mathcal{V}(S^2\times D^1;\phi)} = \mathcal{Z}(S^2\times D^2)[\phi] = \mathcal{D}^2\cdot\left(\mathcal{Z}(D^4)[\phi]\right)^2$.

  To see this, we apply gluing relation by cutting $S^2\times D^2$ into two D^4s along $S^1\times D^2$,

$$\mathcal{Z}(D^2\times S^2)[\phi] = \frac{\mathcal{Z}(D^4)[l_a]\mathcal{Z}(D^4)[l_a]}{\langle l_a|l_a\rangle_{\mathcal{V}(S^1\times D^2;\phi)}}, \tag{C.4}$$

  where the boundary condition on the cut $S^1\times D^2$ is labeled by loop of anyon l_a rounding S^1. We have seen in (C.3) that $\langle l_a|l_a\rangle_{\mathcal{V}(S^1\times D^2;\phi)} = \mathcal{Z}(S^1\times D^3)[l_{\overline{a}}\cup l_a] = 1$. For $\mathcal{Z}(D^4)[l_a]$, we have a bubble of l_a loop on $S^3=\partial D^4$ weighted by quantum dimension d_a. Hence, $\mathcal{Z}(D^4)[l_a] = d_a\mathcal{Z}(D^4)[\phi]$. Therefore,

$$\mathcal{Z}(S^2\times D^2)[\phi] = \mathcal{D}^2\cdot\left(\mathcal{Z}(D^4)[\phi]\right)^2. \tag{C.5}$$

- $\langle\phi|\phi\rangle_{\mathcal{V}(S^3)} = \mathcal{Z}(S^3\times D^1)[\phi] = 1/\mathcal{D}^2$.

To see this, we apply gluing relation by cutting $S^3 \times D^1$ into two D^4s along $S^2 \times D^1$,

$$\mathcal{Z}(S^3 \times D^1)[\phi] = \frac{\mathcal{Z}(D^4)[\phi]\mathcal{Z}(D^4)[\phi]}{\langle\phi|\phi\rangle_{\mathcal{V}(S^2\times D^1;\phi)}}. \tag{C.6}$$

Using (C.5) for $\langle\phi|\phi\rangle_{\mathcal{V}(S^2\times D^1;\phi)} = \mathcal{Z}(S^2 \times D^2)[\phi]$, we have

$$\mathcal{Z}(S^3 \times D^1)[\phi] = \frac{1}{\mathcal{D}^2}. \tag{C.7}$$

- $\mathcal{Z}(D^4)[\phi] = 1/\mathcal{D}$.

  To see this, first we remark that $\mathcal{Z}(D^4)[\phi]$ is positive definite since $\mathcal{Z}(D^4)[\phi]$ is given by norm of some state (C.2); $\mathcal{Z}(D^4)[\phi] > 0$. Then, let us compute $\mathcal{Z}(S^4)$, for which we must have $|\mathcal{Z}(S^4)| = 1$. $\mathcal{Z}(S^4)$ is evaluated by applying gluing formula by cutting S^4 along S^3,

$$\mathcal{Z}(S^4) = \frac{\mathcal{Z}(D^4)[\phi]\mathcal{Z}(D^4)[\phi]}{\langle\phi|\phi\rangle_{\mathcal{V}(S^3)}}. \tag{C.8}$$

  Using (C.7) for $\langle\phi|\phi\rangle_{\mathcal{V}(S^3)} = \mathcal{Z}(S^3 \times D^1)[\phi]$, we have

$$\mathcal{Z}(S^4) = \mathcal{D}^2 \left(\mathcal{Z}(D^4)[\phi]\right)^2. \tag{C.9}$$

  In order for $|\mathcal{Z}(S^4)| = 1$ with positive $\mathcal{Z}(D^4)[\phi]$, we must choose $\mathcal{Z}(D^4)[\phi] = 1/\mathcal{D}$.

Appendix D

1-form LSM theorem is available in the quantum dimer model

Here, we give a simple proof that the result of LSM constraint is applicable for (5.52), even if we take the limit $K \to \infty$ before taking the thermodynamic limit. We check this by seeing if $|\psi_0\rangle$ is a ground state of the gauge theory (5.52), the state $U_{12}|\psi_0\rangle$ also lies in the low energy sector whose energy splitting from $|\psi_0\rangle$ is independent of K and bounded by $O(1/L_1)$. Here, the operator U_{12} is a generator of large gauge transformation, which is defined as

$$U_{12} \equiv \exp\left(\frac{2\pi i}{L_1}\sum_{x_1=0}^{L_1-1} x_1 E_\alpha(x_1,0)\right). \tag{D.1}$$

This statement can be proven in the same manner as the original proof of the LSM theorem (for one dimensional spin system) by Lieb, Schultz and Mattis [50]. We evaluate the difference of the energy expectation values for $|\psi_0\rangle$ and $U_{12}|\psi_0\rangle$ as

$$\begin{aligned}
\delta E[K] &= \langle\psi_0|\left(U_{12}^\dagger H_{\text{eff}}[K]U_{12} - H_{\text{eff}}[K]\right)|\psi_0\rangle \\
&\leq \langle\psi_0|\left(U_{12}^\dagger H_{\text{eff}}[K]U_{12} - H_{\text{eff}}[K]\right)|\psi_0\rangle + \langle\psi_0|\left(U_{12} H_{\text{eff}}[K]U_{12}^\dagger - H_{\text{eff}}[K]\right)|\psi_0\rangle \\
&= 8v\left(\cos\left(\frac{2\pi}{L_1}\right) - 1\right)\langle\psi_0|\left(\sum_{\substack{\{\bigcirc\}\\ x_2=0}} \cos[\text{rot}A]\right)|\psi_0\rangle \\
&\leq 8v\cdot\frac{1}{2}\left(\frac{2\pi}{L_1}\right)^2\cdot L_1 = \frac{16\pi^2 v}{L_1},
\end{aligned} \tag{D.2}$$

where we simply added the term $\langle\psi_0|\left(U_{12}H_{\text{eff}}[K]U_{12}^\dagger - H_{\text{eff}}[K]\right)|\psi_0\rangle$ in the second line, which is non-negative due to the variational principle. Using the similar logic, we find that the variational energy of $U_{12}^n|\psi_0\rangle$ is bounded by $16\pi^2 vn/L_1$. With help of the commutation relation between the momentum in x_1 direction like (5.31), we find at least q mutually orthogonal ground states with distinct momentum when the filling $\nu \equiv Q_2/L_1 = p/q$. Here the upper bound of energy splitting $16\pi^2 vq/L_1$ is independent of K, therefore

$$\lim_{L_1,L_2\to\infty}\lim_{K\to\infty}\delta E[K] \leq \lim_{L_1,L_2\to\infty}\lim_{K\to\infty}\frac{16\pi^2 vq}{L_1} = 0, \tag{D.3}$$

which assures the availability of LSM theorem after taking the limit $K \to \infty$.

Appendix E

LSM theorem for n-form symmetry

In this appendix, we discuss the generalized version of the LSMOH theorem based n-form symmetry. It is straightforward to generalize the logic introduced in Section 5.3 to n-form $U(1)$ symmetry.

E.1 n-form $U(1)$ symmetry in the continuum

Consider a theory written in terms of a n-form $U(1)$ field h, and assume that the action $S[h]$ consists only of $\mathrm{d}h$. The theory is invariant under the shift of h by a flat field

$$h(x) \mapsto h(x) + \omega(x), \qquad \mathrm{d}\omega = 0. \tag{E.1}$$

Gauge equivalence classes of flat n-form $U(1)$ field are classified by the cohomology group

$$[\omega] \in H^n(X; \mathbb{R}/2\pi\mathbb{Z}). \tag{E.2}$$

Then we see that the theory has a global n-form $U(1)$ symmetry

$$h(x) \mapsto h(x) + \theta\lambda(x), \qquad \theta \in \mathbb{R}/2\pi\mathbb{Z}, \tag{E.3}$$

and $[\lambda] \in H^n(X; \mathbb{Z})$.

Objects charged under the n-form $U(1)$ symmetry (E.3) are operators defined on n-dimensional surfaces,

$$V(C) = \exp\left[i \int_C h\right], \qquad C \in Z_n(X), \tag{E.4}$$

which measures a kind of holonomy along C. The n-form symmetry transformation is implemented by an operator $U_\theta(M^{(d-n)})$ supported on $(d-n)$-dimensional manifold $M^{(d-n)}$. We have the equal time commutation relation as

$$U_\theta(M^{(d-n)})V(C) = e^{i\theta(C, M^{(d-n)})} \cdot V(C)U_\theta(M^{(d-n)}) \qquad \text{at equal time}, \tag{E.5}$$

where $(C, M^{(d-n)})$ is the intersection number.

Gauging n-form $U(1)$ symmetry means introducing the flat $(n+1)$-form background $U(1)$ field $c(x)$, $\mathrm{d}c = 0$, and introduce the gauge equivalence relation

$$\begin{aligned} h(x) &\mapsto h(x) + \theta(x)\lambda(x) \\ c(x) &\mapsto c(x) - \mathrm{d}(\theta(x)\lambda(x)) = c(x) - \mathrm{d}\theta(x) \wedge \lambda(x), \end{aligned} \tag{E.6}$$

so that the covariant derivative

$$D_c h := \mathrm{d}h + c \tag{E.7}$$

is invariant. The gauge equivalence classes of $c(x)$ are determined by a kind of holonomy

$$\int_C c \in \mathbb{R}/2\pi\mathbb{Z}, \qquad C \in Z_{n+1}(X). \tag{E.8}$$

i.e.,

$$[c] \in H^{n+1}(X; \mathbb{R}/2\pi\mathbb{Z}). \tag{E.9}$$

E.2 LSM theorem with n-form symmetry

We formulate the above theory on the periodic lattice, whose vertices are labeled as $(x_1, x_2, \ldots, x_d) \in \mathbb{Z}/L_1\mathbb{Z} \times \mathbb{Z}/L_2\mathbb{Z} \times \cdots \times \mathbb{Z}/L_d\mathbb{Z}$, and repeat the same logic as Section 5.3 to derive LSM-type theorem for higher form symmetry. In this case, n-form $U(1)$ field h is assigned on each n-dimensional hypercube. The theory is invariant under the global $U(1)$ transformation

$$h \mapsto h + \theta\lambda \tag{E.10}$$

where $\theta \in \mathbb{R}/2\pi\mathbb{Z}$ is a constant, $d\lambda = 0$ and

$$\sum_{\gamma_n \in C} \lambda_{\gamma_n} \in \mathbb{Z}, \qquad C \in Z_n(X), \tag{E.11}$$

where γ_n is a label of n-dimensional hypercube. The theory is also invariant under the translation $\mathcal{T}_l$ about one unit cell along l-th direction, and assume that neither $U(1)$ nor the translation symmetry is broken.

Then we gauge the $U(1)$ symmetry (E.10) by coupling with a background flat $(n+1)$-form gauge field c defined on $(n+1)$-dimensional hypercube. Consider the field configuration that corresponds to adiabatic insertion

$$\begin{cases} c_{lm_1\ldots m_n} = 0 & t < 0, \\ c_{lm_1\ldots m_n}(\mathbf{x}; t) = \prod_{i=1}^n \delta(x_{m_i}) \cdot 2\pi t/L_l T & 0 \le t < T, \\ c_{lm_1\ldots m_n}(\mathbf{x}; t) = \prod_{i=1}^n \delta(x_{m_i}) \cdot 2\pi/L_l & T \le t, \end{cases} \tag{E.12}$$

and the other components of c are 0.

For the configuration (E.12), the holonomy of c along $(n+1)$-dimensional $x_l x_{m_1} \ldots x_{m_n}$-hyperplane grows gradually from 0 to 2π as time proceeds:

$$\sum_{\gamma_{n+1} \in C} c_{\gamma_{n+1}} = \frac{2\pi t}{T} \qquad 0 \le t < T, \tag{E.13}$$

where γ_{n+1} is a label of $(n+1)$-dimensional hypercube, and C is some $x_l x_{m_1} \ldots x_{m_n}$-hyperplane.

Suppose that the Hamiltonian at $t = 0$ (written as H_0) has finite excitation gap above the ground state, and that the gap does not close during the process of adiabatic flux insertion. At $t = 0$, the ground state $|\psi_0\rangle$ is chosen (when the ground state are degenerate) so that it is an eigenstate of $\mathcal{T}_l$ and a $U(1)$ symmetry transformation operator $Q_{m_1\ldots m_n}$:

$$\begin{aligned}\mathcal{T}_l\,|\psi_0\rangle &= e^{ip_l}\,|\psi_0\rangle\,,\\ Q_{m_1\ldots m_n}\,|\psi_0\rangle &= \nu \prod_{k\neq m_1\ldots m_n} L_k\,|\psi_0\rangle\,,\end{aligned}\tag{E.14}$$

where $Q_{m_1\ldots m_n}$ is a $U(1)$ charge operator associated with $(d-n)$-dimensional hyperplane characterized as $x_{m_1}=\cdots=x_{m_n}=0$, and ν denotes the $U(1)$ charge per unit cell. When the holonomy (E.13) along C reaches the unit flux quantum 2π at $t=T$, the original ground state evolves into some ground state $|\psi_0'\rangle$ of the Hamiltonian at $t=T$ (written as H_0'), that satisfies $\mathcal{T}_l\,|\psi_0'\rangle = e^{ip_l}\,|\psi_0'\rangle$. And the configuration of the flat background $U(1)$ gauge field (E.12) at $t=T$ with the holonomy 2π, is gauge equivalent to that of $t=0$, by the following gauge transformation

$$\begin{aligned}h_{m_1\ldots m_n}(\mathbf{x}) &\mapsto h_{m_1\ldots m_n}(\mathbf{x}) - \prod_{i=1}^{n}\delta(x_{m_i})\cdot 2\pi x_l/L_l,\\ c_{lm_1\ldots m_n}(\mathbf{x}) &\mapsto c_{lm_1\ldots m_n}(\mathbf{x}) - \prod_{i=1}^{n}\delta(x_{m_i})\cdot 2\pi/L_l.\end{aligned}\tag{E.15}$$

We write the symmetry operator corresponding to the above gauge transformation as $U_{lm_1\ldots m_n}$. Then, $U_{lm_1\ldots m_n}\,|\psi_0'\rangle$ is also a ground state of H_0, and there is the following commutation relation between $U_{lm_1\ldots m_n}$ and $\mathcal{T}_l$

$$U_{lm_1\ldots m_n}\mathcal{T}_l U^{\dagger}_{lm_1\ldots m_n} = \mathcal{T}_l \exp\left[-\frac{2\pi i}{L_l}Q_{m_1\ldots m_n}\right].\tag{E.16}$$

Now we obtain the action of $\mathcal{T}_l$ on $U_{lm_1\ldots m_n}\,|\psi_0'\rangle$ using the commutation relation (E.16)

$$\begin{aligned}\mathcal{T}_l U_{lm_1\ldots m_n}\,|\psi_0'\rangle &= e^{ip_l}\exp\left[\frac{2\pi i}{L_l}Q_{m_1\ldots m_n}\right]\cdot U_{lm_1\ldots m_n}\,|\psi_0'\rangle\\ &= \exp\left[ip_l + 2\pi i\nu \prod_{k\neq l,m_1,\ldots,m_n} L_k\right]\cdot U_{lm_1\ldots m_n}\,|\psi_0'\rangle\,.\end{aligned}\tag{E.17}$$

Thus, if we have $\nu = p/q$, with L_l integer multiple of q and $\prod_{k\neq l,m_1,\ldots,m_n} L_k$ mutually prime with q, the momentum of $U_{lm_1\ldots m_n}\,|\psi_0'\rangle$ is written as $p_l + 2\pi r/q$, using some integer r mutually prime with q. Therefore, we obtain at least q mutually orthogonal ground states $|\psi_0\rangle, |\psi_1\rangle, \ldots, |\psi_{q-1}\rangle$ with different momentum, such that

$$|\psi_{k+1}\rangle = U_{lm_1\ldots m_n}\,|\psi_k'\rangle\,,\quad \mathcal{T}_l\,|\psi_k\rangle = \exp\left[i\left(p_l + \frac{2\pi k r}{q}\right)\right]|\psi_k\rangle\,.\tag{E.18}$$

Then, we have proven that

Theorem E.2.1 (LSM theorem for n-form symmetry)

Consider a quantum many-body system defined on a d-dimensional periodic lattice, in the presence of a global n-form $U(1)$ symmetry and a translation symmetry about the l-th primitive lattice vector, and assume that both symmetries are not broken. Then, if the $U(1)$ charge (measured on a $(d-n)$-dimensional hyperplane characterized as $x_{m_1}=\cdots=x_{m_n}=0$ for $m_1,\ldots,m_n\neq l$) per unit cell $\nu = p/q$ at the ground state, only two possibilities are possible for the low energy spectrum:

1. *The system is gapped, and the ground states are at least q-fold degenerate, or*
2. *The system is gapless.*

Bibliography

[1] R. Kobayashi and K. Shiozaki, "Anomaly indicator of rotation symmetry in (3+1)d topological order," arXiv:1901.06195 [cond-mat.str-el].

[2] K. Ryohei, K. Shiozaki, Y. Kikuchi, and S. Ryu, "Lieb-schultz-mattis type theorem with higher-form symmetry and the quantum dimer models," *Physical Review B* **99** no. 1, (2019) 014402.

[3] M. Barkeshli, P. Bonderson, M. Cheng, C.-M. Jian, and K. Walker, "Reflection and time reversal symmetry enriched topological phases of matter: path integrals, non-orientable manifolds, and anomalies," arXiv:1612.07792 [cond-mat.str-el].

[4] D. Gaiotto, A. Kapustin, N. Seiberg, and B. Willett, "Generalized global symmetries," *JHEP* **2015** no. 2, (2015) 172.

[5] D. Gaiotto, A. Kapustin, Z. Komargodski, and N. Seiberg, "Theta, time reversal and temperature," *Journal of High Energy Physics* **2017** no. 5, (2017) 91, arXiv:1703.00501 [hep-th].

[6] X. Chen, Z.-C. Gu, Z.-X. Liu, and X.-G. Wen, "Symmetry protected topological orders and the group cohomology of their symmetry group," *Physical Review B* **87** no. 15, (2013) 155114, arXiv:1106.4772 [cond-mat.str-el].

[7] R. Dijkgraaf and E. Witten, "Topological gauge theories and group cohomology," *Communications in Mathematical Physics* **129** no. 2, (1990) 393–429.

[8] M. Wakui, "On dijkgraaf-witten invariant for 3-manifolds," *Osaka Journal of Mathematics* **29** no. 4, (1992) 675–696. https://ir.library.osaka-u.ac.jp/repo/ouka/all/11650/ojm29_04_02.pdf.

[9] X. Chen, Z.-X. Liu, and X.-G. Wen, "Two-dimensional symmetry-protected topological orders and their protected gapless edge excitations," *Physical Review B* **84** no. 23, (2011) 235141.

[10] J. Wang, X.-G. Wen, and E. Witten, "Symmetric gapped interfaces of spt and set states: systematic constructions," *Physical Review X* **8** no. 3, (2018) 031048.

[11] K. Yonekura, "On the cobordism classification of symmetry protected topological phases," arXiv:1803.10796 [hep-th].

[12] D. S. Freed and M. J. Hopkins, "Reflection positivity and invertible topological phases," arXiv:1604.06527 [hep-th].

[13] H. Song, S.-J. Huang, L. Fu, and M. Hermele, "Topological phases protected by point group symmetry," *Phys. Rev. X* **7** no. 1, (2017) 011020, arXiv:1604.08151 [cond-mat.str-el].

[14] E. Lake, "Anomalies and symmetry fractionalization in reflection-symmetric topological order," *Physical Review B* **94** no. 20, (2016) 205149, arXiv:1608.02736 [cond-mat.str-el].

[15] Y. Qi, C.-M. Jian, and C. Wang, "Folding approach to topological orders enriched by mirror symmetry," arXiv:1710.09391 [cond-mat.str-el].

[16] C. Wang and M. Levin, "Anomaly indicators for time-reversal symmetric topological orders," *Physical review letters* **119** no. 13, (2017) 136801.

[17] Y. Lee and Y. Tachikawa, "A study of time reversal symmetry of abelian anyons," arXiv:1805.02738 [hep-th].

[18] M. Barkeshli and M. Cheng, "Time-reversal and spatial-reflection symmetry localization anomalies in (2+ 1)-dimensional topological phases of matter," *Physical Review B* **98** no. 11, (2018) 115129.

[19] K. Walker. http://canyon23.net/math/tc.pdf.

[20] Y. Tachikawa and K. Yonekura, "On time-reversal anomaly of 2+1d topological phases," *Progress of Theoretical and Experimental Physics* **2017** no. 3, (2017) , arXiv:1610.07010 [hep-th].

[21] Y. Tachikawa and K. Yonekura, "Derivation of the time-reversal anomaly for (2+1)-dimensional topological phases," *Phys. Rev. Lett.* **119** no. 11, (2017) 111603, arXiv:1611.01601 [hep-th].

[22] A. Kapustin, "Symmetry protected topological phases, anomalies, and cobordisms: Beyond group cohomology," arXiv:1403.1467 [cond-mat.str-el].

[23] A. Kitaev, "Toward topological classification of phases with short-range entanglement.". Talk at KITP, 2011-10-21, http://online.kitp.ucsb.edu/online/topomat11/kitaev/.

[24] E. Plamadeala, M. Mulligan, and C. Nayak, "Short-range entangled bosonic states with chiral edge modes and t duality of heterotic strings," *Physical Review B* **88** no. 4, (2013) 045131.

[25] P. Putrov, J. Wang, and S.-T. Yau, "Braiding statistics and link invariants of bosonic/fermionic topological quantum matter in 2+ 1 and 3+ 1 dimensions," *Annals of Physics* **384** (2017) 254–287.

[26] K. Shiozaki, H. Shapourian, and S. Ryu, "Many-body topological invariants in fermionic symmetry-protected topological phases: Cases of point group symmetries," *Physical Review B* **95** (2017) 205139.

[27] N. Tantivasadakarn, "Dimensional reduction and topological invariants of symmetry-protected topological phases," *Physical Review B* **96** no. 19, (2017) 195101, arXiv:1706.09769 [cond-mat.str-el].

[28] K. Walker and Z. Wang, "(3+ 1)-tqfts and topological insulators," *Frontiers of Physics* **7** no. 2, (2012) 150–159.

[29] C. von Keyserlingk, F. Burnell, and S. H. Simon, "Three-dimensional topological lattice models with surface anyons," *Physical Review B* **87** no. 4, (2013) 045107.

[30] A. Kapustin and R. Thorngren, "Higher symmetry and gapped phases of gauge theories," arXiv:1309.4721 [hep-th].

[31] A. Kapustin and N. Seiberg, "Coupling a QFT to a TQFT and Duality," *JHEP* **04** (2014) 001, arXiv:1401.0740 [hep-th].

[32] E. Lake, "Higher-form symmetries and spontaneous symmetry breaking," *arXiv:1802.07747* (2018) . http://arxiv.org/abs/1802.07747.

[33] B. Yoshida, "Topological phases with generalized global symmetries," *Physical Review B* **93** no. 15, (2016) 155131, arXiv:1508.03468 [cond-mat.str-el].

[34] S. Roberts, B. Yoshida, A. Kubica, and S. D. Bartlett, "Symmetry-protected topological order at nonzero temperature," *Physical Review A* **96** no. 2, (2017) 022306, arXiv:1611.05450 [quant-ph].

[35] X.-G. Wen, "Emergent (anomalous) higher symmetries from topological orders and from dynamical electromagnetic field in condensed matter systems," arXiv:1812.02517 [cond-mat.str-el].

[36] C. Wang, A. Nahum, M. A. Metlitski, C. Xu, and T. Senthil, "Deconfined quantum critical points: symmetries and dualities," *Phys. Rev.* **X7** no. 3, (2017) 031051, arXiv:1703.02426 [cond-mat.str-el].

[37] Y. Tanizaki and Y. Kikuchi, "Vacuum structure of bifundamental gauge theories at finite topological angles," *JHEP* **06** (2017) 102, arXiv:1705.01949 [hep-th].

[38] Z. Komargodski, A. Sharon, R. Thorngren, and X. Zhou, "Comments on Abelian Higgs Models and Persistent Order," arXiv:1705.04786 [hep-th].

[39] Z. Komargodski, T. Sulejmanpasic, and M. Ünsal, "Walls, Anomalies, and (De)Confinement in Quantum Anti-Ferromagnets," arXiv:1706.05731 [cond-mat.str-el].

[40] H. Shimizu and K. Yonekura, "Anomaly constraints on deconfinement and chiral phase transition," arXiv:1706.06104 [hep-th].

[41] M. A. Metlitski and R. Thorngren, "Intrinsic and emergent anomalies at deconfined critical points," arXiv:1707.07686 [cond-mat.str-el].

[42] D. Gaiotto, Z. Komargodski, and N. Seiberg, "Time-Reversal Breaking in QCD_4, Walls, and Dualities in 2+1 Dimensions," arXiv:1708.06806 [hep-th].

[43] M. Yamazaki, "Relating 't Hooft Anomalies of 4d Pure Yang-Mills and 2d $\mathbb{CP}^{N-1}$ Model," arXiv:1711.04360 [hep-th].

[44] A. Cherman and M. Unsal, "Critical behavior of gauge theories and Coulomb gases in three and four dimensions," arXiv:1711.10567 [hep-th].

[45] Y. Tanizaki, T. Misumi, and N. Sakai, "Circle compactification and ' t Hooft anomaly," *JHEP* **12** (2017) 056, arXiv:1710.08923 [hep-th].

[46] Y. Tanizaki, Y. Kikuchi, T. Misumi, and N. Sakai, "Anomaly matching for the phase diagram of massless $\mathbb{Z}_N$-QCD," *Phys. Rev. D* **97** no. 5, (2018) 054012, arXiv:1711.10487 [hep-th].

[47] M. Guo, P. Putrov, and J. Wang, "Time Reversal, SU(N) Yang-Mills and Cobordisms: Interacting Topological Superconductors/Insulators and Quantum Spin Liquids in 3+1D," arXiv:1711.11587 [cond-mat.str-el].

[48] T. Sulejmanpasic and Y. Tanizaki, "C-P-T anomaly matching in bosonic quantum field theory and spin chains," *Phys. Rev. B* **97** no. 14, (2018) 144201, arXiv:1802.02153 [hep-th].

[49] R. Raussendorf, S. Bravyi, and J. Harrington, "Long-range quantum entanglement in noisy cluster states," *Physical Review A* **71** no. 6, (2005) 062313, arXiv:0407255 [quant-ph].

[50] E. Lieb, T. Schultz, and D. Mattis, "Two soluble models of an antiferromagnetic chain," *Ann. Phys. (N.Y.)* **16** no. 3, (1961) 407–466.

[51] M. Oshikawa, "Commensurability, excitation gap, and topology in quantum many-particle systems on a periodic lattice," *Phys. Rev. Lett.* **84** no. 7, (2000) 1535.

[52] M. B. Hastings, "Lieb-schultz-mattis in higher dimensions," *Phys. Rev. B* **69** no. 10, (2004) 104431.

[53] X.-G. Wen, *Quantum field theory of many-body systems*. Oxford Univ. Press, New York, 2004.

[54] M. Cheng, M. Zaletel, M. Barkeshli, A. Vishwanath, and P. Bonderson, "Translational symmetry and microscopic constraints on symmetry-enriched topological phases: A view from the surface," *Physical Review X* **6** no. 4, (2016) 041068, arXiv:1511.02263 [cond-mat.str-el].

[55] S. A. Parameswaran, A. M. Turner, D. P. Arovas, and A. Vishwanath, "Topological order and absence of band insulators at integer filling in non-symmorphic crystals," *Nature Physics* **9** (May, 2013) 299–303, arXiv:1212.0557 [cond-mat.str-el].

[56] R. Roy, "Space group symmetries and low lying excitations of many-body systems at integer fillings," *ArXiv e-prints* (Dec., 2012) , arXiv:1212.2944 [cond-mat.str-el].

[57] S. C. Furuya and M. Oshikawa, "Symmetry protection of critical phases and global anomaly in $1+1$ dimensions," *ArXiv e-prints* (Mar., 2015) , arXiv:1503.07292 [cond-mat.stat-mech].

[58] H. Watanabe, H. C. Po, A. Vishwanath, and M. Zaletel, "Filling constraints for spin-orbit coupled insulators in symmorphic and nonsymmorphic crystals," *Proc. Natl. Acad. Sci.* **112** no. 47, (2015) 14551–14556.

[59] H. Watanabe, H. C. Po, M. P. Zaletel, and A. Vishwanath, "Filling-enforced gaplessness in band structures of the 230 space groups," *Phys. Rev. Lett.* **117** no. 9, (2016) 096404.

[60] X. Yang, S. Jiang, A. Vishwanath, and Y. Ran, "Dyonic Lieb-Shultz-Mattis Theorem and Symmetry Protected Topological Phases in Decorated Dimer Models," *ArXiv e-prints* (May, 2017) , arXiv:1705.05421 [cond-mat.str-el].

[61] G. Y. Cho, C.-T. Hsieh, and S. Ryu, "Anomaly manifestation of lieb-schultz-mattis theorem and topological phases," *Phys. Rev. B* **96** no. 19, (2017) 195105.

[62] M. A. Metlitski and R. Thorngren, "Intrinsic and emergent anomalies at deconfined critical points," *arXiv:1707.07686* (2017) . http://arxiv.org/abs/1707.07686.

[63] C.-M. Jian, Z. Bi, and C. Xu, "Lieb-schultz-mattis theorem and its generalizations from the perspective of the symmetry-protected topological phase," *Phys. Rev. B* **97** no. 5, (2018) 054412.

[64] Y. Qi, C. Fang, and L. Fu, "Ground state degeneracy in quantum spin systems protected by crystal symmetries," *ArXiv e-prints* (May, 2017) , arXiv:1705.09190 [cond-mat.str-el].

[65] S.-J. Huang, H. Song, Y.-P. Huang, and M. Hermele, "Building crystalline topological phases from lower-dimensional states," *Phys. Rev. B* **96** no. 20, (Nov., 2017) 205106, arXiv:1705.09243 [cond-mat.str-el].

[66] M. Cheng, "Fermionic Lieb-Schultz-Mattis Theorems and Weak Symmetry-Protected Phases," *ArXiv e-prints* (Apr., 2018) , arXiv:1804.10122 [cond-mat.str-el].

[67] Y. Yao, C.-T. Hsieh, and M. Oshikawa, "Anomaly matching and symmetry-protected critical phases in $su(n)$ spin systems in 1+1 dimensions," *arXiv:1805.06885* (2018) . https://arxiv.org/abs/1805.06885.

[68] N. E. Bonesteel, "Valence bonds and the lieb-schultz-mattis theorem," *Phys. Rev. B* **40** (Nov, 1989) 8954–8960. https://link.aps.org/doi/10.1103/PhysRevB.40.8954.

[69] G. Misguich, C. Lhuillier, M. Mambrini, and P. Sindzingre, "Degeneracy of the ground-state of antiferromagnetic spin-1/2 hamiltonians," *Eur. Phys. J. B* **26** no. 2, (2002) 167–183. https://epjb.epj.org/articles/epjb/abs/2002/06/b01640/b01640.html.

[70] E. Fradkin and S. A. Kivelson *Mod. Phys. Lett.* **B4** (1990) 225.

[71] R. Moessner, S. Sondhi, and P. Chandra, "Phase diagram of the hexagonal lattice quantum dimer model," *Phys. Rev. B* **64** no. 14, (2001) 144416.

[72] D. S. Rokhsar and S. A. Kivelson, "Superconductivity and the quantum hard-core dimer gas," *Phys. Rev. Lett.* **61** no. 20, (1988) 2376.

[73] E. Ardonne, P. Fendley, and E. Fradkin, "Topological order and conformal quantum critical points," *Ann. Phys.* **310** no. 2, (2004) 493–551.

[74] E. Fradkin, D. A. Huse, R. Moessner, V. Oganesyan, and S. L. Sondhi, "Bipartite rokhsar–kivelson points and cantor deconfinement," *Phys. Rev. B* **69** no. 22, (2004) 224415.

[75] E. Fradkin, *Field theories of condensed matter physics*. Cambridge University Press, England, 2013.

[76] R. Moessner and K. Raman, "Quantum dimer models, trieste lectures (2007)," *arXiv:0809.3051* (2008) . http://arxiv.org/abs/0809.3051.

[77] A. Vishwanath, L. Balents, and T. Senthil, "Quantum criticality and deconfinement in phase transitions between valence bond solids," *Phys. Rev. B* **69** no. 22, (2004) 224416.

[78] S. Papanikolaou, K. S. Raman, and E. Fradkin, "Devil's staircases, quantum dimer models, and stripe formation in strong coupling models of quantum frustration," *Phys. Rev. B* **75** no. 9, (Mar., 2007) 094406, cond-mat/0611390.

[79] M. Hermele, M. P. A. Fisher, and L. Balents, "Pyrochlore photons: The $u(1)$ spin liquid in a $s = 1/2$ three-dimensional frustrated magnet," *Phys. Rev. B* **69** no. 6, (2004) 064404.

[80] T. Lan, L. Kong, and X.-G. Wen, "Classification of (3+ 1) D Bosonic Topological Orders: The Case When Pointlike Excitations Are All Bosons," *Phys. Rev. X* **8** no. 2, (2018) 021074, `arXiv:1704.04221 [cond-mat.str-el]`.

[81] M. G. Alford, K.-M. Lee, J. March-Russell, and J. Preskill, "Quantum field theory of non-Abelian strings and vortices," *Nuclear Physics B* **384** no. 1-2, (1992) 251–317.

[82] M. Bucher, H.-K. Lo, and J. Preskill, "Topological approach to Alice electrodynamics," *Nuclear Physics B* **386** no. 1, (1992) 3–26.

[83] M. d. W. Propitius, "Topological interactions in broken gauge theories," `arXiv:9511195 [hep-th]`.

[84] S. Beigi, P. W. Shor, and D. Whalen, "The quantum double model with boundary: condensations and symmetries," *Communications in mathematical physics* **306** no. 3, (2011) 663–694.